A Study of Chirality Induction Mechanism in Cyclocopolymerization of Bis(4-vinylbenzoate)s with Styrene

Makoto Obata

Hokkaido University

September, 1999

A Study of Chirality Induction Mechanism in Cyclocopolymerization of Bis(4-vinylbenzoate)s with Styrene

A Dissertation for the Degree of Doctor of Engineering

Makoto Obata

Hokkaido University

September, 1999

Acknowledgments

The author would like to express his sincere gratitude to Professor Kazuaki Yokota (Division of Molecular Chemistry, Graduate School of Engineering, Hokkaido University) for his help in preparing the thesis and the many useful suggestions for its improvement. The author is deeply grateful to Associate Professor Toyoji Kakuchi (Division of Bioscience, Graduate School of Engineering, Hokkaido University) for his helpful advice and valuable suggestions with continuous encouragement throughout this work. The author would like to acknowledge Assistant Professor Toshifumi Satoh (Division of Molecular Chemistry, Graduate School of Engineering, Hokkaido University), Associate Professor Osamu Haba (Department of Material Science and Engineering, Yamagata University) for making a number of helpful suggestions.

The author enjoyed working with his colleagues because the friendship and good humor of the members in the laboratory created a pleasant and stimulating environment in which to work. In particular, the author is very thankful to Mr. Yasushi Morimoto, Mr. Yukio Yamauchi, Mr. Hiro-omi Shimomura, Mr. Yui Sugiura, Mr. Kazunobu Kamino, Mr. Atsushi Narumi, Mr. Noriaki Yamamoto, Mr. Masashi Tsuji, Mr. Hiroshi Nakade, Mr. Tadashi Ishibashi, and Dr. Takahiro Uesaka for their contribution to this work.

The author is indebted to Assistant Professor Yuji Mikata (Department of Chemistry, Faculty of Science, Nara Women's University) and Assistant Professor Yasushi Kawai (Laboratory of Bioorganic Chemistry, Institute for Chemical Research, Kyoto University) for X-ray structural analysis.

Finally, the author would like to thank Research Fellowships of the Japan Society for the Promotion of Science for Young Scientists for its support of this work.

Makoto Obata

Contents

Chapter 1
Introduction

1.1 Stereochemical Control in Radical Polymerization

Free radical polymerization of vinyl monomers is an important method for producing polymers. Control of the stereochemistry (i.e., the tacticity) in free radical polymerization reactions has been investigated since 1955 when Natta pointed out that two different stereochemical arrangements (namely, isotactic and syndiotactic) could be formed through vinyl polymerization.[1] The control of stereochemistry in free radical reaction is generally more difficult than other types of reaction in organic synthesis as well as polymer synthesis.[2-4] Since free radical polymerization methods are convenient, the control of stereochemistry in the polymerization have been attempted using matrixes[5,6], magnetic field[7], acidic solvents[8], transition metal complexes[9,10], and auxiliaries[11-16].

As for the stereochemical control using an auxiliary, radical polymerization of various esters of acrylic acid have been investigated. Most methacrylates produce a polymer having high content of *r* diad in radical polymerization. However, Okamoto et al. reported that the radical polymerization of bulky esters of methacrylic acid such as triphenylmethyl and 1-phenyldibenzosuberyl methacrylate produced highly isotactic polymer (Chart 1.1).[12] The obtained polymer could be converted to poly(methyl methacrylate) (PMMA) by the acidic hydrolysis and methyl esterification. The isospecificity in this radical polymerization was caused to the thermodynamically stable forms of ω-end radical having a higher possibility of meso addition.[13]

Chart 1.1

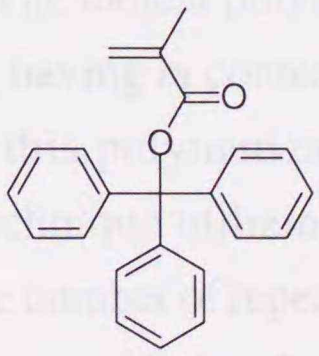

triphenylmethyl methacrylate

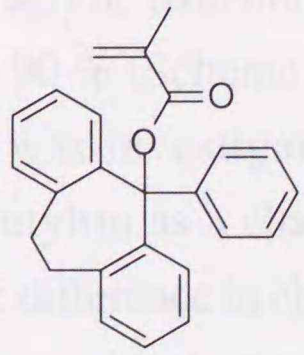

1-phenyldibenzosuberyl methacrylate

Chart 1.2

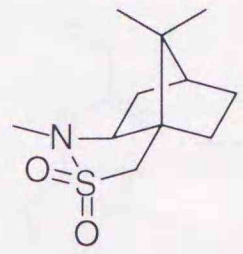

Oppolzer's camphor sultam[17-20]

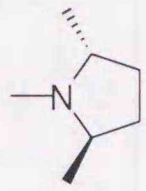

Chiral pyrrolidine derivatives[21-27]

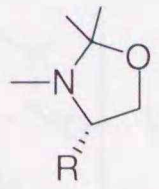

Chiral oxazolidine derivatives[28-31]

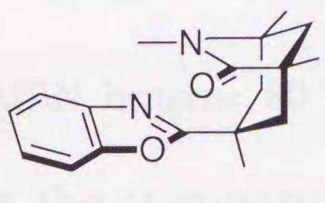

Chiral Kemp's triacid derivatives[33]

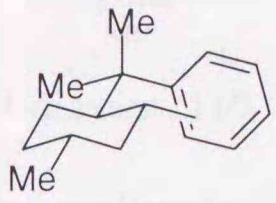

Menthyl derivatives[32]

Scheme 1.1

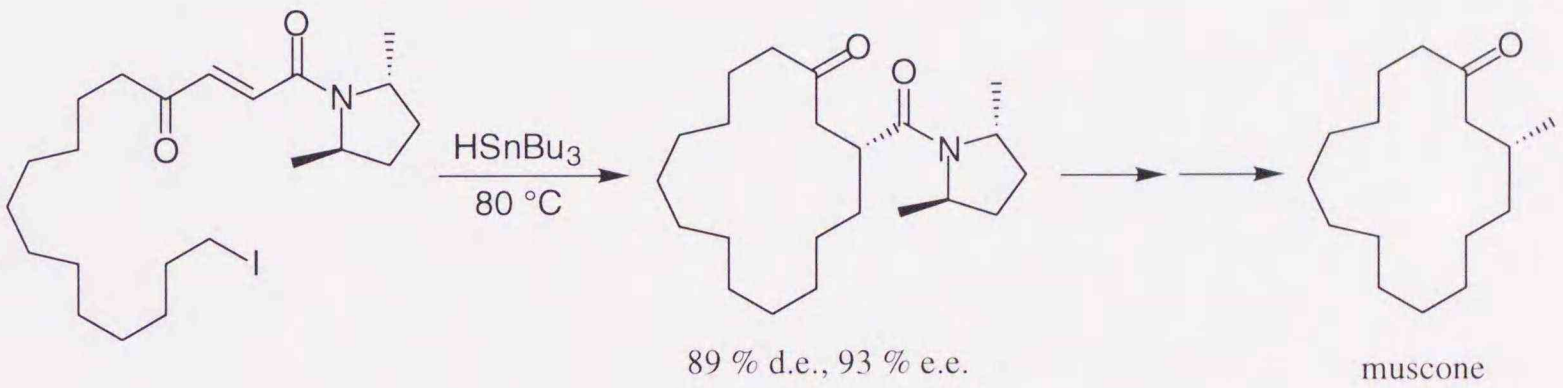

89 % d.e., 93 % e.e.

muscone

Rationally designed chiral auxiliaries can be used for asymmetric synthesis by means of free radical reactions (Chart 1.2).[17-33] Chiral pyrrolidines and oxazolidines were widely used to control acyclic stereochemistry in the radical addition (Scheme 1.1[23]). Porter et al. applied chiral oxazolidine auxiliaries to the radical polymerization of acrylamide.[14] The radical polymerization of acrylic oxazolidides produced highly isotactic polymer having *m* contents more than 90 % (Scheme 1.2). In addition, the stereocontrol in this polymerization system was investigated using the radical telomerization technique utilizing allyltri-*n*-butyltin as a chain transfer reagent.[16] Because of a large number of repeating units, the difference in chain ends is negligible. Hence, after cleavage of the chiral auxiliary, vinyl polymer is optically inactive although the chiral auxiliary exhibits diastereofacial selection in the vinyl polymerization. For asymmetrci polymerization to synthesize an optically active polymer due to main chain chirality, therefore, it is necessary that the rational approach

Scheme 1.2

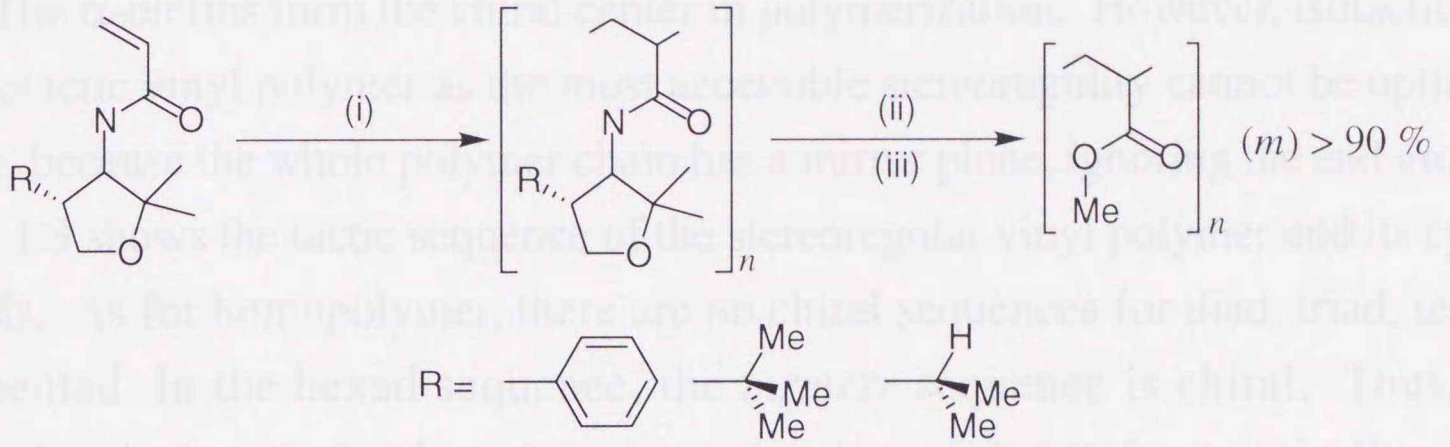

Conditions: (i) AIBN, benzene, 80 °C; (ii) 12*N* HCl, 1,4-dioxane, 110 °C; (iii) CH_2N_2, benzene

to break down the symmetric property of the polymer chain as well as the stereochemical control by the chiral auxiliary.

1.2 Optically Active Polymer due to Main Chain Chirality

The α-olefins form the chiral center in polymerization. However, isotactic and syndiotactic vinyl polymer as the most accessible stereoregulity cannot be optically active, because the whole polymer chain has a mirror plane, ignoring the end groups. Chart 1.3 shows the tactic sequence of the stereoregular vinyl polymer and its cyclic models. As for homopolymer, there are no chiral sequences for diad, triad, tetrad, and pentad. In the hexad sequence, the *mrmrrr* sequence is chiral. Thus, the stereochemical control at hexad sequence level is needed to form optically active homopolymer of α-olefins at least.

Chart 1.3

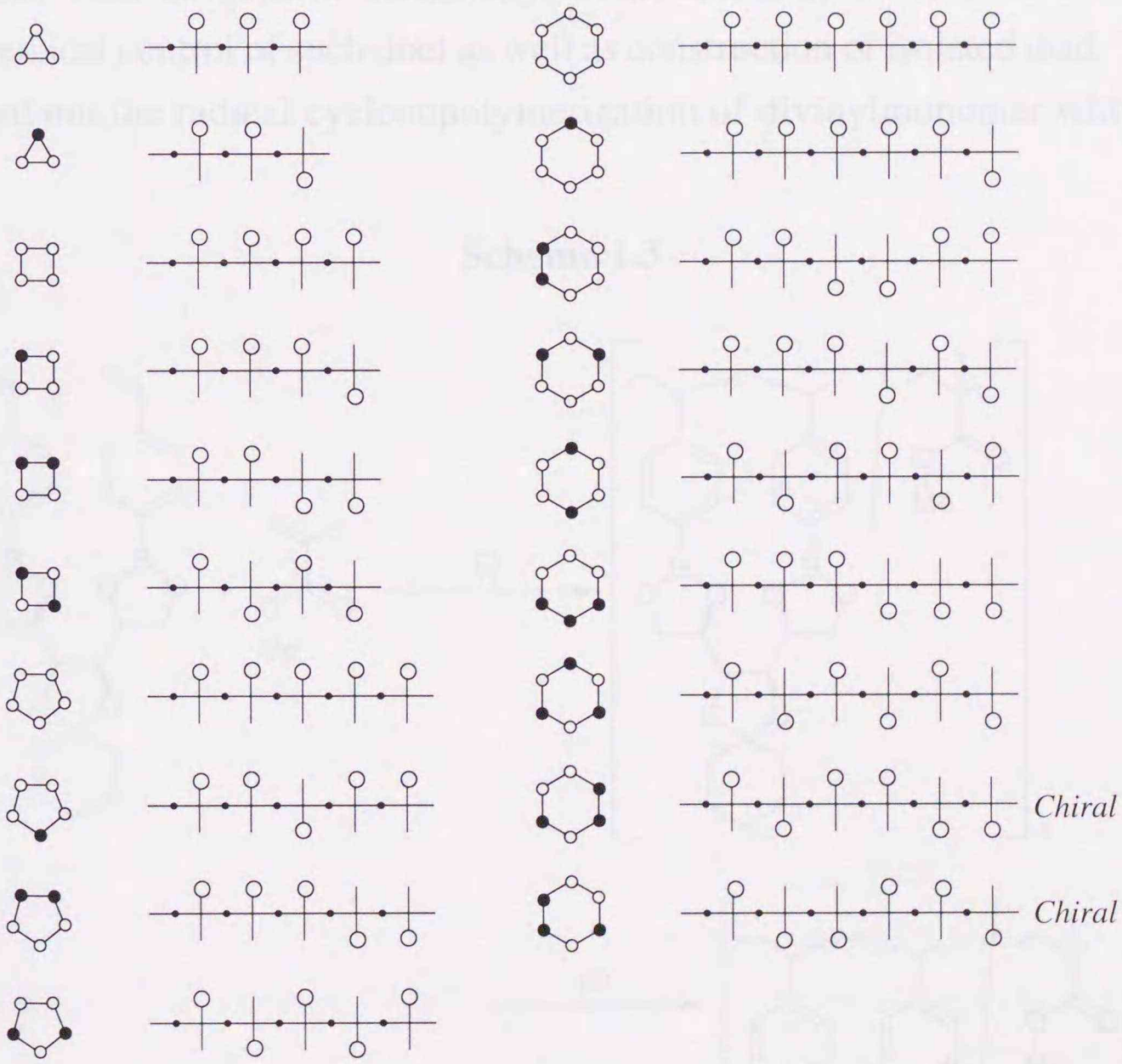

Chart 1.4

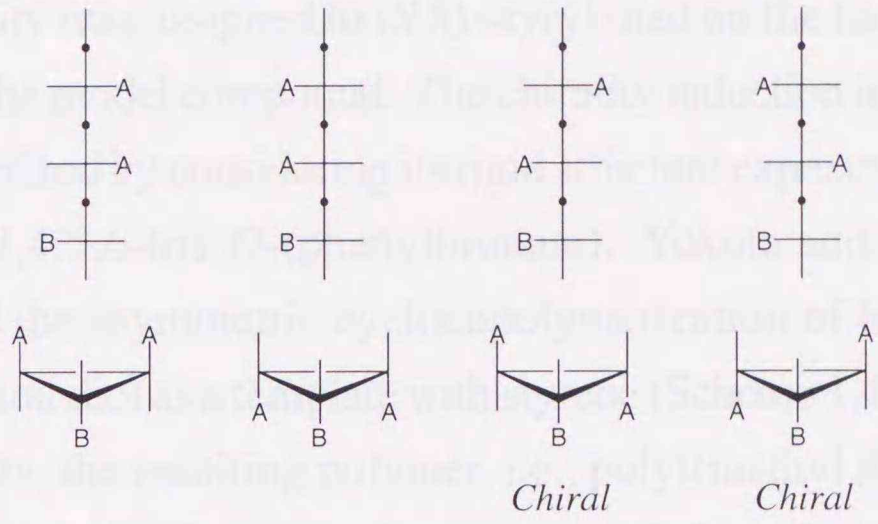

The same consideration can be applied to copolymer sequence as shown in Chart 1.4. Two of the four possible triad sequences A-A-B in a copolymer are chiral. In order to the synthesis of an optically active polymer due to such chiral A-A-B sequence, asymmetric cyclocopolymerization of divinyl monomer having a chiral auxiliary (template) with an achiral monovinyl comonomer is a versatile method for stereochemical control of such diad as well as construction of isolated diad. Wulff et al. carried out the radical cyclocopolymerization of divinylmonomer with methyl

Scheme 1.3

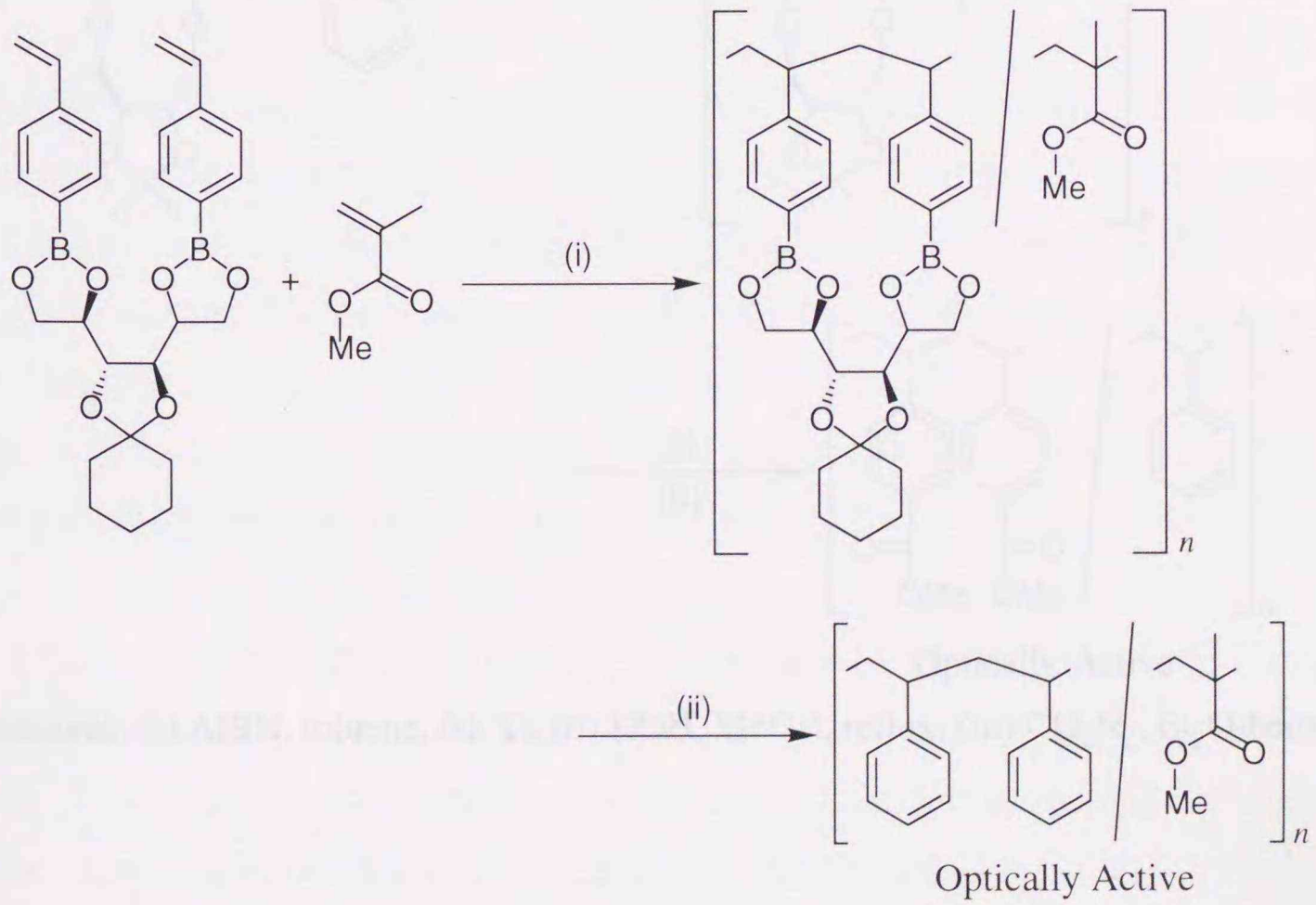

Condictions: (i) AIBN, toluene, 60 °C; (ii) $AgNO_3$, NH_3

methacrylate (Scheme 1.3).[34] After removal of the chiral template using $AgNO_3$/NH_3, the resulting poly[styrene-*co*-(methyl methacrylate)] showed an optical activity. The origin of chirality was assigned to (*S*,*S*)-styryl diad on the basis of the sign of the specific rotation of the model compound. The chirality induction in this polymerization system was characterized by considering its rigid structure expexcted by X-ray analysis of D-mannitol 1,2:3,4:5,6-tris-*O*-(phenylbronate). Yokota and Kakuchi have been extensively studied the asymmetric cyclocopolymerization of bis(4-vinylbenzoate) derivatives using chiral diol as a template with styrene (Scheme 1.4).[35,36] After removal of the chiral template, the resulting polymer, i.e., poly[(methyl 4-vinylbenzoate)-*co*-styrene], showed an optically active due to main chain chirality. In addition, the chiral configuration of the main chain could be characterized using the CD exciton chirality method[37] by CD spectroscopy.

Scheme 1.4

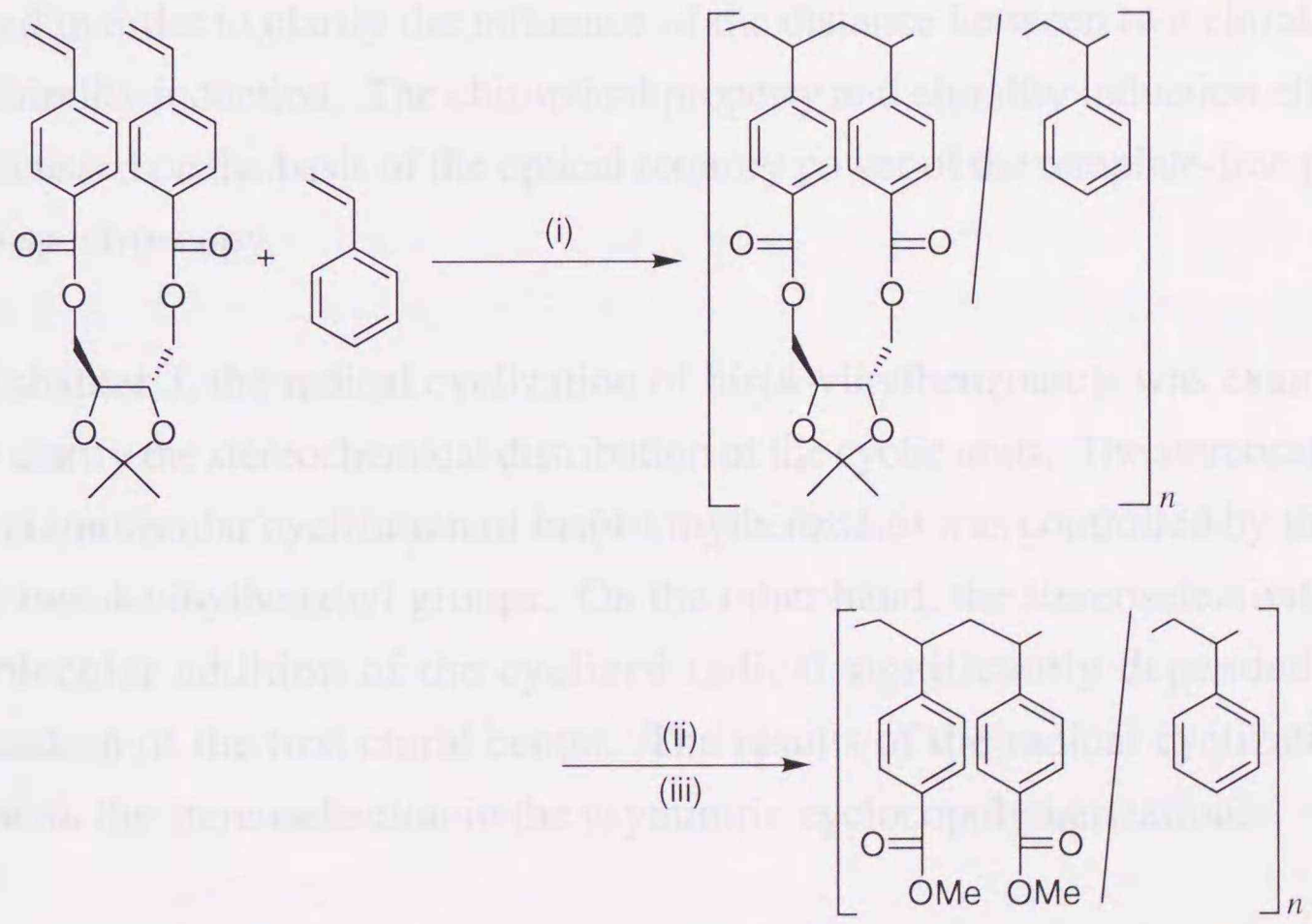

Optically Active

Conditions: (i) AIBN, toluene, 60 °C; (ii) KOH, MeOH, reflux; (iii) CH_2N_2, Et_2O-benzene

1.3 Object and Outline of the Thesis

Asymmetric cyclocopolymerization of bis(4-vinylbenzoate) having a chiral template with styrene has beed extensively studied. The specific rotation of poly[(methyl 4-vinylbenzoate)-*co*-styrene] significantly depends on the structural characteristics of the chiral template. However, we little know about the relationship among the optical rotatory power of the resulting polymer, structural characteristics of the template, and chirality induction mechanism of the chiral template because of flexiblity in these divinyl monomers.

The objects of this study are to examine fresh approaches for the quantitative estimation of the chirality induction and to clarify the chirality induction mechanism.

The outline of this thesis is as follows:

In chapter 2, the cyclocopolymerizations of (2*S*,3*S*)-2,3-butanediyl, (2*S*,4*S*)-2,4-pentanediyl, and (2*S*,5*S*)-2,5-hexanediyl bis(4-vinylbenzoate)s with styrene were examined in order to clarify the influence of the distance between two chiral centers on the chirality induction. The chiroptical property and chirality induction efficiency were discussed on the basis of the optical rotatory power of the template-free polymer and CD spectroscopy.

In chapter 3, the radical cyclization of bis(4-vinylbenzoate)s was examined in order to clarify the stereochemical distribution of the cyclic units. The stereoselectivity in the intramolecular cyclization of bis(4-vinylbenzoate) was controlled by the chiral twist of two 4-vinylbenzoyl groups. On the other hand, the stereoselectivity in the intermolecular addition of the cyclized radical significantly depended on the configuration of the first chiral center. The results of the radical cyclization was agreed with the stereoselection in the asymmtric cyclocopolymerization.

In chapter 4, the chirality induction mechanism in the radical cyclization of bis(4-vinylbenzoate) having a chiral template was studied using a computational method. The semiempirical molecular orbital calculation indicated that the chiral template biases two conformational elements, namely chiral twist of 4-vinylbenzoyl groups and chiral orientation of two carbonyl groups. The two states play an important

role in the stereoselctivity in intra- and intermolecular radical reaction, respectively. This chirality induction mechanism could conclusively explain the stereoselctivity in the radical cyclization.

In chapter 5, total monomer concentration effect on the chirality induction were estimated in the cyclocopolymerizations of (2*S*,3*S*)-2,3-butanediyl, (2*S*,4*S*)-2,4-pentanediyl, and (2*S*,5*S*)-2,5-hexanediyl bis(4-vinylbenzoate)s with styrene. The molecular weight has no influence on the chiroptical properties of the template-free polymer as long as DP_n' of the template-free polymer ranges from 32 to 21. In this DP_n' range, the specific rotation of the template-free polymer increased with a decrease in the total monomer concentration during the polymerization. This effect could be explained by considering the chirality induction mechanism established in chapter 4.

In chapter 6, conformational effect of monomer on the chirality induction was estimated in the cyclocopolymerization of 2,3-bis-*O*-(4-vinylbenzoyl)-L-tartarate and (2*S*,3*S*)-1,4-dimethoxy-2,3-butandiyl bis(4-vinylbenzoate) with styrene. Although these templates have an identical configuration on the chiral center, the sense of chiral twist of two 4-vinylbenzoyl groups was different between the tartarate derivative and its decarbonyl analog. The tartarate derivative was unsuitable for chirality induction, whereas its decarbonyl analog effectively acted as a template. This conformational effect was discussed on the basis of the chirality induction mechanism established in chapter 4.

In chapter 7, the cyclocopolymerization of 1,2:5,6-di-*O*-isopropylidene-3,4-di-*O*-methacryloyl-D-mannitol with styrene. The resulting polymer was converted to poly[(methyl methacrylate)-*co*-styrene]. The cotacticity of poly[(methyl methacrylate)-*co*-styrene] could be estimated by ^{13}C NMR spectroscopy. The origin of chirality was discussed on the basis of the chiroptical properties and tactic sequence of poly[(methyl methacrylate)-*co*-styrene].

Finally, chapter 8 summarizes the results in this study.

1.4 References

(1) Natta, G. *J. Polym. Sci.* **1955**, *16*, 143.

(2) Giese, B. *Angew. Chem. Int. Ed. Engl.* **1989**, *28*, 969.

(3) Porter, N. A.; Giese, B.; Curran, D. P. *Acc. Chem. Res.* **1991**, *24*, 296.

(4) Samadja, W. *Synlett* **1994**, 1.

(5) Buter, R.; Tan, Y. Y.; Challa, G. *J. Polym. Sci., A-1* **1973**, *11*, 2975.

(6) Gons, J.; Vorenkamp, E. J.; Challa, G. *J. Polym. Sci., Polym. Chem. Ed.* **1977**, *15*, 3031.

(7) Turro, N. J.; Pierola, I. F.; Chung, C.-J. *J. Polym. Sci., Polym. Chem. Ed.* **1983**, *21*, 1085.

(8) Yamada, K.; Nakano, T.; Okamoto, Y. *Macromolecules* **1998**, *31*, 7598.

(9) Nakano, T.; Okamoto, Y. *Polym. Preprints, Japan* **1995**, *44*, 1108.

(10) Nakano, T.; Ishigaki, Y.; Okamoto, Y. *Polym. Preprints, Japan* **1997**, *46*, 138.

(11) Yuki, H.; Hatada, K.; Niinomi, T.; Kikuchi, Y. *Polym. J.* **1970**, *1*, 36.

(12) Nakano, T.; Mori, M.; Okamoto, Y. *Macromolecules* **1993**, *26*, 867.

(13) Nakano, T.; Matsuda, A.; Okamoto, Y. *Polym. J.* **1996**, *28*, 556.

(14) Porter, N. A.; Allen, T. R.; Breyer, R. A. *J. Am. Chem. Soc.* **1992**, *114*, 7676.

(15) Wu, W.-X.; McPhail, A. T.; Porter, N. A. *J. Org. Chem.* **1994**, *59*, 1302.

(16) Porter, N. A.; Carter, R. L.; Mero, C. L.; Roepel, M. G.; Curran, D. P. *Tetrahedron* **1996**, *52*, 4181.

(17) Oppolzer, W. *Tetrahedron* **1987**, *43*, 1969.

(18) Oppolzer, W. *Pure Appl. Chem.* **1988**, *60*, 39.

(19) Curran, D. P.; Shen, W.; Zhang, J.; Heffner, T. A. *J. Am. Chem. Soc.* **1990**, 112, 6738.

(20) Curran, D. P.; Shen, W.; Zhang, J.; Geib, S. J.; Lin, C.-H. *Heterocycles* **1994**, *37*, 1773.

(21) Schlessinger, R. H.; Iwanowicz, E. J. *Tetrahedron Lett.* **1987**, *28*, 2083.

(22) Short, R. P.; Kennedy, R. M.; Masamune, S. *J. Org. Chem.* **1989**, *54*, 1755.

(23) Porter, N. A.; Lacher, B.; Chang, V. H.-T.; Magnin, D. R. *J. Am. Chem. Soc.* **1989**, *111*, 8309.

(24) Porter, N. A.; Scott, D. M.; Lacher, B.; Giese, B.; Zeitz, H.-G.; Lindner, H. T. *J. Am. Chem. Soc.* **1989**, *111*, 8311.

(25) Scott, D. M.; McPhail, A. T.; Porter, N. A. *Tetrahedron Lett.* **1990**, *31*, 1679.

(26) Porter, N. A.; Swann, E.; Nally, J.; McPhail, A. T. *J. Am. Chem. Soc.* **1990**, *112*, 6740.
(27) Giese, B.; Zehnder, M.; Roth, M.; Zeitz, H.-G. *J. Am. Chem. Soc.* **1990**, *112*, 6741.
(28) Radinov, R.; Mero, C. L.; McPhail, A. T.; Porter N. A. *Tetrahedron Lett.* **1995**, *36*, 8183.
(29) Porter, N. A.; Bruhnke, J. D.; Wu, W.-X.; Rosenstein, I. J.; Breyer, R. A. *J. Am. Chem. Soc.* **1991**, *113*, 7788.
(30) Badone, D.; Bernassau, J.-M., Cardamone, R.; Guzzi, U. *Angew. Chem. Int. Ed. Engl.* **1996**, *35*, 535.
(31) Sibi, M. P.; Ji, J. *J. Am. Chem. Soc.* **1996**, *118*, 3063.
(32) Nishida, M.; Ueyama, E.; Hayashi, H.; Ohtake, Y.; Yamaura, Y.; Yanagimura, E.; Yonemitsu, O.; Nishida, A.; Kawahara, N. *J. Am. Chem. Soc.* **1994**, *116*, 6455.
(33) Stack, J. G.; Curran, D. P.; Geib, S. V.; Rebek, Jr. J.; Ballester, P. *J. Am. Chem. Soc.* **1992**, *114*, 7007.
(34) Wulff, G. *Angew. Chem. Int. Ed. Engl.* **1989**, *28*, 21.
(35) Yokota, K.; Kakuchi, T.; Uesaka, T.; Obata, M. *Acta Polym.* **1997**, *48*, 459.
(36) Kakuchi, T.; Uesaka, T.; Obata, M.; Yokota, K. *Kobunshi Ronbunshu* **1997**, *54*, 684.
(37) Harada, N.; Nakanishi, K. *Circular Dichroic Spectroscopy Exciton Coupling in Organic Stereochemistry*; Oxford University Press: Oxford, U. K., **1983**.

Chapter 2

Asymmetric Cyclocopolymerization of (2S,3S)-2,3-Butanediyl, (2S,4S)-2,4-Pentanediyl, and (2S,5S)-2,5-Hexanediyl Bis(4-vinylbenzoate)s with Styrene

2.1 Introduction

For the asymmetric cyclocopolymerization of bis(4-vinylbenzoate) having chiral templates with styrene, the chirality induction depends on the structural characteristics of the templates, i.e., the distance, the torsion angle, the rotational freedom, and the steric crowding between two 4-vinylbenzoyl groups. A series of compounds as template need to design adequately for the elucidation of these effects. (2*S*,3*S*)-2,3-Butanediol, (2*S*,4*S*)-2,4-pentanediol, and (2*S*,5*S*)-2,5-hexanediol are well suitable for the purpose that is to clarify the effect of the distance between two 4-vinylbenzoyl groups on chirality induction.

In this chapter, the cyclocopolymerizations of (2*S*,3*S*)-2,3-butanediyl, (2*S*,4*S*)-2,4-pentanediyl, and (2*S*,5*S*)-2,5-hexanediyl bis(4-vinylbenzoate)s with styrene were examined (Scheme 2.1). The effect of the distance between two 4-vinylbenzoyl groups was discussed on the basis of the chiroptical property of the template-free polymer.

Scheme 2.1

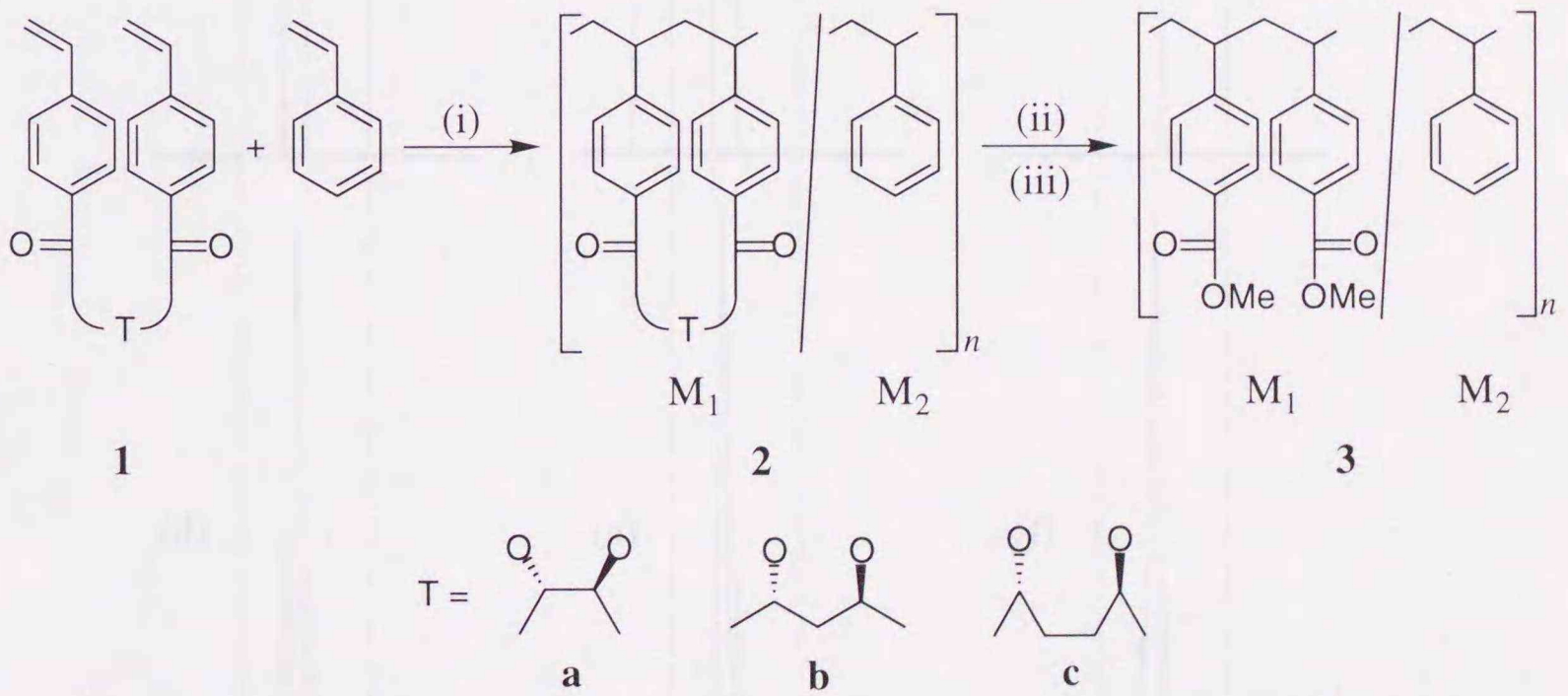

1 **2** **3**

a **b** **c**

Conditions: (i) AIBN, toluene, 60 °C; (ii) KOH, MeOH, reflux; (iii) CH_2N_2, Et_2O

2.2 Results and Discussion

2.2.1 Cyclocopolymerization.

The cyclocopolymerizations of (2*S*,3*S*)-2,3-butanediyl, (2*S*,4*S*)-2,4-pentanediyl, and (2*S*,5*S*)-2,5-hexanediyl bis(4-vinylbenzoate)s (**1a**, **1b**, and **1c**, respectively, M_1) with styrene (M_2) were carried out using AIBN in toluene at 60 °C. The results are listed in Table 2.1. The polymerization systems were homogeneous and the resulting polymers **2a**-**c** were soluble in chloroform and tetrahydrofuran. The number-average molecular weights (M_ns) of polymers **2a**-**c** decreased with an increase of the mole fraction of styrene in the feed. The degree of polymerization decreased from 66, 104, and 51 for polymers **2a**, **2b**, and **2c**, respectively, to 22 for all of them. The higher and lower limits are intrinsic in the bis(4-vinylbenzoate)s and styrene, respectively,

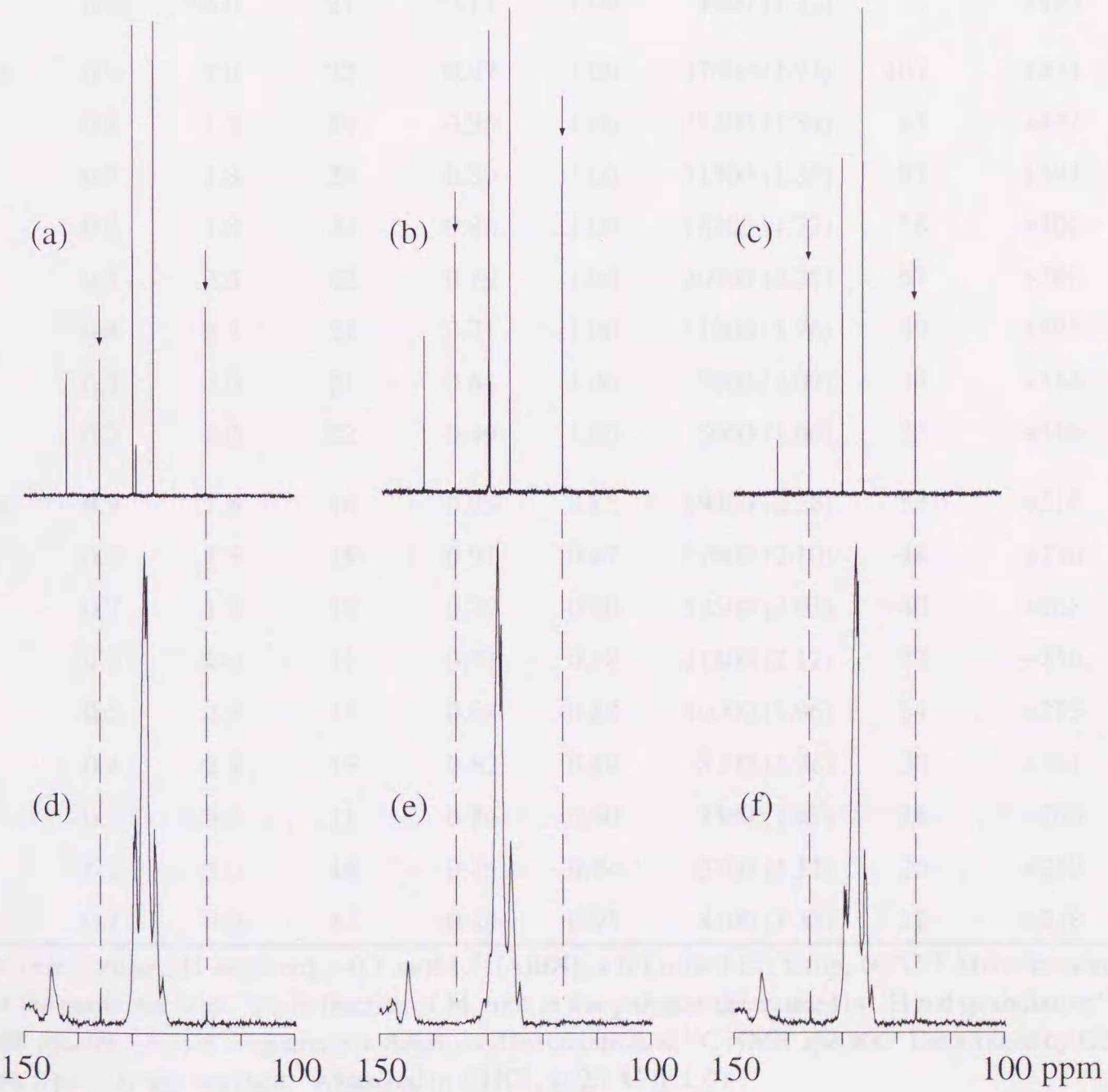

Figure 2.1. Expanded ^{13}C NMR spectra of monomers **1a** (a), **1b** (b), and **1c** (c) and polymers **2a** (d), **2b** (e), and **2c** (f).

Table 2.1. Cyclocopolymerizations of (2*S*,3*S*)-2,3-butanediyl, (2*S*,4*S*)-2,4-pentanediyl, and (2*S*,5*S*)-2,5-hexanediyl bis(4-vinylbenzoate)s (**1a**, **1b**, and **1c**, respectively, M_1) with styrene (M_2).[a]

M_1	F_1[b]	Time (h)	Yield (%)	f_1[c]	f_c[d]	M_n (M_w/M_n)[e]	DP_n	$[\alpha]^{23}_{435}$[f]
1a	0.9	2.5	24	0.99	0.86	22900 (3.41)	66	+278
	0.8	2.0	16	0.90	0.87	19300 (2.05)	59	+304
	0.7	3.5	28	0.79	0.89	18700 (1.76)	63	+313
	0.6	2.5	19	0.77	0.88	15200 (2.34)	52	+315
	0.5	3.0	9	0.66	0.89	10700 (1.78)	40	+307
	0.4	3.6	19	0.65	0.90	10200 (2.12)	39	+314
	0.3	5.5	25	0.51	0.94	7900 (1.62)	34	+319
	0.2	6.0	18	0.46	0.89	6100 (1.83)	28	+291
	0.1	12.5	14	0.30	0.94	3900 (1.67)	22	+252
	0.05	68.0	27	0.11	1.00	4400 (1.32)	34	+150
1b	0.9	1.0	22	0.97	1.00	37000 (1.73)	104	+434
	0.8	1.5	24	0.95	1.00	29300 (1.89)	83	+423
	0.7	1.8	24	0.89	1.00	31300 (1.89)	93	+394
	0.6	1.8	23	0.86	1.00	18300 (1.72)	56	+405
	0.5	2.5	22	0.79	1.00	20900 (2.25)	67	+386
	0.4	2.3	22	0.71	1.00	11200 (1.76)	39	+395
	0.3	4.0	21	0.61	1.00	9000 (2.09)	34	+354
	0.2	5.0	22	0.49	1.00	5000 (1.60)	22	+319
1c	0.9	1.5	16	0.95	0.85	19200 (2.28)	53	+218
	0.8	1.5	15	0.91	0.87	17000 (2.10)	48	+250
	0.7	1.7	18	0.77	0.90	12500 (2.03)	40	+268
	0.6	2.0	11	0.71	0.88	11200 (2.12)	37	+256
	0.5	2.5	17	0.68	0.88	10000 (1.96)	34	+275
	0.4	2.8	15	0.62	0.89	8200 (1.76)	30	+261
	0.3	3.5	11	0.56	0.90	7300 (1.67)	28	+263
	0.2	5.0	14	0.45	0.94	5700 (1.51)	25	+259
	0.1	8.0	11	0.29	0.95	4100 (1.33)	22	+218

[a] Solvent, toluene; $[\mathbf{1}+\text{styrene}]_0 = 0.1$ mol·L^{-1}; $[\text{AIBN}]_0 = 6.1$ mmol·L^{-1}; temp, 60 °C. [b] Mole fraction of **1** in the monomer feed. [c] Mole fraction of M_1 unit in the polymer determined by ^{1}H and quantitative ^{13}C NMR spectra. [d] Extent of cyclization determined by quantitative ^{13}C NMR spectra. [e] Determined by GPC using a polystyrene standard. [f] Measured in $CHCl_3$ at 23 °C (*c* 1.0).

under the cyclocopolymerization conditions. Figure 2.1 shows the ^{13}C NMR spectra of monomers **1a-c** and polymers **2a-c**. The peaks due to the vinyl groups disappeared in the ^{13}C NMR spectrum of polymer **2b**, and thus, the monomer **1b** was suggested to polymerize with complete cyclization. However, polymers **2a** and **2c** contained a small amount of residual double bonds. The extent of cyclization (f_c) was estimated from the area ratio between the peaks of the carbonyl and vinyl carbons in the inverse gated decoupling ^{13}C NMR spectra of polymers **2a** and **2c**. The f_c values for polymers **2a** and **2c** increased with increasing M_2 fraction. Hence, the cyclization tendency increased in the order of **1a** ≅ **1c** < **1b**. The mole fraction of M_1 unit in polymer **2** was estimated from area ratio of the aromatic and carbonyl carbon region in the inverse gated decoupling ^{13}C NMR spectrum as listed in Table 2.1. The monomer reactivity ratio $r_1 = 3.41$ and $r_2 = 0.38$ for **1a**/St, $r_1 = 3.81$ and $r_2 = 0.28$ for **1b**/St, and $r_1 = 1.97$ and $r_2 = 0.21$ for **1c**/St, which were calculated by the Kelen-Tüdös plots.[1] Figure 2.2 shows the composition curves calculated on the basis of Mayo-Lewis equation.[2]

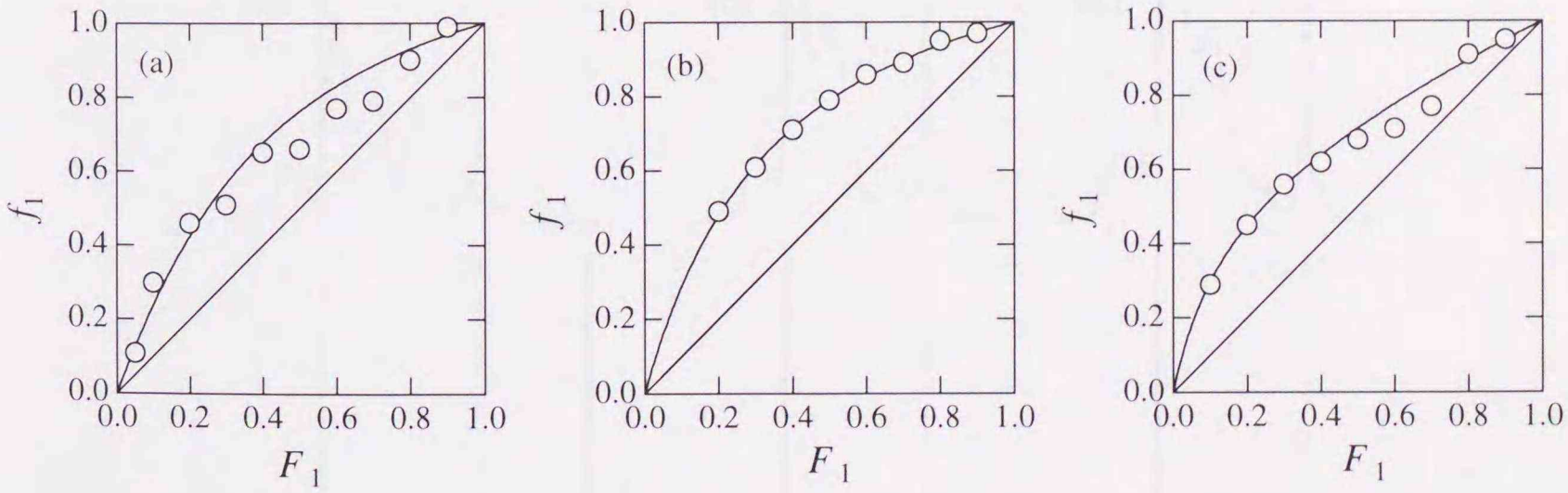

Figure 2.2. Composition curves for the radical cyclocopolymerizations of monomers **1a** (a), **1b** (b), and **1c** (c) with styrene. Conditions: solvent, toluene; $[\mathbf{1}+\text{styrene}]_0 = 0.1$ mol·L^{-1}; $[\text{AIBN}]_0 = 6.1$ mmol·L^{-1}; temp, 60 °C.

2.2.2 Removal of the Template from Polymer ***2***

The chirality induction in the cyclocopolymerization should be confirmed by quantitatively removing the chiral template from polymer **2**. The removal of the chiral template from **2** was carried out using KOH in aqueous MeOH. The hydrolyzed polymer was then treated with diazomethane. Figure 2.3 shows the ^{1}H NMR spectra of the methylated polymers derived from **2a**-**c**. The peaks due to the chiral template (i.e., the peaks at 5.3-5.4 ppm assigned to methine proton of the chiral template) disappeared so that the lack of chiral templates was confirmed for each polymer. Therefore, the template-free polymers were poly[(methyl 4-vinylbenzoate)-*co*-styrene] (**3**). Table 2.2 lists the results of the synthesis of polymer **3**.

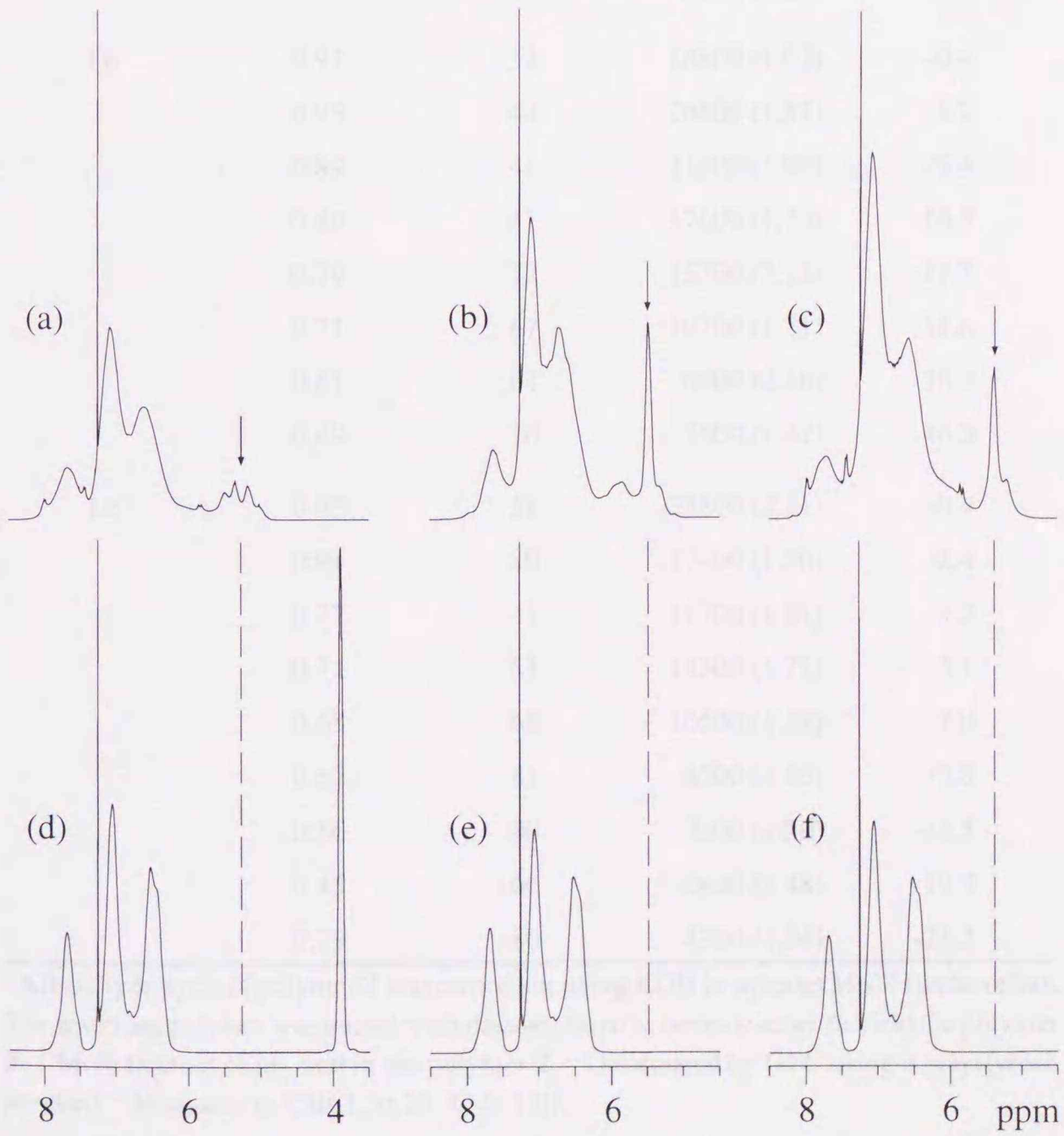

Figure 2.3. Expanded ^{1}H NMR spectra of polymers **2a** (a), **2b** (b), and **2c** (c) and thier template-free polymers **3a** (d), **3b** (e), and **3c** (f).

Table 2.2. Hydrolysis and methyl esterification of polymers **2a-c**.[a]

M_1	f_1[b]	Yield (%)	M_n (M_w/M_n)[c]	$[\alpha]^{23}_{435}$[d]
1a	0.99	27	21400 (1.72)	-1.3
	0.90	68	18000 (1.71)	-1.6
	0.79	46	14400 (1.42)	-1.9
	0.77	71	14300 (1.58)	-2.2
	0.66	73	9200 (1.76)	-2.6
	0.65	69	10100 (1.51)	-3.7
	0.51	56	7200 (1.53)	-4.7
	0.46	80	5800 (1.55)	-7.2
	0.30	61	3800 (1.48)	-8.4
	0.11	62	2500 (1.52)	-8.4
1b	0.97	32	28800 (1.92)	-0.4
	0.95	44	26800 (1.87)	-5.2
	0.89	41	21800 (1.98)	-9.4
	0.86	41	17600 (1.76)	-16.3
	0.79	72	15700 (2.12)	-19.7
	0.71	67	10700 (1.71)	-31.6
	0.61	64	6900 (2.16)	-36.4
	0.49	70	5500 (1.47)	-46.3
1c	0.95	58	22800 (2.11)	-0.4
	0.91	80	17400 (1.76)	-2.4
	0.77	47	11700 (1.81)	-4.2
	0.71	61	13300 (1.72)	-5.1
	0.68	68	10500 (1.58)	-7.0
	0.62	81	8200 (1.65)	-9.8
	0.56	80	7300 (1.50)	-14.5
	0.45	66	6400 (1.48)	-19.5
	0.29	80	4300 (1.54)	-24.2

[a] Alkali hydrolysis of polymer **2** was carried out using KOH in aqueous MeOH under reflux. The resulting polymer was treated with diazomethane in benzene-ether to yield the polymer **3**. [b] Mole fraction of M_1 unit in the polymer **2**. [c] Determined by GPC using a polystyrene standard. [d] Measured in $CHCl_3$ at 23 ℃ (*c* 1.0).

*2.2.3 Chiroptical Properties of Polymers **3a-c***

Even after removal of the chiral templates, the obtained polymers, i.e., poly[(methyl 4-vinylbenzoate)-*co*-styrene]s (**3a-c**), showed an optical activity as listed in Table 2.2. The specific rotation ($[\alpha]_{435}$, *c* 1.0, $CHCl_3$) increased with a decrease in the M_1 fraction in the polymer and varied from -1° to -8° for **3a**, from 0° to -46° for **3b**, and from 0° to -24° for **3c**. These optical activities originated in the chiral configuration of the main chain possessing numerous chiral centers. As described in chapter 1, the minimum chiral repeating unit is generated in a racemo diad of the M_1 unit separated by M_2 units, namely, the isolated benzoate diad. On the first-order Markov model and perfect cyclization, the weight fraction of the isolated benzoate diad (W_1) could be calculated as follows:[3]

$$W_1 = W_{M1}\left(\frac{[M_2]}{r_1[M_1]+[M_2]}\right) \qquad (2.1)$$

W_{M1} is the weight fraction of the M_1 unit. Figure 2.4 shows the specific rotations of

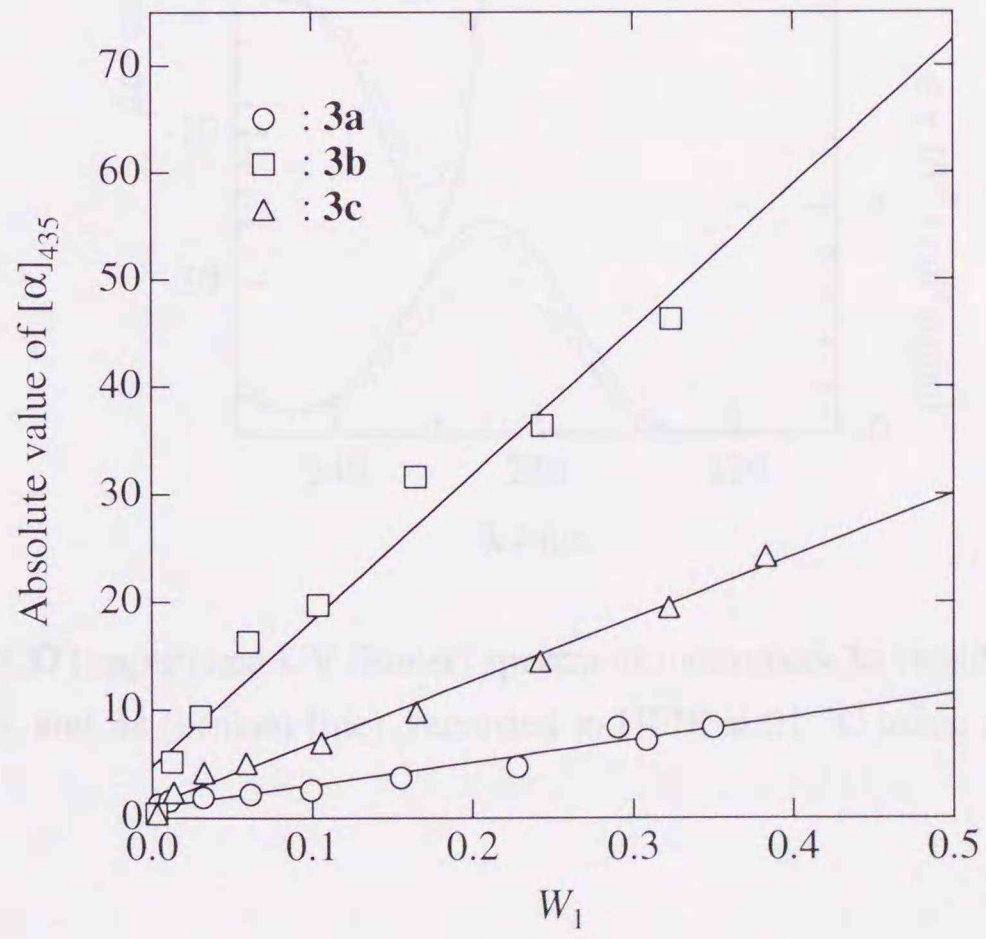

Figure 2.4. Specific rotations ($[\alpha]_{435}$, *c* 0.1, $CHCl_3$) *versus* weight fraction of the isolated benzoate diad (W_1) in polymers **3a** (○), **3b** (□), and **3c** (△). The W_1 values were calculated according to eq. 2.1.

polymers **3a-c** as a function of W_1. Each of the polymers showed a good linearity of the plots. This result means that the source of chirality in polymer **3** is attributable to the isolated benzoate diad. Here the slope of the plots gives the specific rotation per isolated benzoate diad. Therefore, the chirality induction efficiency increased in order of **1a** < **1c** < **1b**. Figure 2.5 shows the CD and UV spectra of monomers **1a-c**. The CD spectra exhibit the split Cotton effect with a positive first and a negative second Cotton effects. According to the CD exciton chirality method[4], these CD spectra indicate that two 4-vinylbenzoyl groups twist clockwise. On the other hand,

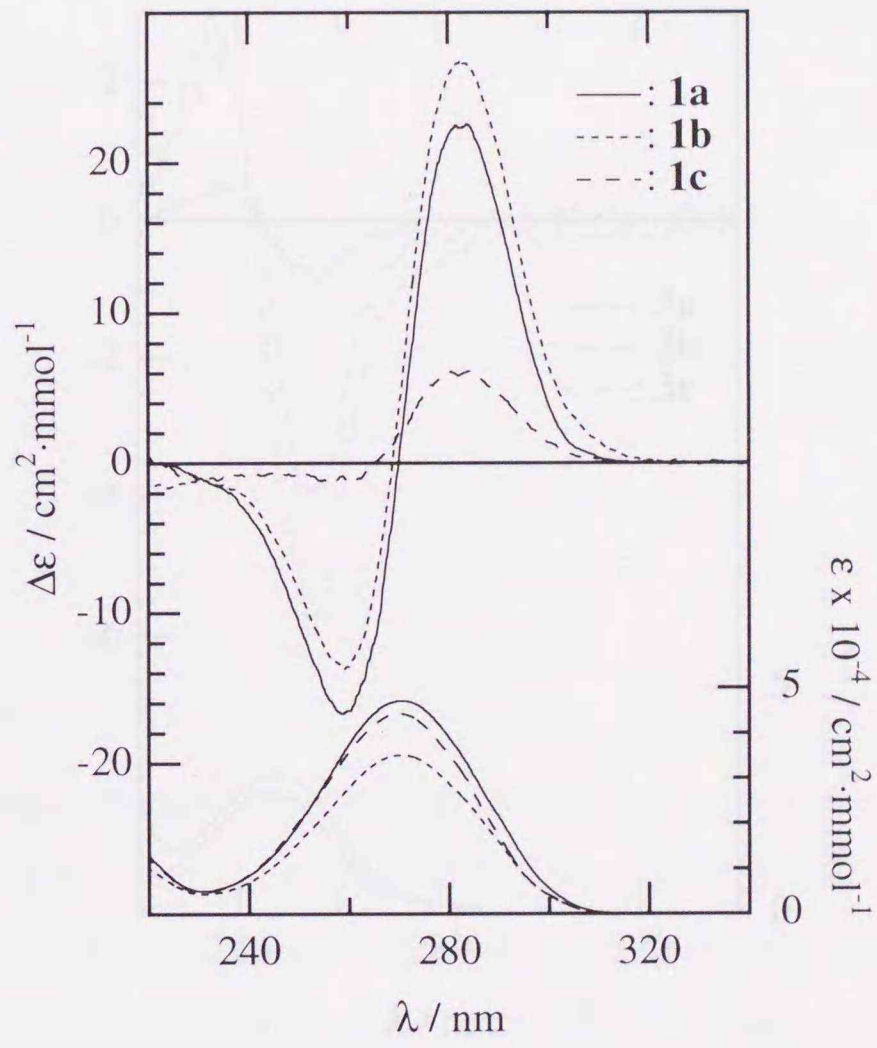

Figure 2.5. CD (upper) and UV (lower) spectra of monomers **1a** (solid line), **1b** (short broken line), and **3c** (broken line), recorded in HFIP at 21 °C using a path length of 5mm.

the CD spectra of polymers **3a-c** show the split Cotton effect with a negative first and a positive second Cotton effects (Figure 2.6). These CD spectra indicate that the adjacent two methyl benzoate units twist counterclockwise. On the assumption of the zigzag conformation under the conditions of CD spectral measurements, one would expect that polymer **3** favors a segmental distribution with a high contents of (*R*,*R*)-racemo benzoate diads. The templates having (*S*,*S*)-configuration, thus, induced the chirality of the (*R*,*R*)-racemo configuration in the main chain as summarized in Scheme 2.2.

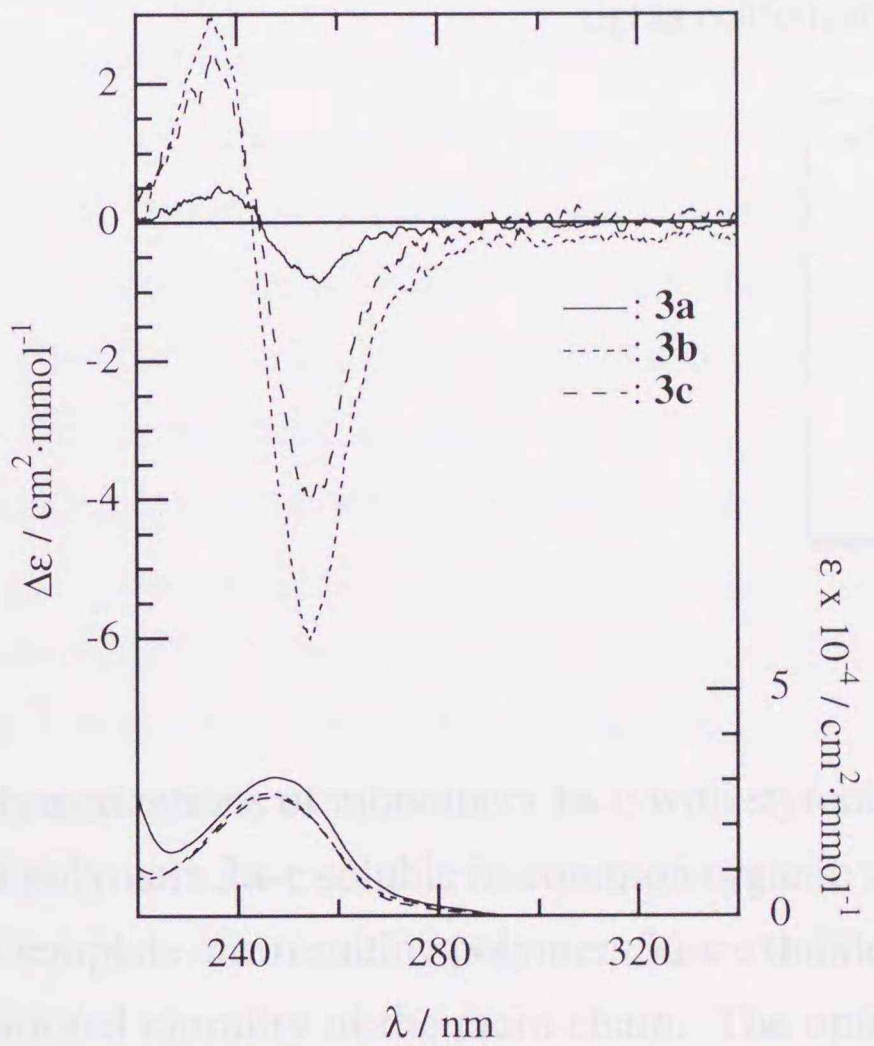

Figure 2.6. CD (upper) and UV (lower) spectra of polymers **3a** (f_1 = 0.11, solid line), **3b** (f_1 = 0.49, short broken line), and **3c** (f_1 = 0.24, broken line). The Δε and ε values were based on the concentration of the methyl benzoate diad unit.

Scheme 2.2

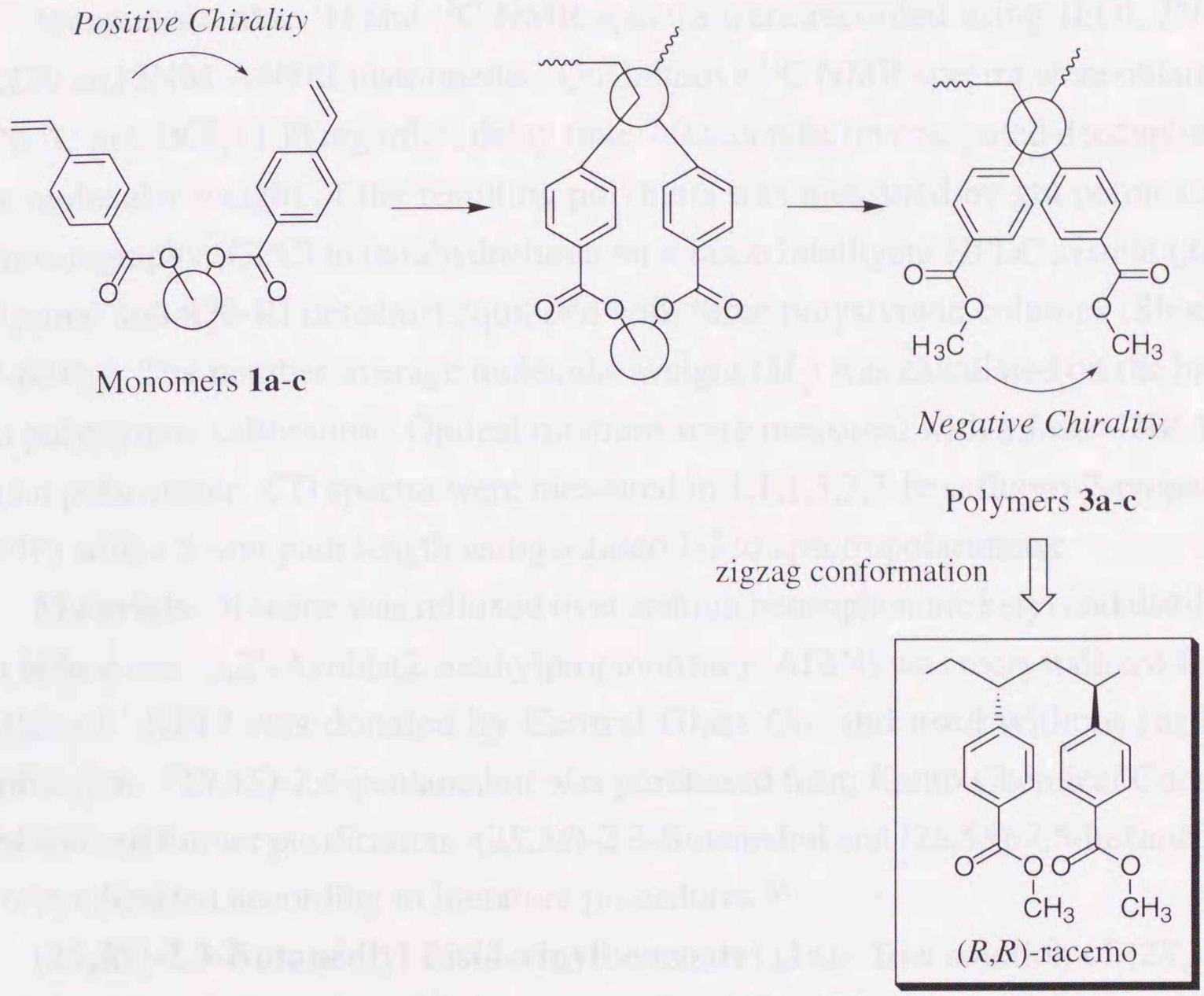

2.3 Conclusions

The cyclocopolymerizations of monomers **1a-c** with styrene proceeded without crosslinking to yield polymers **2a-c** soluble in common organic solvents. Even after removal of the chiral template, the resulting polymers **3a-c** exhibited an optical activity due to the configurational chirality of the main chain. The optical activity of **3a-c** was attributable to the isolated benzoate diad, and the chirality induction efficiency of the chiral template increased in the order of **a** < **c** < **b**, namely, 1,2-diol < 1,4-diol < 1,3-diol. According to the CD exciton chirality method, adjacent two methyl benzoate units predominately take an (*R*,*R*)-racemo configuration in polymers **3a-c**. Hence, the templates in monomer **1** transmitted its chirality to the main chain to form an enantiomeric (*R*,*R*)-racemo configuration in polymers **3a-c**.

2.4 Experimental Section

Measurements. ^{1}H and ^{13}C NMR spectra were recorded using JEOL JNM-EX270 and JNM-A400II instruments. Quantitative ^{13}C NMR spectra were obtained at 30 °C in $CDCl_3$ (100 mg·mL^{-1}; delay time 7.0 seconds; inverse gated decoupling). The molecular weight of the resulting polymers was measured by gel permeation chromatography (GPC) in tetrahydrofuran on a Jasco Intelligent HPLC system (880-PU pump and 830-RI detector) equipped with three polystyrene columns (Shodex KF-804L). The number-average molecular weight (M_n) was calculated on the basis of a polystyrene calibration. Optical rotations were measured with a Jasco DIP-140 digital polarimeter. CD spectra were measured in 1,1,1,3,3,3-hexafluoro-2-propanol (HFIP) with a 5 mm path length using a Jasco J-720 spectropolarimeter.

Materials. Toluene was refluxed over sodium benzophenone ketyl and distilled just before use. 2,2'-Azobis(2-methylpropionitrile) (AIBN) was recrystallized from methanol. HFIP was donated by Central Glass Co. and used without further purification. (2*S*,4*S*)-2,4-pentanediol was purchased from Kanto Chemical Co. and used without further purification. (2*S*,3*S*)-2,3-Butanediol and (2*S*,5*S*)-2,5-hexanediol were synthesized according to literature procedures.[5,6]

(2*S*,3*S*)-2,3-Butanediyl Bis(4-vinylbenzoate) (1a). To a solution of (2*S*,3*S*)-2,3-butanediol (8.6 g, 95 mmol) in dry pyridine (600 mL) was gradually added 4-vinylbenzoyl chloride (32.5 g, 195 mmol) at 5 - 10 °C, and then the mixture was heated at 80 °C with stirring for 4 hr. After dilution of the solution with water on cooling, the whole was stirred further for 1 hr and extracted with ether. The solvent was removed, and then the residue was purified by squat column chromatography on silica gel (Kiesel Gel 60) with hexane/diethyl ether (vol. ratio 3/1) to give **1a** as a white powder. Yield 24.3 g (69.3 mmol, 73 %). $[\alpha]_{435}$ = +72.2°, $[\alpha]_D$ = +30.8° ($CHCl_3$, 23 °C, *c* 1.0). ^{1}H NMR (270 MHz, $CDCl_3$): δ (ppm) = 7.99 (d, ^{3}J = 8.25 Hz, 4H, Ar), 7.43 (d, ^{3}J = 8.25 Hz, 4H, Ar), 6.74 (dd, $^{3}J_{trans}$ = 17.8 Hz, $^{3}J_{cis}$ = 10.9 Hz, 2H, =CH-), 5.84 (d, $^{3}J_{trans}$ = 17.2 Hz, 2H, $=CH_2$), 5.39-5.30 (m, 4H, $=CH_2$ and OCH), 1.42 (d, ^{3}J = 5.9 Hz, 6H, CH_3). ^{13}C NMR (67.8 MHz, $CDCl_3$): δ (ppm) =165.6 (C=O), 142.0, 129.9, 129.3, 126.0 (Ar), 135.9 (=CH-), 116.4 ($=CH_2$), 72.2 (OCH), 16.3 (CH_3). Anal. Calcd for $C_{22}H_{22}O_4$ (350.4): C 75.41; H 6.33. Found: C 67.84; H 6.16.

(2*S*,4*S*)-2,4-Pentanediyl Bis(4-vinylbenzoate) (1b). The same procedure as that for **1a** was applied to a mixture of (2*S*,4*S*)-2,4-pentanediol (4.2 g, 40 mmol) , 4-

vinylbenzoyl chloride (14 g, 84 mmol) and 200 mL of pyridine. The crude product was purified by column chromatography on silica gel (Kiesel Gel 60) with hexane/ethyl acetate (vol. ratio 15/85) to give **1b** as a sticky liquid. Yield 10.4 g (28.6 mmol, 71.5 %). $[\alpha]_{435}$ = +516.5°, $[\alpha]_D$ = +216.8° ($CHCl_3$, 23 °C, *c* 1.0). ^{1}H NMR (400 MHz, $CDCl_3$): δ (ppm) = 7.92 (d, ^3J = 8.4 Hz, 4H, Ar), 7.36 (d, ^3J = 8.3 Hz, 4H, Ar), 6.70 (dd, $^3J_{trans}$ = 17.6 Hz, $^3J_{cis}$ = 10.9 Hz, 2H, =CH-), 5.81 (d, $^3J_{trans}$ = 17.5 Hz, 2H, =CH_2), 5.33 (d, $^3J_{cis}$ = 10.8 Hz, 2H, =CH_2), 5.28-5.36 (m, 2H, OCH), 2.08 (t, ^3J = 6.3 Hz, 2H, CH_2), 1.40 (d, ^3J = 6.3 Hz, 6H, CH_3). ^{13}C NMR (100 MHz, $CDCl_3$): δ (ppm) = 165.6 (C=O), 141.7, 129.8, 129.6, 125.9 (Ar), 136.0 (=CH-), 116.3 (=CH_2), 68.2 (CH), 42.1 (CH_2), 20.5 (CH_3). Anal. Calcd for $C_{23}H_{24}O_4$ (364.4): C 75.79; H 6.64. Found: C 76.21; H6.79.

(2*S*,5*S*)-2,5-Hexanediyl Bis(4-vinylbenzoate) (1c). The same procedure as that for **1a** was applied to a mixture of (2*S*,5*S*)-2,5-hexanediol (4.3 g, 36 mmol) , 4-vinylbenzoyl chloride (18.3 g, 110 mmol) and 200 mL of pyridine. The crude product was purified by column chromatography on alumina with hexane/diethyl ether (vol. ratio 4/1), followed by recrystallization from hexane to give **1c** as a white powder. Yield 8.5 g (22.5 mmol, 62 %). $[\alpha]_{435}$ = +60.2°, $[\alpha]_D$ = +23.6° ($CHCl_3$, 23 °C, *c* 0.1). ^{1}H NMR (270 MHz, $CDCl_3$): δ (ppm) = 7.99 (d, ^3J = 8.2 Hz, 4H, Ar), 7.45 (d, ^3J = 8.2 Hz, 4H, Ar), 6.75 (dd, $^3J_{trans}$ = 17.5 Hz, $^3J_{cis}$ = 10.9 Hz, 2H, =CH-), 5.85 (d, $^3J_{trans}$ = 17.5 Hz, 2H, =CH_2), 5.37 (d, $^3J_{cis}$ = 10.9 Hz, 2H, =CH_2), 5.16-5.23 (m, 2H, CH), 1.94-1.66 (m, 4H, CH_2), 1.36 (d, ^3J = 6.3 Hz, 6H, CH_3). ^{13}C NMR (67.8 MHz, $CDCl_3$): δ (ppm) = 165.9 (C=O), 141.8, 129.8, 126.0 (Ar), 136.0 (-CH=), 116.4 (=CH_2), 71.1 (CH), 31.8 (CH_2), 20.0 (CH_3). Anal. Calcd. for $C_{24}H_{26}O_4$ (378.5): C 76.17; H 6.92. Found: C 76.10; H 6.98.

Cyclocopolymerization. The cyclocopolymerization of **1** with styrene was carried out using AIBN in toluene at 60 °C. After an appropriate time, the polymerization mixture was poured into methanol and the precipitate was filtered. The obtained white powder was purified by reprecipitation with chloroform-methanol and dried *in vacuo*.

Poly[(methyl 4-vinylbenzoate)-*co*-styrene] (3). The removal of the chiral template from polymers **2** was carried out using methanolic KOH. After neutralization with hydrochloric acid, the solution was dialyzed using a cellophane tube, and later concentrated by freeze-drying. The hydrolyzed copolymers were treated with diazomethane in benzene/ether, whereupon polymers **3** were obtained. The procedures

of dialysis and freeze-drying lowered the yields of **3** as shown in Table 1.

2.5 References

(1) Kelen, T.; Tüdös, F. *J. Macromol. Sci. Chem.* **1975**, *A9(1)*, 1.

(2) Mayo, F. R.; Lewis, F. M. *J. Amer. Chem. Soc.* **1944**, *66*, 1594.

(3) Ito, K.; Yamashita, Y. *J. Polym. Sci. Part A: Polym. Chem.* **1965**, *3*, 2165.

(4) Harada, N.; Nakanishi, K. *Circular Dichroic Spectroscopy Exciton Coupling in Organic Stereochemistry*; Oxford University Press: Oxford, U. K, **1983**.

(5) Schurig, V.; Koppenhoefer, B.; Buerkle, W. *J. Org. Chem.* **1980**, *45*, 538.

(6) Lieser, J. K. *Synth. Commun.* **1983**, *13*, 765.

Chapter 3

Stereoselectivity in Radical Cyclization of Bis(4-vinylbenzoate) having a Chiral Template.

3.1 Introduction

The previous chapter clarified that the chirality induction efficiency depended on the distance between two chiral centers in the chiral template. However, an unsettled question is how the distance between two chiral centers concerns with chirality induction. In order to resolve the question, it is necessary to construct the rational mechanism for chirality induction on the basis of a stereochemical distribution of the isolated benzoate diads.

The first report of the analysis of the stereochemical process for the asymmetric cyclocopolymerization was presented by Wulff and Küneweg.[1] The radical cyclizations of 3,4-*O*-cyclohexylidene-D-mannitol 1,2:5,6-bis-*O*-[(4-vinylphenyl)boronate] and 3,4-*O*-cyclohexylidene-D-mannitol 1,2:5,6-bis-*O*-[(4-vinylnaphthyl-1)boronate] were examined using an excess amount of radical initiator. However the excessive use of radical initiator induced the primary radical termination, namely, the recombination between the cyclized radical and the initiator. This reaction essentially differed from the intermolecular propagation in the radical cyclocopolymerization. The radical cyclization, therefore, must be designed to produce

Scheme 3.1

the suitable cyclic compound as the model of the constitutional repeating unit formed by the cyclopolymerization. The use of an appropriate chain transfer becomes the first step to solve the subject.

In this chapter, the radical cyclization of bis(4-vinylbenzoate) was examined using tri-*n*-butyltin hydride or allyltri-*n*-butyltin as a chain transfer reagent (Scheme 3.1). The stereoselectivities in the intramolecular cyclization and the intermolecular addition were discussed on the basis of a distribution of stereoisomers of the obtained cyclic unimer.

3.2 Results and Discussion

3.2.1 Radical Cyclization using Tri-n-butyltin Hydride

The radical cyclizations of monomers **1a-f** were carried out using benzyl bromide, AIBN, and tri-*n*-butyltin hydride as a chain transfer reagent (Scheme 3.2). Reaction profile is described as follows (see Scheme 3.1). (1) An isobutyronitrile radical due to thermal homolysis of AIBN reacts with benzyl bromide to generate the benzyl radical which is a model for a propagating species in the polymerization. (2) The benzyl radical attacks one of the vinyl groups in the monomer to form an intermediate radical **4** (The monomer has C_2 symmetry and the two vinyl groups are equal in reactivity). (3) Radical **4** attacks the other vinyl groups to form a cyclized radical **5**

Scheme 3.2

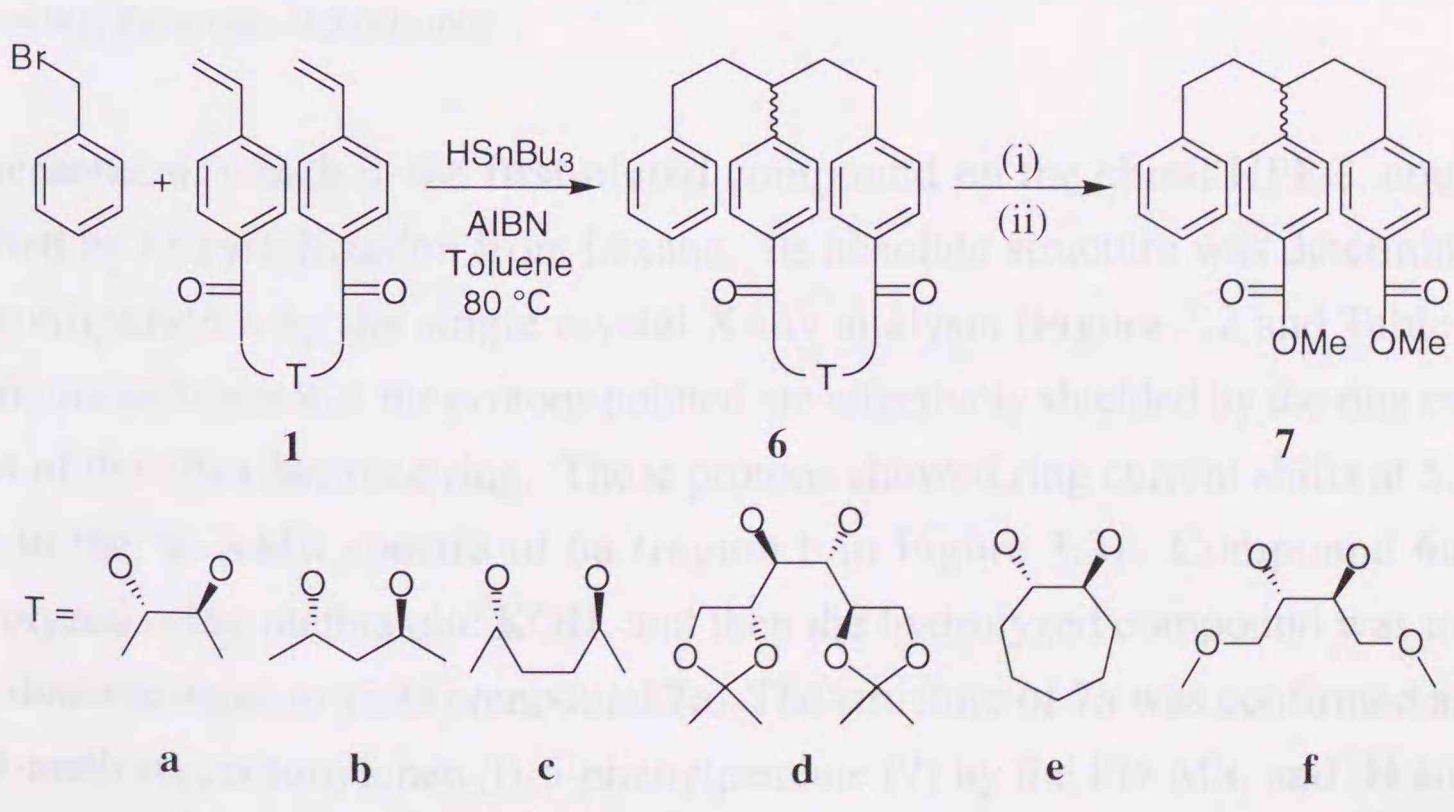

1 **6** **7**

a **b** **c** **d** **e** **f**

Conditions: (i) KOH / MeOH, reflux, (ii) CH_2N_2 / Ether

with a chiral center. (4) Radical **5** leads to form the cyclic compound **6** through the reaction with tri-*n*-butyltin hydride. Although radical **5** tends to attack another monomer to yield the higher oligomers and polymers, tri-*n*-butyltin hydride as a chain transfer reagent depress the undesirable tendency.

3.2.2 Structural Elucidation for Stereochemical Analysis

Compound **6a**, which consisted of two diastereomers, was isolated from the reaction mixture using preparative HPLC. Moreover, its diastereomers could be separate into two parts using chiral HPLC (Figure 3.1). In addition, one of the

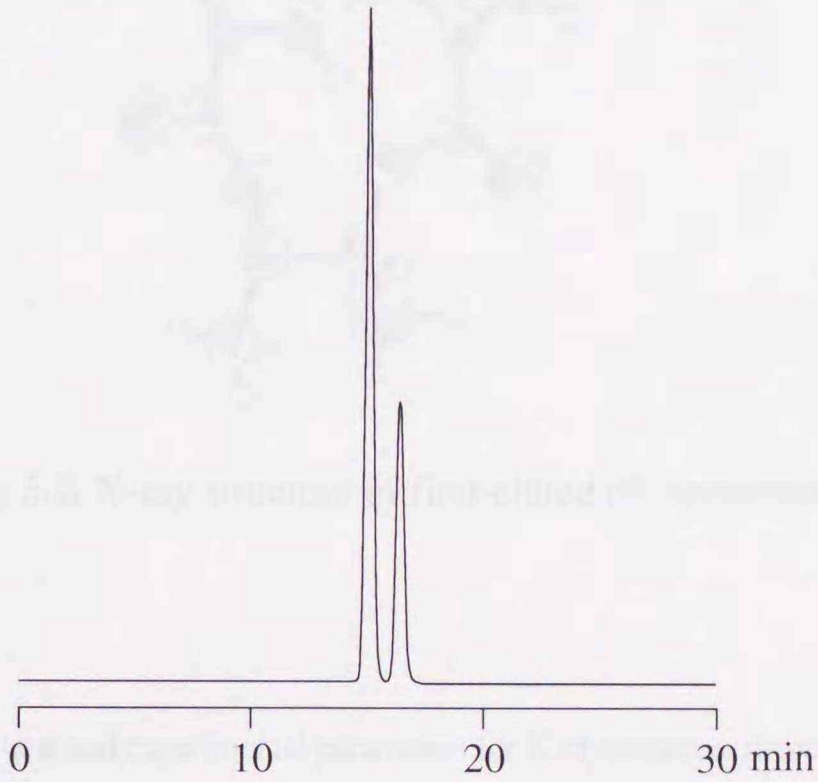

Figure 3.1. Chromatogram of **6a**. Column, CHIRALCEL OD; eluent, hexane/2-propanol = 9/1; flow rate, 0.5 mL·min^{-1}.

diastereomers, which is the first-eluted compound on the chiral HPLC, could be purified by recrystallization from hexane. Its absolute structure was determined as (*R*)-configuration by the single crystal X-ray analysis (Figure 3.2 and Table 3.1). The figure indicates that the protons pointed are effectively shielded by the ring current effect of the other benzene ring. These protons showed ring current shifts at 5.8-6.5 ppm in the ^{1}H NMR spectra of **6a** (region b in Figure 3.3). Compound **6a** was hydrolyzed using methanolic KOH, and then the hydrolyzed compound was treated with diazomethane to yield compound **7a**. The structure of **7a** was confirmed as 1,3-bis(4-methoxycarbonylphenyl)-5-phenylpentane (**7**) by the FD-MS, and ^{1}H and ^{13}C NMR spectra as shown in Figure 3.4 as well as the single crystal X-ray analysis of

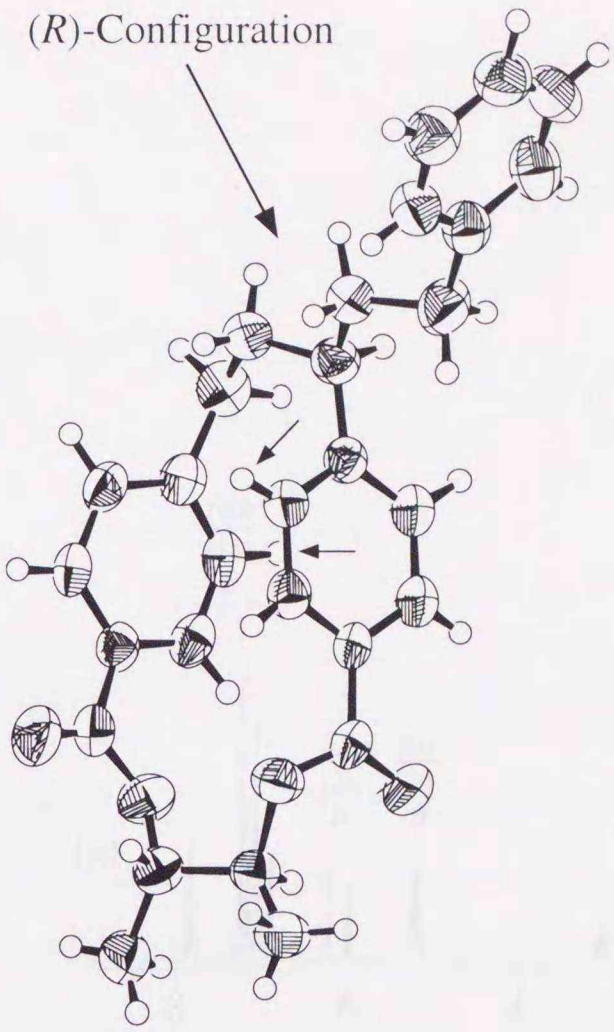

Figure 3.2. X-ray structure of first-eluted diastereomer of **6a**.

Table 3.1. Crystal data and experimental parameters for X-ray structure determination of first-eluted diastereomer **6a**.

crystal data		experimental parameters	
molecular formura	$C_{29}H_{30}O_4$	radiation	CuKα (λ = 1.54178 Å)
molecular weight	442.55	scan type	ω - 2θ
crystal system	orthorhombic	scan rate / deg·min^{-1}	8.0 (up to 3 scans)
space group	$P2_12_12_1$	scan width / deg	1.15 + 0.30tan θ
crystal size / mm	0.40 x 0.50 x 0.40	2θ range	47.5 - 60.0°
a / Å	10.1725(9)	no. of unique data	2486 (R_{int} = 0.029)
b / Å	25.615(2)	no. of obsd data	2201
c / Å	9.257(1)	no. of variables	419
V / Å^3	2412.2(3)	*R*	0.047
Z	4	R_w	0.063
D_{calcd} / g·cm^{-3}	1.219	goodness of fit	1.02

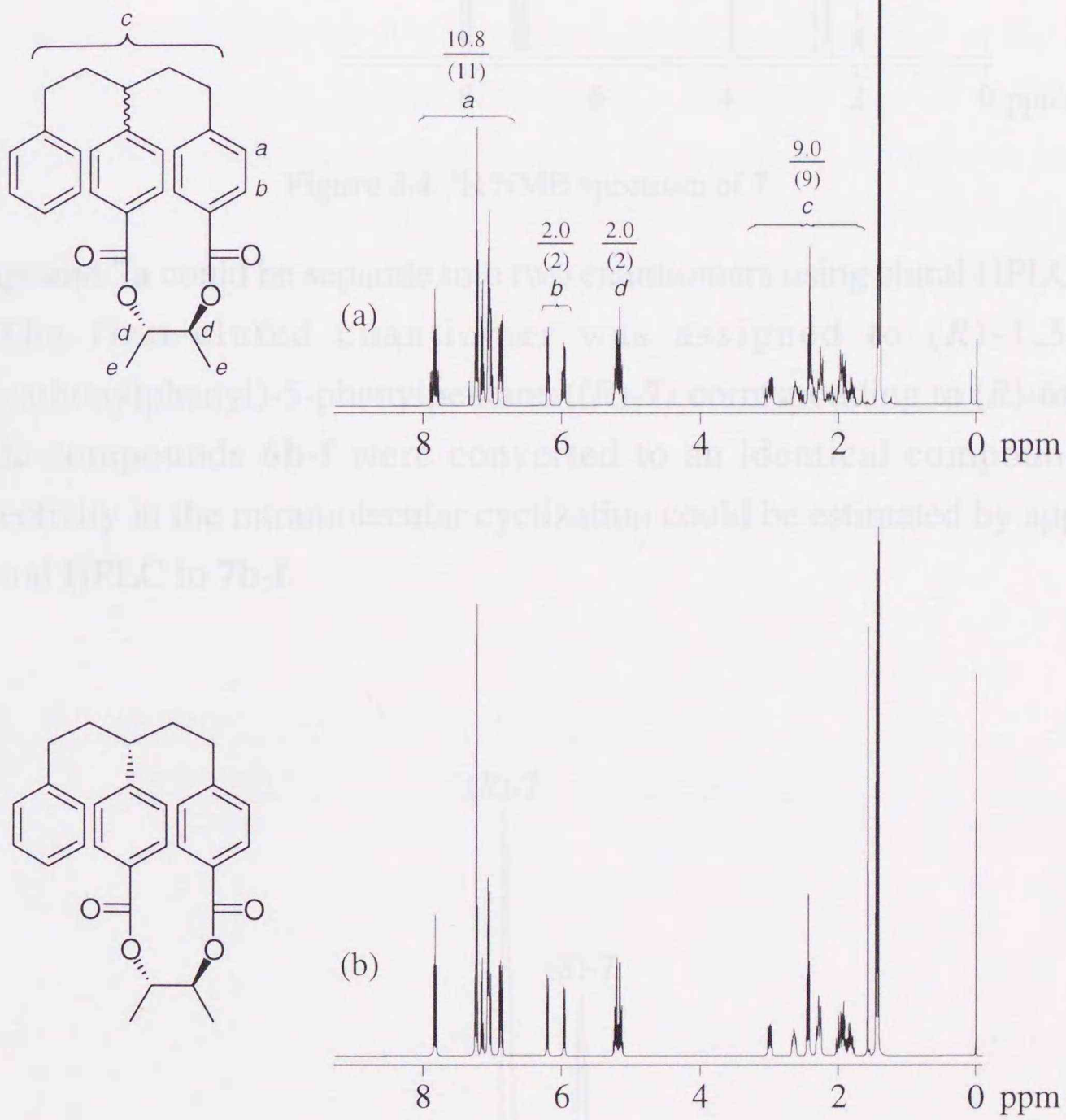

Figure 3.3. ^{1}H NMR spectra of diastereomeric mixture (a) and first-eluted diastereomer of **6a** (b).

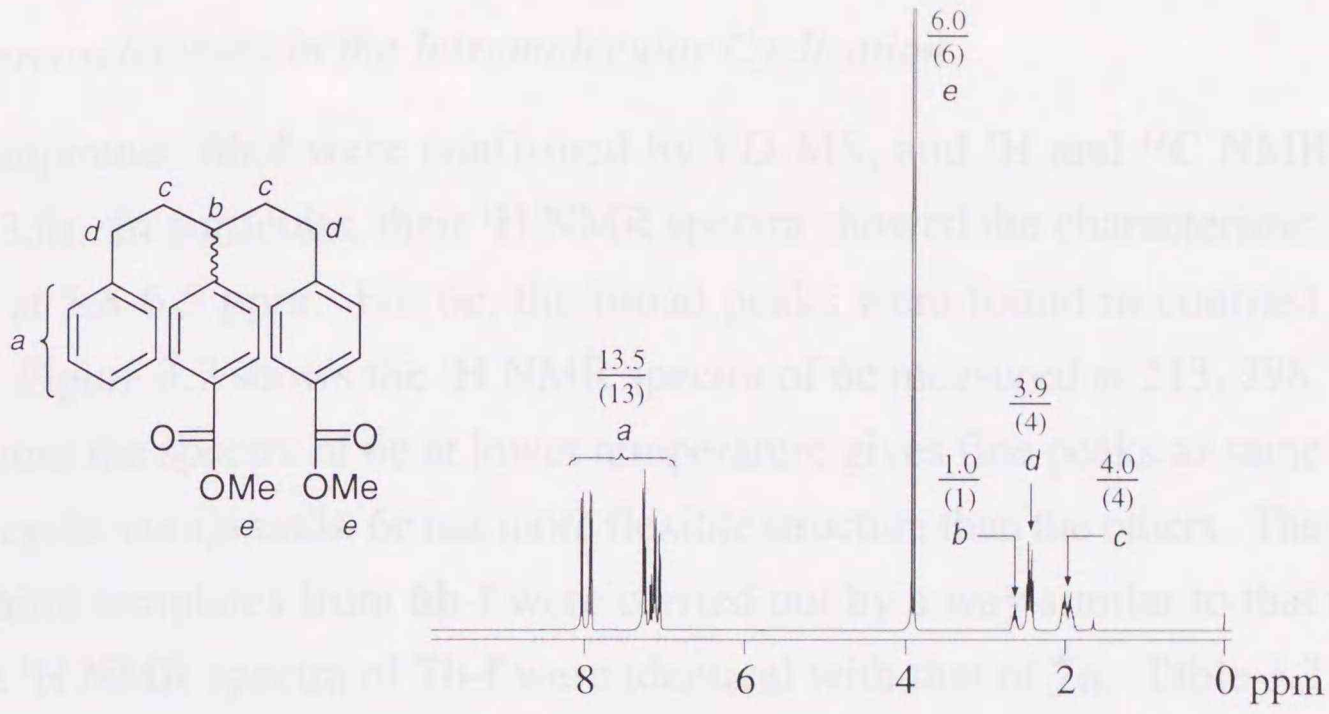

Figure 3.4. ^{1}H NMR spectrum of **7**.

6a. Compound **7a** could be separate into two enantiomers using chiral HPLC (Figure 3.5). The first-eluted enantiomer was assigned to (*R*)-1,3-bis(4-methoxycarbonylphenyl)-5-phenylpentane ((*R*)-**7**) corresponding to (*R*)-**6a**. Since the cyclic compounds **6b-f** were converted to an identical compound **7**, the stereoselectivity in the intramolecular cyclization could be estimated by application of the chiral HPLC to **7b-f**.

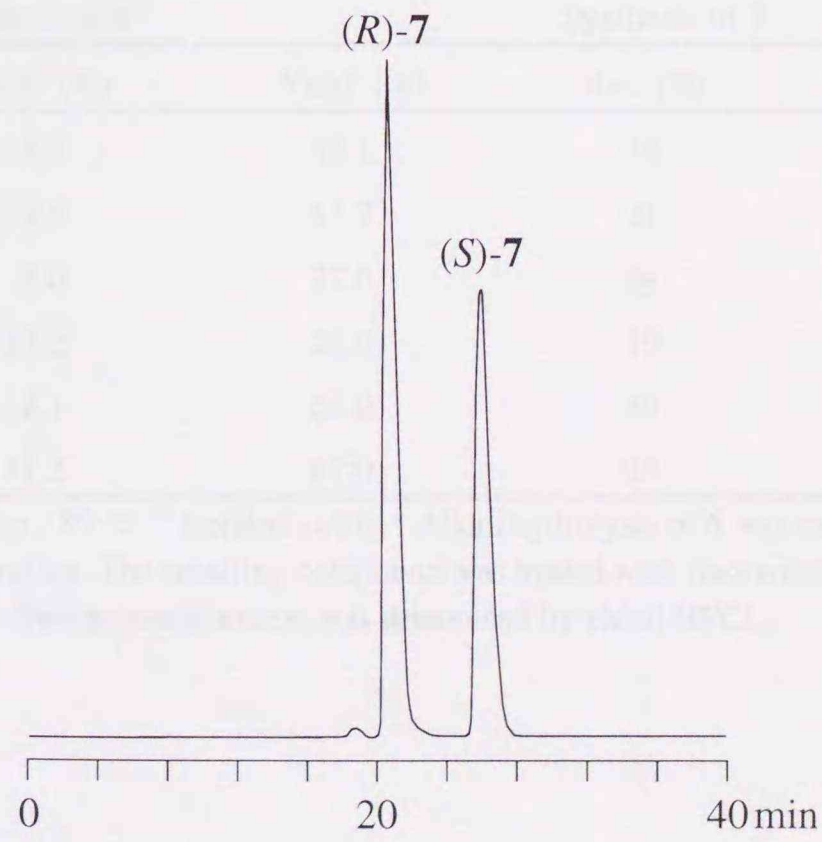

Figure 3.5. Optical resolution of **7a**. Column, CHIRALCEL OD; eluent, hexane/2-propanol = 8/2; flow rate, 0.5 mL·min^{-1}.

3.2.3 Stereoselectivity in the Intramolecular Cyclization

Compounds **6b-f** were confirmed by FD-MS, and ^{1}H and ^{13}C NMR spectra (Figure 3.6). In particular, their ^{1}H NMR spectra showed the characteristic shielded protons at 5.8-6.5 ppm. For **6c**, the broad peaks were found in contrast to other spectra. Figure 3.7 shows the ^{1}H NMR spectra of **6c** measured at 213, 298, and 313 K. Because the spectra of **6c** at lower temperature gives fine peaks as same as those of other cyclic compounds, **6c** has more flexible structure than the others. The removal of the chiral templates from **6b-f** were carried out by a way similar to that used for **6a**. The ^{1}H NMR spectra of **7b-f** were identical with that of **7a**. Table 3.2 lists the results of the radical cyclization using tri-*n*-butyltin hydride. Monomers **1a**, **1b**, **1c**, **1e**, and **1f** preferentially formed the cyclic compounds **7** with an (*R*)-configuration rather than a (*S*)-configuration. Monomer **1d** showed the stereoselectivity opposite to the other monomers. These results agree with the cyclocopolymerization results. The extent of stereoselectivity in the intramolecular cyclization was varied from 19 to 39 % d.e.

Table 3.2. Results of radical cyclization using tri-*n*-butyltin hydride.

	Synthesis of **6**[a]	Synthesis of **7**[c]		
Monomer	Yield[b] (%)	Yield[d] (%)	d.e.[e] (%)	Major Configuration
1a	13.9	52.1	34	(*R*)
1b	19.5	53.7	21	(*R*)
1c	8.6	72.0	24	(*R*)
1d	13.2	28.0	19	(*S*)
1e	12.1	62.0	39	(*R*)
1f	11.2	87.0	27	(*R*)

[a] Solvent, toluene; temp., 80 °C. [b] Isolated yields. [c] Alkali hydrolysis of **6** was carried out using KOH in aqueous MeOH under reflux. The resulting compound was treated with diazomethane in ether to yield **7**. [d] Isolated yields. [e] The diastereomeric excess was determined by chiral HPCL.

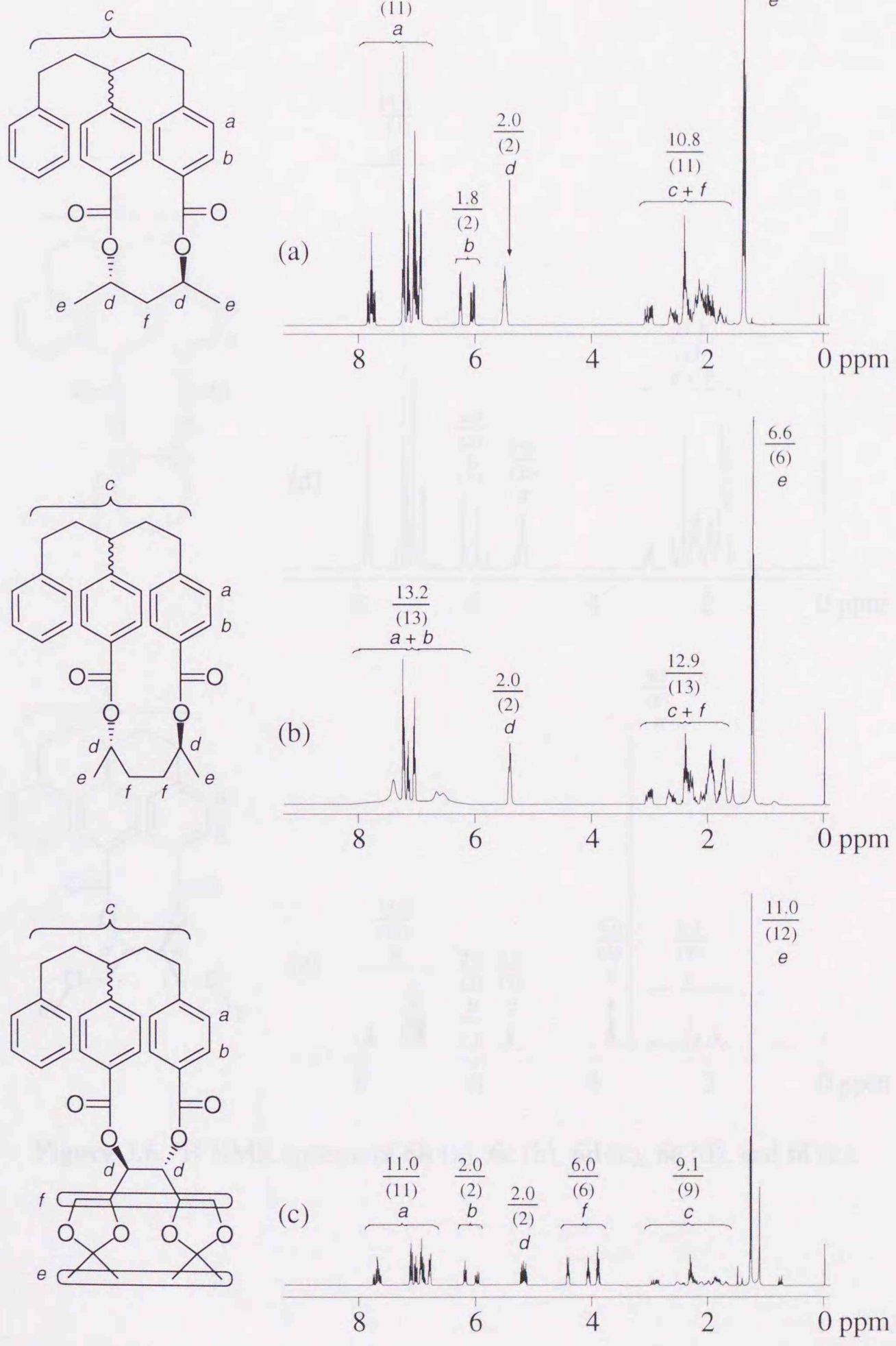
c
a
b
d
e
f
(a)
11.5
(11)
a
1.8
(2)
b
2.0
(2)
d
10.8
(11)
c + f
5.9
(6)
e
8
6
4
2
0 ppm
(b)
13.2
(13)
a + b
2.0
(2)
d
12.9
(13)
c + f
6.6
(6)
e
(c)
11.0
(11)
a
2.0
(2)
b
2.0
(2)
d
6.0
(6)
f
9.1
(9)
c
11.0
(12)
e

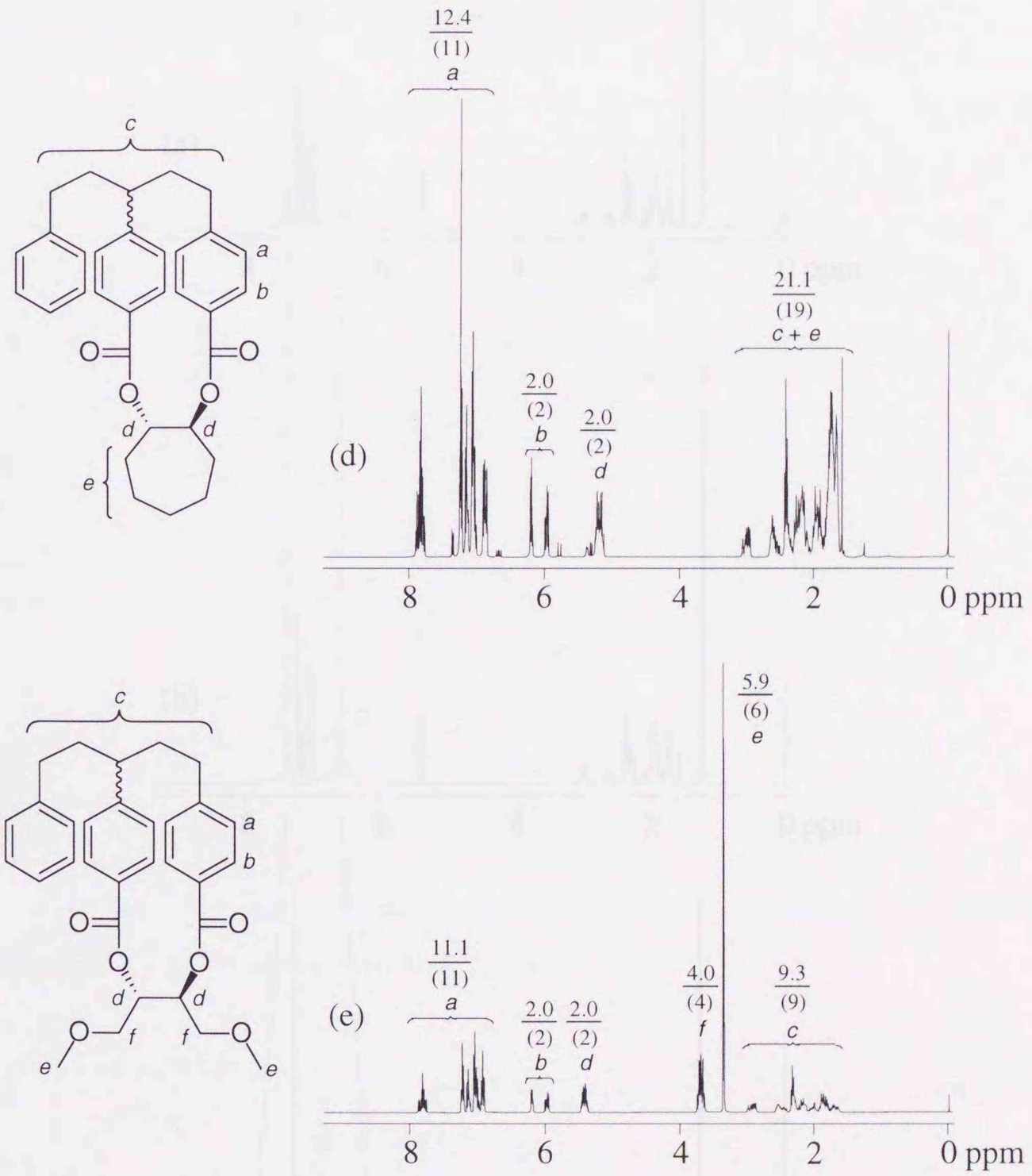

Figure 3.6. ^{1}H NMR spectra of **6b** (a), **6c** (b), **6d** (c), **6e** (d), and **6f** (e).

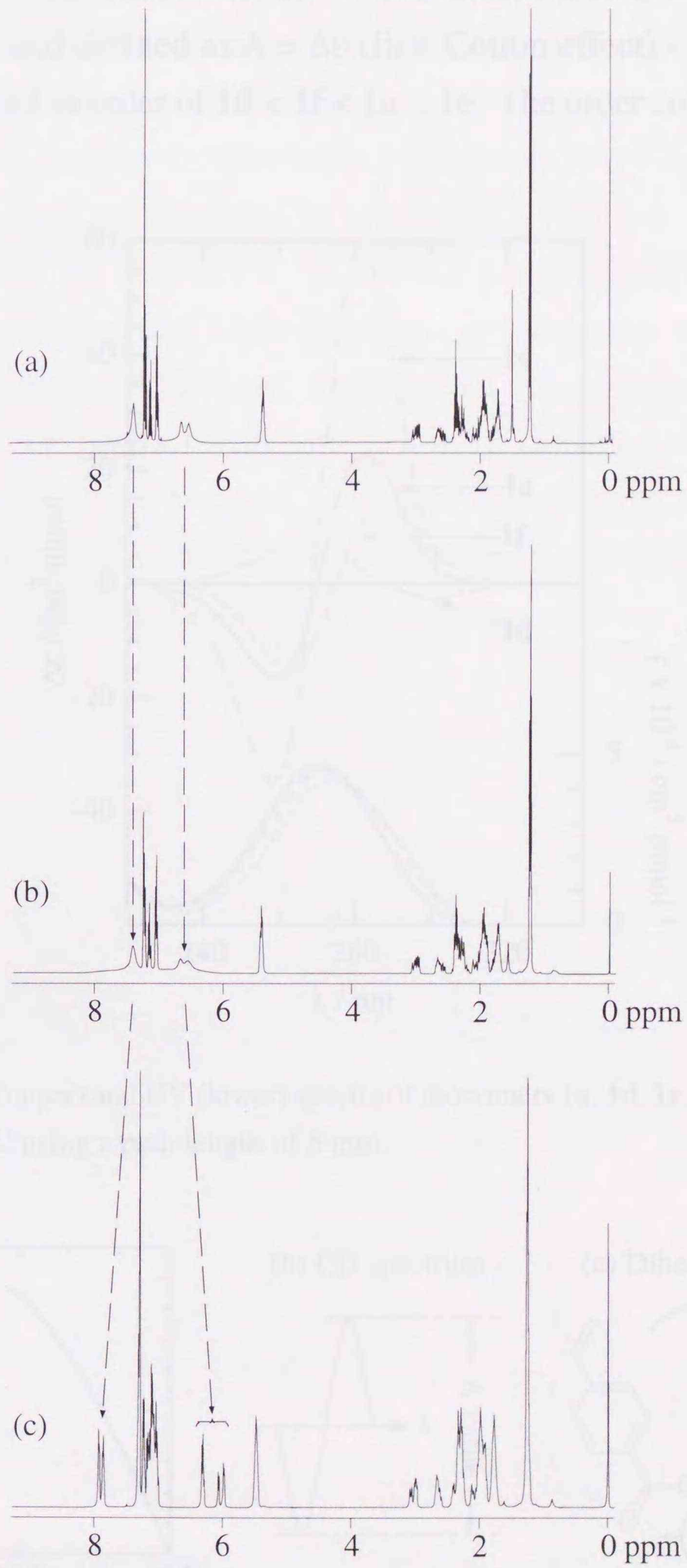

Figure 3.7. ^{1}H NMR spectra of **6c** recorded at 313 (a), 298 (b), and 213 K (c).

The chirality induction in the intramolecular cyclization should be attributable to the chiral twist of two 4-vinylbenzoyl groups. Figure 3.8 shows the CD and UV spectra of monomers **1a**, **1d**, **1e**, and **1f**. The A value, which is characteristics of the split Cotton effect and defined as A = Δε (first Cotton effect) - Δε (second Cotton effect), was increased in order of **1d** < **1f** < **1a** < **1e**. The order coincided with that of

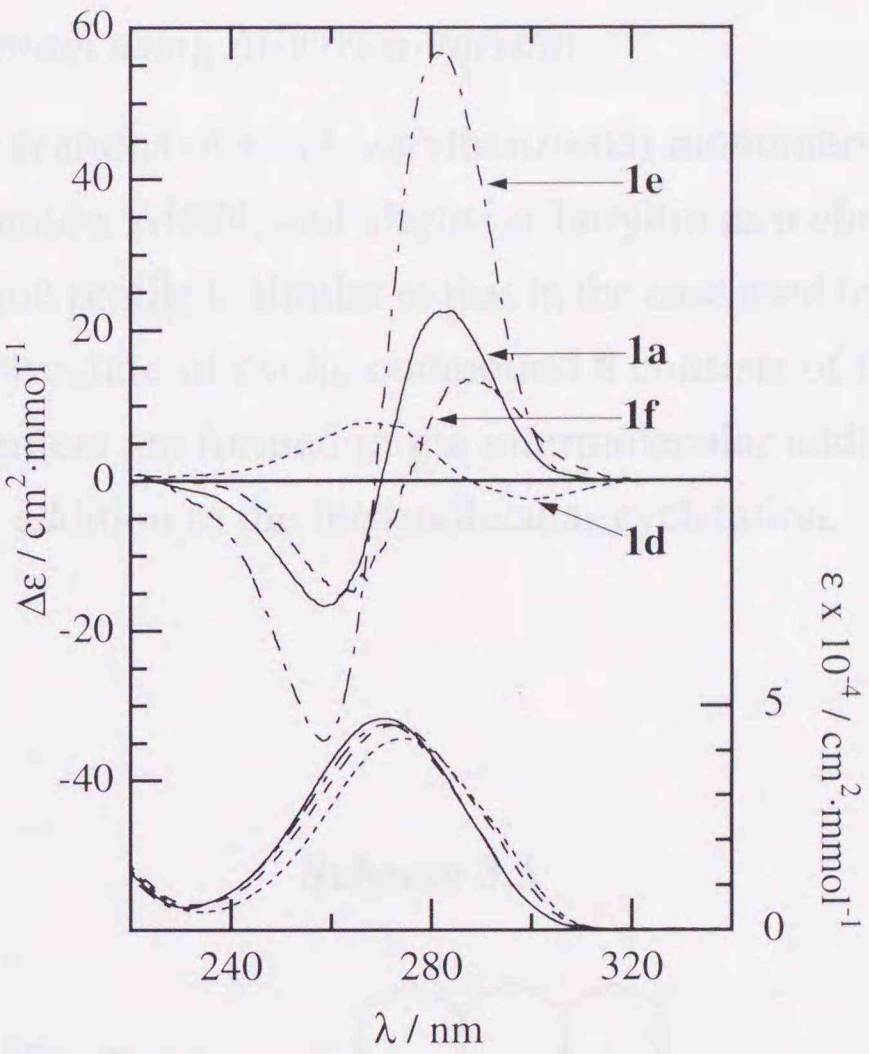

Figure 3.8. CD (upper) and UV (lower) spectra of monomers **1a**, **1d**, **1e**, and **1f**, recorded in HFIP at 21 °C using a path length of 5 mm.

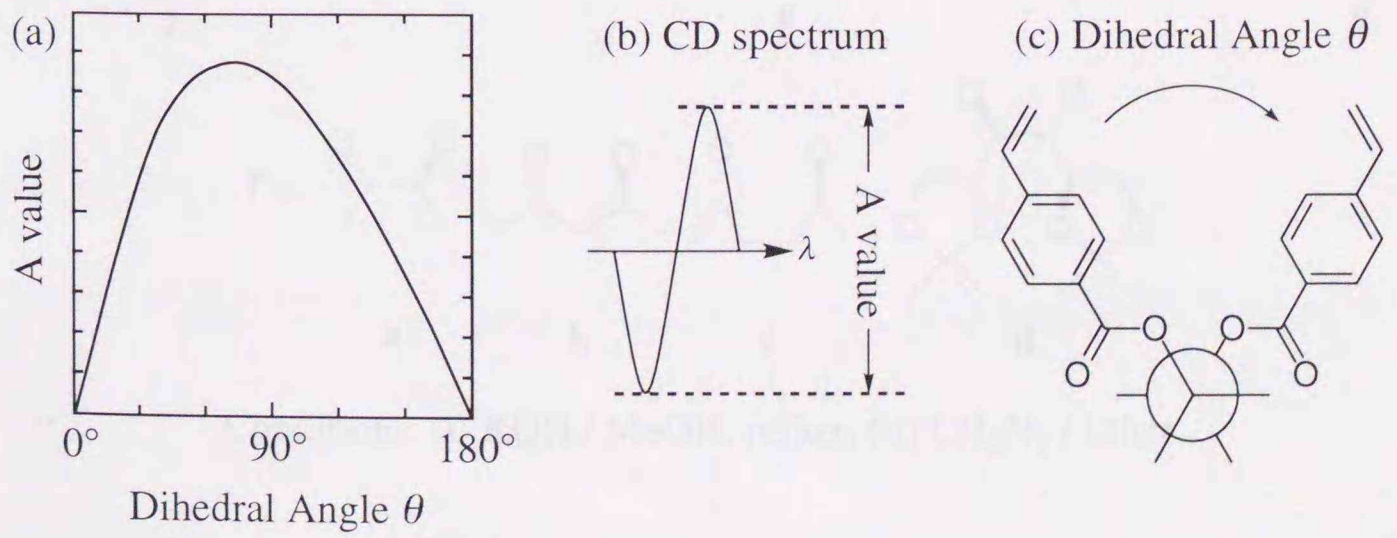

Figure 3.9. Angular dependence of the A value of split Cotton effect (a) with definitions of the A value on the ordinate (b) and of the dihedral angle θ on the abscissa (c).

stereoselectivity for the intramolecular cyclization, i.e., **1d** (19 % d.e.) < **1f** (27 % d.e.) < **1a** (34 % d.e.) < **1e** (39 % d.e.). Since monomers **1a**, **1d**, **1e**, and **1f** are the 4-vinylbenzoates of 1,2-diols, the A value only depends on a dihedral angle between two 4-vinylbenzoyl groups. The angular dependence of the A value is illustrated in Figure 3.9. Consequently, the stereoselectivity in the intramolecular cyclization was improved with an increase in the dihedral angle between two 4-vinylbenzoyl groups.

3.2.4 Radical Cyclization using Allyltri-n-butyltin

The radical cyclizations of bis(4-vinylbenzoate) monomers **1a-d** were carried out using benzyl bromide, AIBN, and allyltri-*n*-butyltin as a chain transfer reagent (Scheme 3.3). Reaction profile is similar to that in the case used tri-*n*-butyltin hydride (Scheme 3.1). The structure of cyclic compound **8** consists of four stereoisomeric forms. The chiral centers are formed in the intermolecular addition of radical **5** to allyltri-*n*-butyltin, in addition to the intramolecular cyclization.

Scheme 3.3

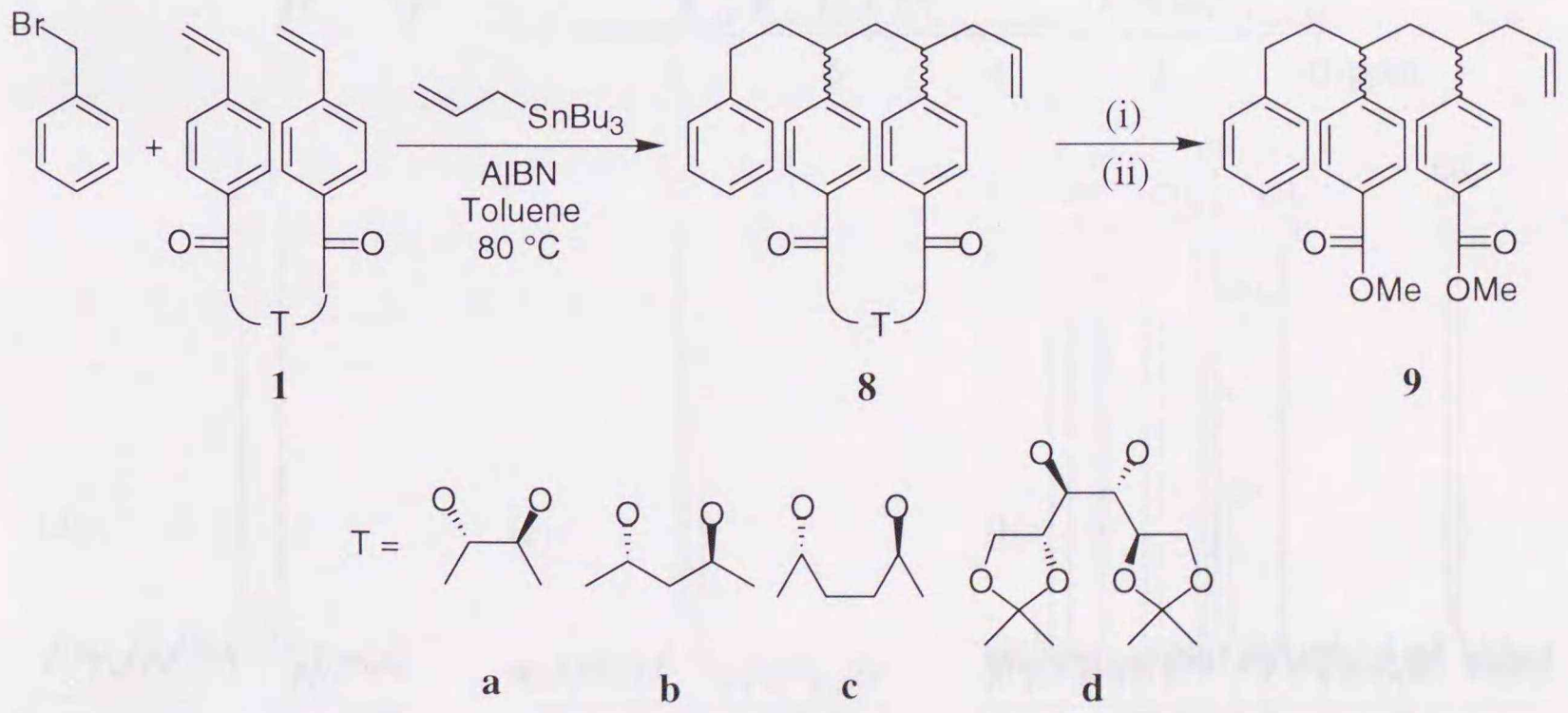

Conditions: (i) KOH / MeOH, reflux, (ii) CH_2N_2 / Ether

3.2.5 Structural Elucidation for Stereochemical Analysis

Cyclic compound **8a** containing four stereoisomers was obtained from the reaction mixture using preparative HPLC, and confirmed by the FD-MS, ^{1}H and ^{13}C NMR spectra (Figure 3.10). The shielded protons characteristically appeared at 5.8-6.5 ppm in analogy with the case of **6a**. The olefinic carbons were found as peaks at 116 and 136 ppm in the ^{13}C NMR spectrum. Cyclic compound **8a** was hydrolyzed using methanolic KOH, and then the resulting compound was treated with diazomethane to yield compound **9a**. This compound **9a** should consist of four stereoisomers as shown in Chart 3.1. The chiral HPLC, therefore, was used for the

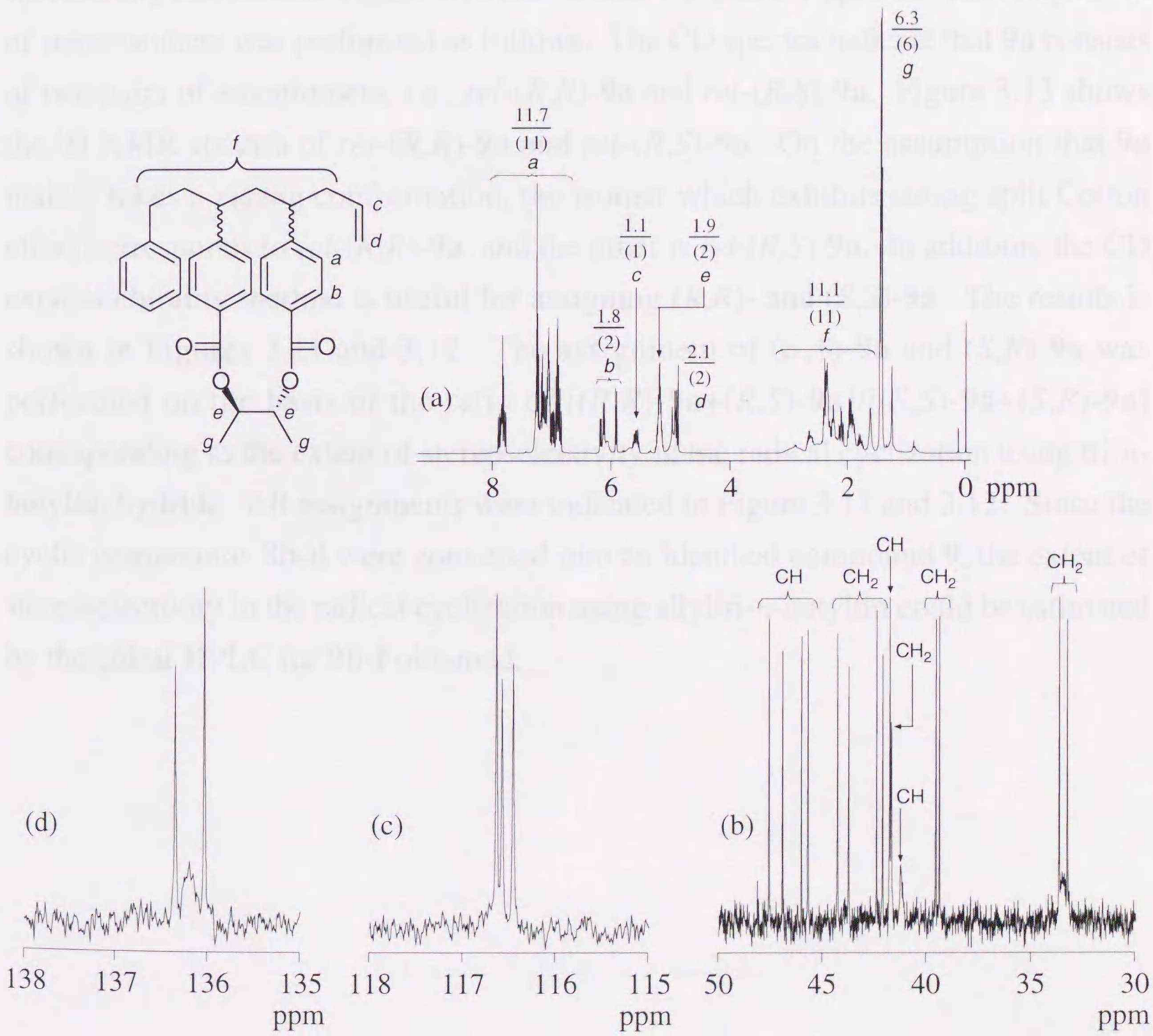

Figure 3.10. ^{1}H NMR spectrum of **8a** (a) and expanded ^{13}C NMR spectra of **8a** in the main chain region (b), in the allyl methylene region (c), and in the allyl methine region (d).

Chart 3.1

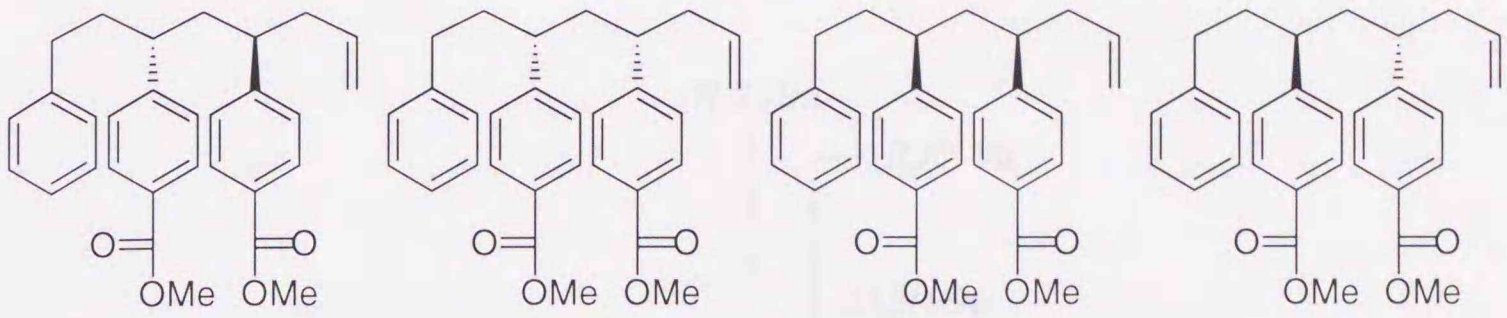

(*R*,*R*)-**9** (*R*,*S*)-**9** (*S*,*R*)-**9** (*S*,*S*)-**9**

separation of these stereoisomers. The resolution in the chromatogram of **9a** is satisfactory, as shown in Figure 3.11. The isolation of each stereoisomer also was successfully carried out. Figure 3.12 shows their CD and UV spectra. The assignment of stereoisomers was performed as follows: The CD spectra indicate that **9a** consists of two pairs of enantiomers, i.e., *rel*-(*R*,*R*)-**9a** and *rel*-(*R*,*S*)-**9a**. Figure 3.13 shows the ^{1}H NMR spectra of *rel*-(*R*,*R*)-**9a** and *rel*-(*R*,*S*)-**9a**. On the assumption that **9a** mainly takes a zigzag conformation, the isomer which exhibits strong split Cotton effect corresponds to *rel*-(*R*,*R*)-**9a**, and the other is *rel*-(*R*,*S*)-**9a**. In addition, the CD exciton chirality method is useful for assigning (*R*,*R*)- and (*S*,*S*)-**9a**. The results is shown in Figures 3.11 and 3.12. The assignment of (*R*,*S*)-**9a** and (*S*,*R*)-**9a** was performed on the basis of the ratio of [(*R*,*R*)-**9a**+(*R*,*S*)-**9a**]/[(*S*,*S*)-**9a**+(*S*,*R*)-**9a**] corresponding to the extent of stereoselectivity in the radical cyclization using tri-*n*-butyltin hydride. All assignments were indicated in Figure 3.11 and 3.12. Since the cyclic compounds **8b-d** were converted into an identical compound **9**, the extent of stereoselectivity in the radical cyclization using allyltri-*n*-butyltin could be estimated by the chiral HPLC for **9b-f** obtained.

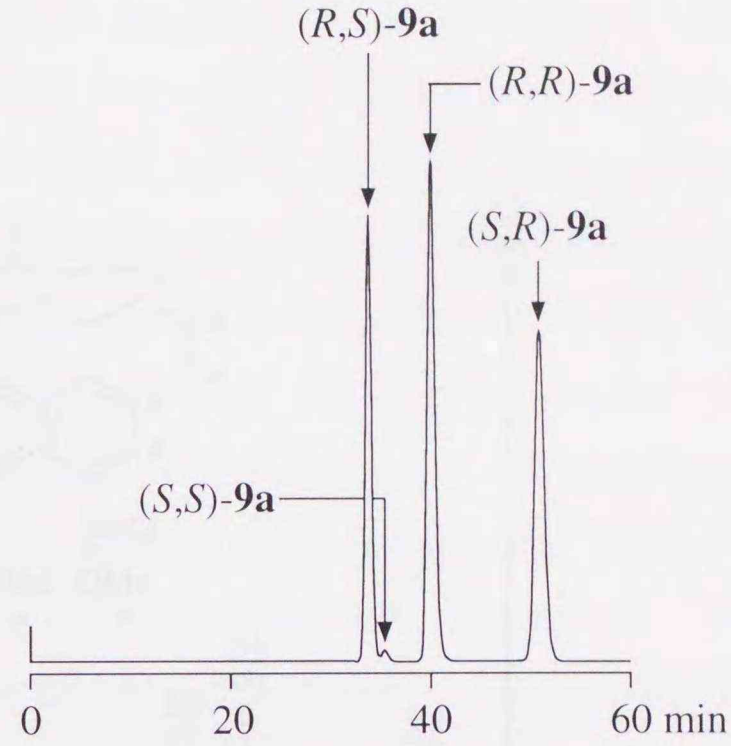

Figure 3.11. Separation of **9a** into each stereoisomer. Column, CHIRALCEL OD; eluent, hexane/2-propanol = 9/1; flow rate, 0.2 mL·min^{-1}.

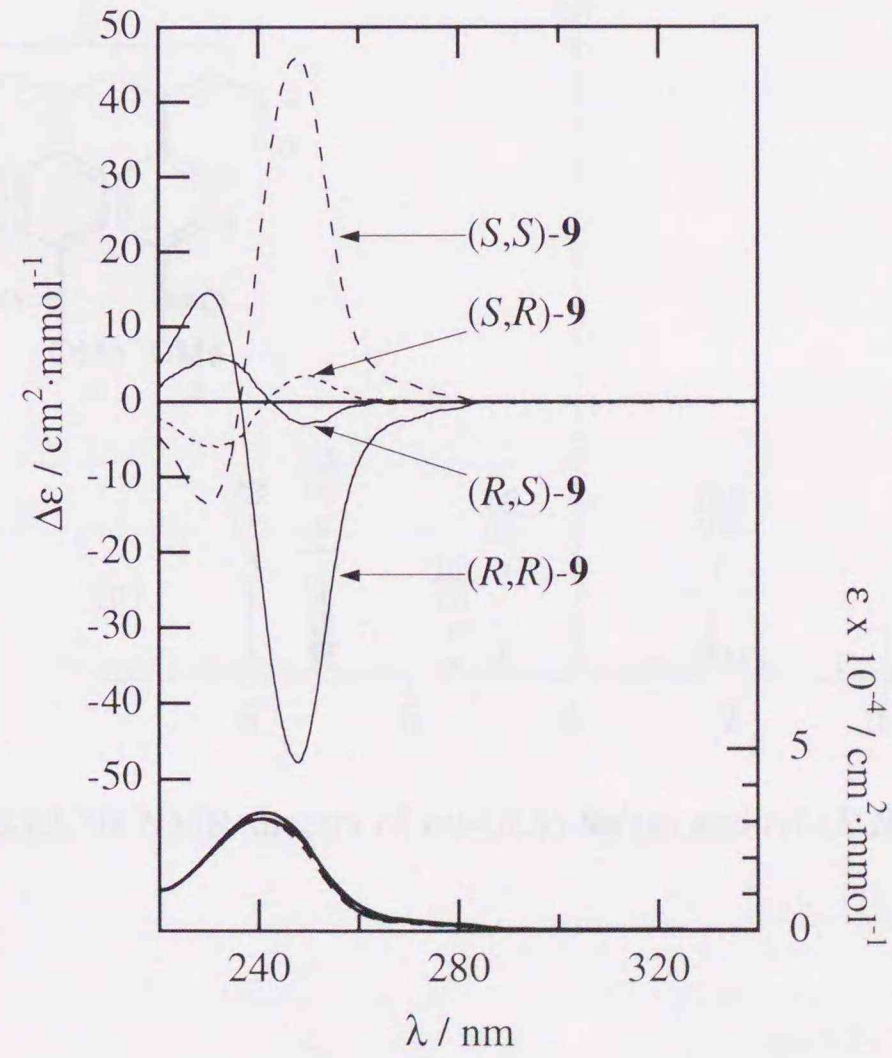

Figure 3.12. CD (upper) and UV (lower) spectra of isolated stereoisomer of **9a**, recorded in acetonitrile at 21 °C using a path length of 5 mm.

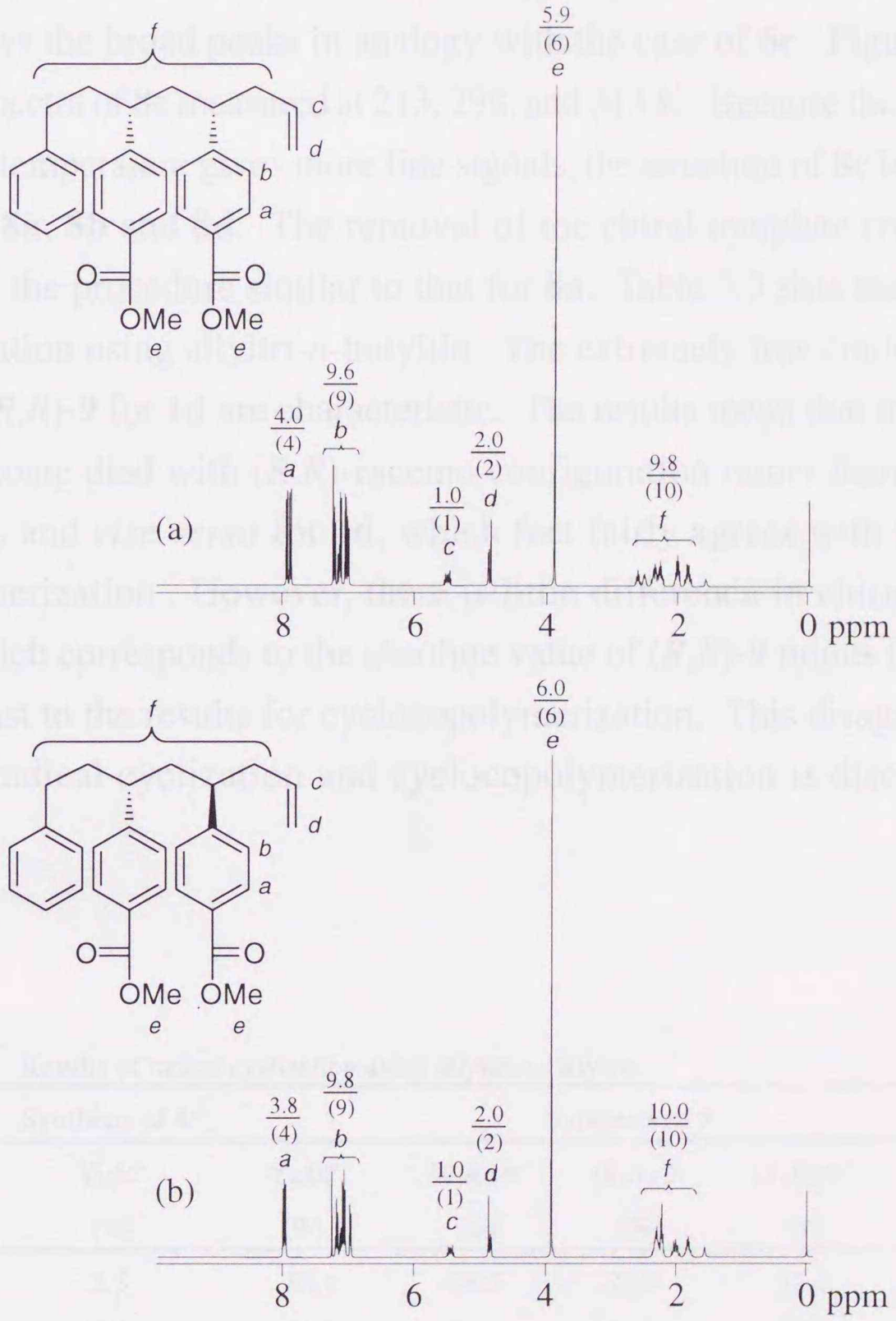

Figure 3.13. ^{1}H NMR spectra of *rel*-(*R*,*S*)-**9a** (a) and *rel*-(*R*,*R*)-**9a** (b).

3.2.6 Stereoselectivity in the Overall Process

Cyclic compounds **8b-d** were confirmed by the FD-MS, ^{1}H and ^{13}C NMR spectra (Figure 3.14). In particular, the characteristic peaks due to shielded protons and the peaks due to vinyl carbons were observed at 5.8-6.5 ppm in ^{1}H NMR spectra and at 116 and 136 ppm in ^{13}C NMR spectra of **8b-d**, respectively. For **8c**, the ^{1}H NMR spectrum shows the broad peaks in analogy with the case of **6c**. Figure 3.15 shows the ^{1}H NMR spectra of **8c** measured at 213, 298, and 313 K. Because the measurements of **8c** at lower temperature gives more fine signals, the structure of **8c** is more flexible than those of **8a**, **8b** and **8d**. The removal of the chiral template from **8b-d** were carried out by the procedure similar to that for **8a**. Table 3.3 lists the results of the radical cyclization using allyltri-*n*-butyltin. The extremely low contents of (*S*,*S*)-**9** for **1a-c** and (*R*,*R*)-**9** for **1d** are characteristic. The results mean that monomers **1a-c** form the benzoate diad with (*R*,*R*)-racemo configuration rather than (*S*,*S*)-racemo configuration, and *vise versa* for **1d**, which fact fairly agrees with the results for cyclocopolymerization. However, there is little difference in chirality induction efficiency, which corresponds to the absolute value of (*R*,*R*)-**9** minus (*S*,*S*)-**9**, among **1a-d** in contrast to the results for cyclocopolymerization. This disagreement result between the radical cyclization and cyclocopolymerization is discussed in later chapters.

Table 3.3. Results of radical cyclization using allyltri-*n*-butyltin.

Monomer	Synthesis of **8**[a]	Synthesis of **9**[c]				
	Yield[b] (%)	Yield[d] (%)	(*R*,*R*)-**9**[e] (%)	(*R*,*S*)-**9**[e] (%)	(*S*,*R*)-**9**[e] (%)	(*S*,*S*)-**9**[e] (%)
1a	2.3	88.1	38.5	27.9	32.8	0.8
1b	5.4	88.3	39.0	16.9	43.8	0.3
1c	4.0	90.2	39.9	22.6	36.7	0.8
1d	3.9	89.3	0.6	36.4	22.2	40.8

[a] Solvent, toluene; temp., 80 °C. [b] Isolated yields. [c] Alkali hydrolysis of **6** was carried out using KOH in aqueous MeOH under reflux. The resulting compound was treated with diazomethane in ether to yield **7**. [d] Isolated yields. [e] The composition of stereoisomers was determined by chiral HPCL.

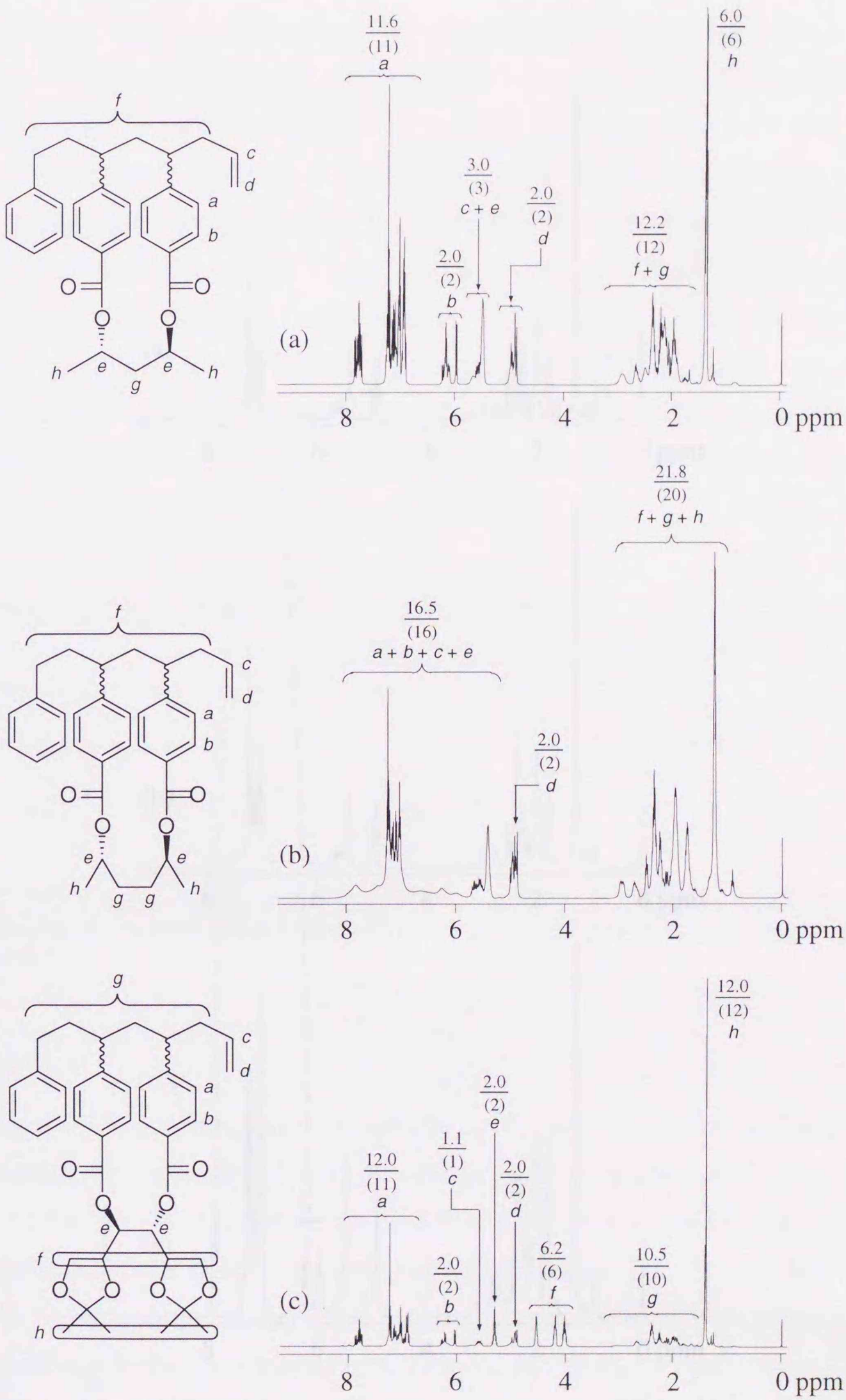

Figure 3.14. ^{1}H NMR spectra of **8b** (a), **8c** (b), and **8d** (c).

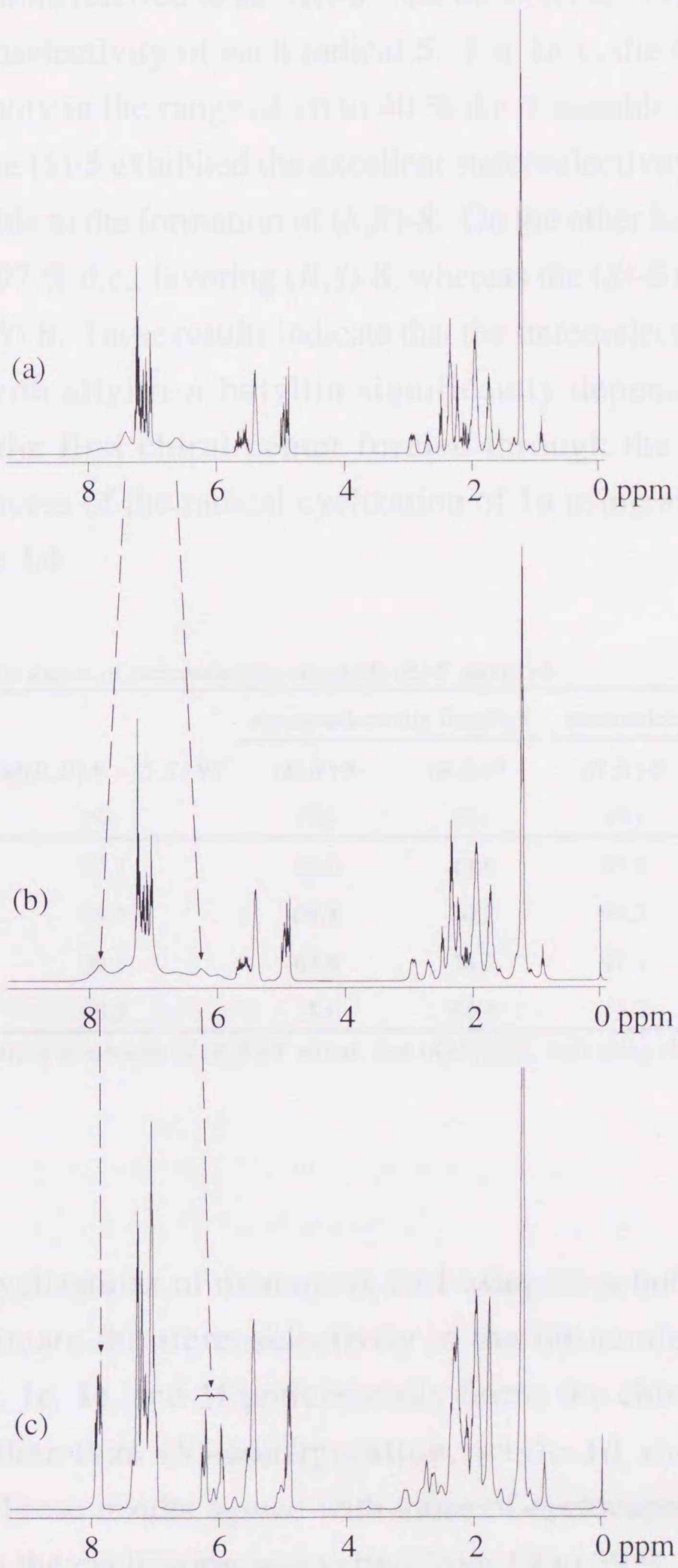

Figure 3.15. ^{1}H NMR spectra of **8c** recorded at 313 (a), 298 (b), and 213 K (c).

In the radical cyclization, there are two kinds of stereoisomeric forms in radical **5**. One of the forms, which has the (*R*)-configuration at the chiral center formed through the cyclization, referred to as "(*R*)-**5**" and the other to "(*S*)-**5**". Table 3.4 lists the extent of stereoselectivity of each radical **5**. For **1a-c**, the (*R*)-**5** exhibited the lower stereoselectivity in the range of 16 to 40 % d.e. favorable to the formation of (*R*,*R*)-**8**, whereas the (*S*)-**5** exhibited the excellent stereoselectivity in the range of 95 to 99 % d.e. favorable to the formation of (*S*,*R*)-**8**. On the other hand, for **1d**, the (*R*)-**5** exhibited that of 97 % d.e., favoring (*R*,*S*)-**8**, whereas the (*S*)-**5** exhibited that of 30 % d.e., favoring (*S*,*S*)-**8**. These results indicate that the stereoselectivity in the reaction of the radical **5** with allyltri-*n*-butyltin significantly depends on the absolute configuration of the first chiral center formed through the cyclization. The stereochemical process of the radical cyclization of **1a** using allyltri-*n*-butyltin is outlined in Scheme 3.4.

Table 3.4. The extent of stereoselectity of radcals (*R*)-**5** and (*S*)-**5**.

		steresoselectivity for (*R*)-**5**		stereoselectivity for (*S*)-**5**	
Monomer	Abs[(*R*,*R*)-**9** - (*S*,*S*)-**9**][a]	(*R*,*R*)-**9**	(*R*,*S*)-**9**	(*S*,*R*)-**9**	(*S*,*S*)-**9**
	(%)	(%)	(%)	(%)	(%)
1a	37.7	58.0	42.0	97.6	2.4
1b	38.7	69.8	30.2	99.3	0.7
1c	39.1	63.8	36.2	97.9	2.1
1d	40.2	1.6	98.4	35.2	64.8

[a] The absolute values of content of (*R*,*R*)-**9** minus that of (*S*,*S*)-**9**, indicating chirality induction efficiency .

3.3 Conclusion

The radical cyclizations of monomers **1a-f** using tri-*n*-butyltin hydride were carried out to estimate the stereoselectivity in the intramolecular cyclization. Monomers **1a**, **1b**, **1c**, **1e**, and **1f** preferentially forms the chiral center with (*R*)-configuration rather than (*S*)-configuration, while **1d** shows the opposite stereoselectivity. These results agreed with those of cyclocopolymerization. The stereoselectivity in the cyclization was varied from 19 to 39 % d.e. For the bis(4-vinylbenzoate)s of 1,2-diols (i.e., **1a**, **1d**, **1e**, and **1f**), the diastereomeric excess increased with an increase in the A value of the split Cotton effect in the CD spectra, indicating that the stereoselectivity in the cyclization was improved with an increase

Scheme 3.4

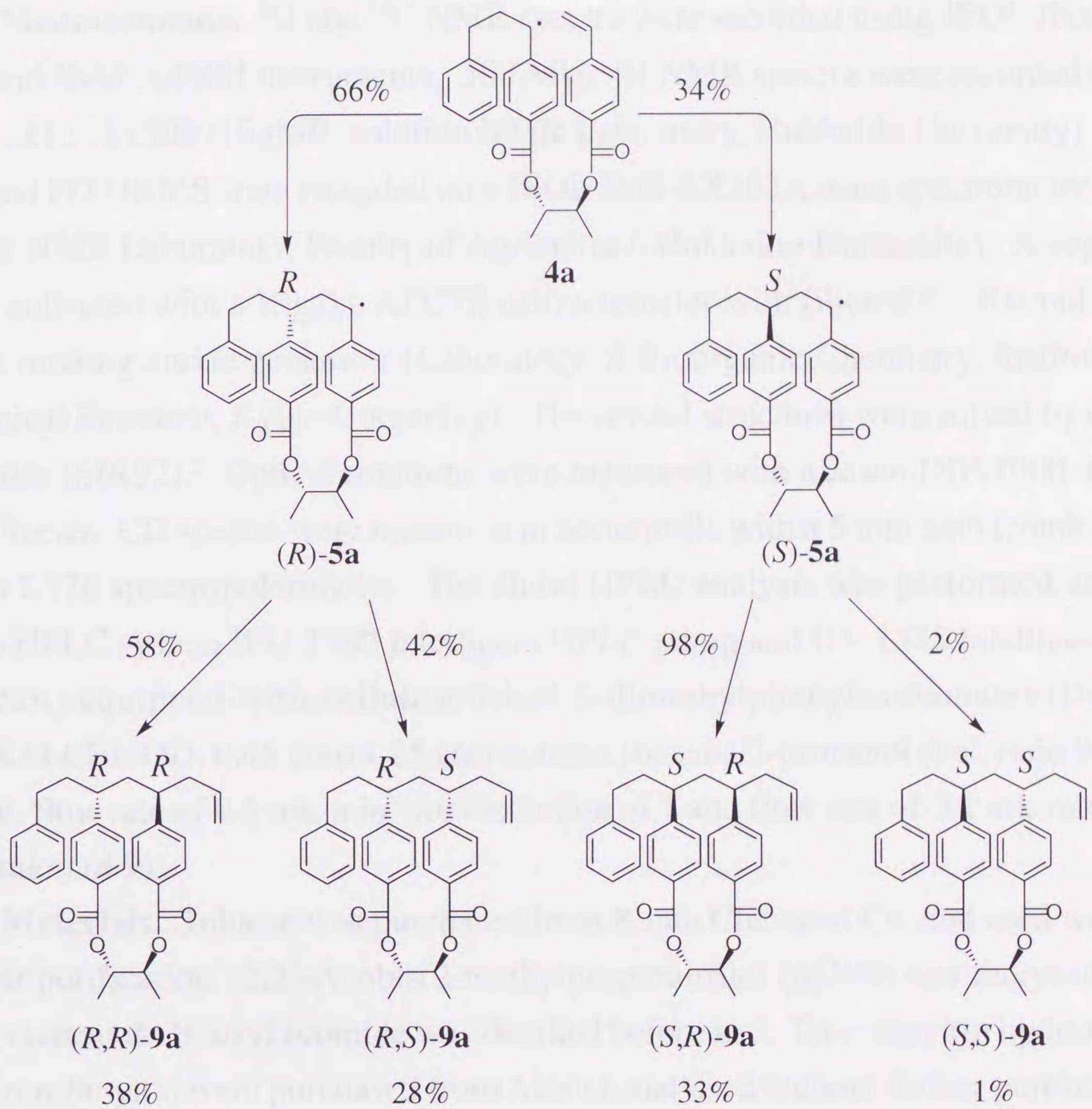

in the dihedral angle between two 4-vinylbenzoyl groups.

The radical cyclizations of **1a-d** using allyltri-*n*-butyltin were carried out to estimate the stereoselectivity in the intermolecular addition of the cyclized radical **5**. The results shows the extremely low content of (*S*,*S*)-**9** for **1a-c** and (*R*,*R*)-**9** for **1d**, indicating that the second stereoselectivity during the addition of radical **5** depends on the absolute configuration of the first chiral center. Therefore, monomers **1a-c** form the benzoate diad with (*R*,*R*)-racemo configuration rather than that with (*S*,*S*)-racemo configuration, and *vise versa* for **1d**, which fact agrees with the results for cyclocopolymerization.

3.4 Experimental Section

Measurements. ^{1}H and ^{13}C NMR spectra were recorded using JEOL JNM-EX 270 and JNM-A400II instruments. 500 MHz ^{1}H NMR spectra were recorded using JEOL ALPHA500 (High-Resolution NMR Laboratory, Hokkaido University). FD-MS and FD-HRMS were recorded on a JEOL JMS-SX102A mass spectrometer (GC-MS & NMR Laboratory, Faculty of Agriculture, Hokkaido University). X-ray data were collected with a Rigaku AFC7R diffractometer with filtered Cu-Kα radiation and a rotating anode generator (Laboratory of Bioorganic Chemistry, Institute for Chemical Research, Kyoto University). The crystal structures were solved by direct methods (SIR92).[2] Optical rotations were measured with a Jasco DIP-1000 digital polarimeter. CD spectra were measured in acetonitrile with a 5 mm path length using Jasco J-720 spectropolarimeter. The chiral HPLC analysis was performed using a Jasco HPLC system (PU-1580 Intelligent HPLC pump and UV-1575 Intelligent UV detector) equipped with cellulose-tris(3,5-dimethylphenylcarbamate) (Daicel, CHIRALCEL OD, 0.46 cmϕ x 25 cm) column (hexane/2-propanol (vol. ratio 9/1) as eluent, flow rate of 0.5 mL·min^{-1} for resolution of **7** and flow rate of 0.2 mL·min^{-1} for resolution of **9**).

Materials. Toluene was purchased from Kanto Chemical Co. and used without further purification. 2,2'-Azobis(2-methylpropionitrile) (AIBN) was recrystallized from methanol. Benzyl bromide was distilled before use. Tri-*n*-butyltin hydride and allyltri-*n*-butyltin were purchased from Aldrich and used without further purification. 1,2:5,6-Di-*O*-isopropylidene-D-mannitol[3], (1*S*,2*S*)-1,2-cycloheptanediol[4], and (2*S*,3*S*)-1,4-dimethoxy-2,3-butanediol[5] were synthesized according to literature procedures.

Separation of the Cyclic Compound. The preparative HPLC for the isolation of the cyclic compound was performed using Jasco HPLC system (PU-986 Intelligent preparative pump and UVIDEC-100-III UV Spectrophotometer) equipped with silica gel-ODS (Kanto, Mightysil RP-18 250-20) column.

Removal of the Chiral Template. The cyclic compound and 5 wt% methanolic KOH solution (50 eq. to carboxyl groups) were placed in 50 mL flask and refluxed for 1 hour. The resulting mixture was neutralized with hydrochloric acid. After removal of water under reduced pressure, the residue was treated with diazomethane in ether, whereupon template-free compound.

1,2:5,6-Di-*O*-isopropylidene-3,4-bis-*O*-(4-vinylbenzoyl)-D-mannitol (1d). The same procedure as that for **1a** in chapter 2 was applied to a mixture of 1,2:5,6-di-*O*-isopropylidene-D-mannitol (11 g, 43 mmol), 4-vinylbenzoyl chloride (22 g, 130 mmol) and 250 mL of pyridine. The crude product was purified by column chromatography on alumina with dichloromethane to give **1d** as a white solid. Yield 4.1 g (7.8 mmol, 18 %). $[\alpha]_{435}$ = +172.2°, $[\alpha]_D$ = +75.1° ($CHCl_3$, 21 °C, *c* 0.1). ^{1}H NMR (270 MHz, $CDCl_3$): δ (ppm) = 8.02 (d, ^3J = 8.2 Hz, 4H, Ar), 7.48 (d, ^3J = 8.3 Hz, 4H, Ar), 6.76 (dd, $^3J_{trans}$ = 17.5 Hz, $^3J_{cis}$ = 10.9 Hz, 2H, =CH-), 5.88 (d, $^3J_{trans}$ = 17.5 Hz, 2H, =CH_2), 5.70 (d, ^3J = 5.3 Hz, 2H, OCH), 5.41 (d, $^3J_{cis}$ = 10.9 Hz, 2H, =CH_2), 4.40-4.34 (m, 2H, CH), 4.04-3.91 (m, 4H, CH_2), 1.31 (s, 6H, CH_3), 1.30 (s, 6H, CH_3). ^{13}C NMR (67.8 MHz, $CDCl_3$): δ (ppm) = 165.6 (C=O), 142.9, 130.5, 128.9, 126.7 (Ar), 136.30 (=CH-), 117.4 (=CH_2), 110.0 (C), 75.3 (CH), 72.5 (CH), 66.2 (CH_2), 26.9 (CH_3), 25.7 (CH_3). Anal. Calcd. for $C_{30}H_{34}O_8$ (522.6): C 68.95; H 6.56. Found: C 69.93; H 6.53.

(1*S*,2*S*)-1,2-Cycloheptanediyl Bis(4-vinylbenzoate) (1e). The same procedure as that for **1a** in chapter 2 was applied to a mixture of (1*S*,2*S*)-1,2-cycloheptanediol (1.0 g, 7.7 mmol), 4-vinylbenzoyl chloride (4.4 g, 26.4 mmol) and 100 mL of pyridine. The crude product was purified by column chromatography on alumina with hexane/diethyl ether (vol. ratio 4/1) to give **1e** as a white solid. Yield 2.4 g (6.1 mmol, 79.4 %). $[\alpha]_{435}$ = +579.7°, $[\alpha]_D$ = +237.9° ($CHCl_3$, 23 °C, *c* 0.1). ^{1}H NMR (270 MHz, $CDCl_3$): δ (ppm) = 7.92 (d, ^3J = 8.6 Hz, 4H, Ar), 7.38 (d, ^3J = 8.6 Hz, 4H, Ar), 6.75 (dd, $^3J_{trans}$ = 17.8 Hz, $^3J_{cis}$ = 10.9 Hz, 2H, =CH-), 5.80 (d, $^3J_{trans}$ = 17.5 Hz, 2H, =CH_2), 5.44-5.38 (m, 2H, OCH), 5.33 (d, $^3J_{cis}$ = 10.9 Hz, 2H, =CH_2), 2.07-1.60 (m, 10H, cyclic-CH_2). ^{13}C NMR (67.8 MHz, $CDCl_3$): δ (ppm) = 165.6 (C=O), 141.8, 129.9, 129.4, 126.0 (Ar), 136.0 (=CH-), 116.4 (=CH_2), 76.5 (OCH), 30.4, 28.2, 22.8 (cyclic-CH_2). Anal. Calcd. for $C_{25}H_{26}O_4$ (390.5): C 76.90; H 6.71. Found: C 76.73; H 6.83.

(2*S*,3*S*)-1,4-Dimethoxy-2,3-butanediyl Bis(4-vinylbenzoate) (1f). The same procedure as that for **1a** in chapter 2 was applied to a mixture of (2*S*,3*S*)-1,4-dimethoxy-2,3-butanediol (2.2 g, 14.6 mmol), 4-vinylbenzoyl chloride (7.2 g, 43.2 mmol) and 120 mL of pyridine. The crude product was purified by column chromatography on silica gel (Kiesel Gel 60) with hexane/diethyl ether (vol. ratio 1/1) to give **1f** as a sticky liquid. Yield 5.4 g (13.2 mmol, 90.3 %). $[\alpha]_{435}$ = +67.5°, $[\alpha]_D$ = +23.2° ($CHCl_3$, 23 °C, *c* 1.0). ^{1}H NMR (270 MHz, $CDCl_3$): δ (ppm) = 8.00 (d, ^3J = 8.5 Hz, 4H, Ar), 7.43 (d, ^3J = 8.5 Hz, 4H, Ar), 6.72 (dd, $^3J_{trans}$ = 17.7 Hz, $^3J_{cis}$ = 10.9 Hz, 2H, =CH-),

5.84 (d, $^3J_{trans}$ = 17.6 Hz, 2H, =CH_2), 5.66 (m, 2H, OCH), 5.36 (d, $^3J_{cis}$ = 11.0 Hz, 2H, =CH_2), 3.72 (m, 4H, CH_2), 3.37 (s, 6H, CH_3). ^{13}C NMR (67.5 MHz, $CDCl_3$): δ (ppm) = 165.6 (C=O), 142.1, 130.0, 128.8, 126.1 (Ar), 135.9 (=CH-), 116.5 (=CH_2), 71.4 (OCH), 71.1 (CH_2), 59.3 (CH_3). Anal. Calcd for $C_{24}H_{26}O_6$ (410.5): C 70.23; H 6.38. Found: C 70.14; H 6.54.

(6*S*,7*S*)-6,7-Dimethyl-5,8-dioxa-4,9-dioxo-1-(2-phenylethyl)-[3,6]-*p*-cyclophane (6a). Dry toluene (800 mL) was placed into 1 L flask. This solution was degassed by bubbling nitrogen through for 1 hr and preheated at 80 °C. To this solution, a solution of (2*S*,3*S*)-2,3-butanediyl bis(4-vinylbenzoate) (**1a**) (282 mg, 0.8 mmol) and benzyl bromide (1mL, 8 mmol) were added 5 times at intervals of 24 hrs, and tri-*n*-butyltin hydride (220 mL, 0.8 mmol) and a portion of AIBN (ca. 30 mg) were added a 10 times at intervals of 12 hrs under nitrogen atmosphere. After removal of the solvent, reaction mixture was roughly purified by column chromatography. Further purification was performed by preparative HPLC (CH_3CN/H_2O (vol. ratio 9/1) as eluent, 10 mL/min) to give a diastereomeric mixture **6a** as a colorless solid (247 mg, 13.9 %). FD-HRMS m/z for $C_{29}H_{30}O_4$ calcd 442.2144, found 442.2126 (Error -4.1 ppm, -1.8 mmu).

(6*S*,8*S*)-6,8-Dimethyl-5,9-dioxa-4,10-dioxo-1-(2-phenylethyl)-[3,7]-*p*-cyclophane (6b). The same procedure as that for **6a** was applied to a mixture of (2*S*,4*S*)-2,4-pentanediyl bis(4-vinylbenzoate) (**1b**) (292 mg, 0.8 mmol x 5), benzyl bromide (1mL, 8 mmol x 5), tri-*n*-butyltin hydride (220 mL, 0.8 mmol x 10), and AIBN (ca. 30 mg x 10) in dry toluene (800 mL). The crude product was roughly purified by column chromatography. Further purification was performed by preparative HPLC (CH_3CN/H_2O (vol. ratio 9/1) as eluent, 10 mL/min) to give a diastereomeric mixture **6b** as a colorless solid (356 mg, 19.5 %). FD-HRMS m/z for $C_{30}H_{32}O_4$ calcd 456.2301, found 456.2319 (Error +4.0 ppm, +1.8 mmu).

(6*S*,9*S*)-6,9-Dimethyl-5,10-dioxa-4,11-dioxo-10-dioxo-1-(2-phenylethyl)-[3,8]-*p*-cyclophane (6c). The same procedure as that for **6a** was applied to a mixture of (2*S*,5*S*)-2,5-hexanediyl bis(4-vinylbenzoate) (**1c**) (303 mg, 0.8 mmol x 4), benzyl bromide (1mL, 8 mmol x 4), tri-*n*-butyltin hydride (220 mL, 0.8 mmol x 8), and AIBN (ca. 30 mg x 8) in dry toluene (800 mL). The crude product was roughly purified by column chromatography. Further purification was performed by preparative HPLC (CH_3CN/H_2O (vol. ratio 9/1) as eluent, 10 mL/min) to give a diastereomeric mixture **6c** as a colorless solid (130 mg, 8.6 %). FD-HRMS m/z for

$C_{31}H_{34}O_4$ calcd 470.2457, found 470.2470 (Error +2.7 ppm, +1.3 mmu).

(6*R*,7*R*)-6,7-Bis[(4*S*)-2,2-dimethyl-1,3-dioxolane-4-yl]-7-Dimethyl-5,8-dioxa-4,9-dioxo-1-(2-phenylethyl)-[3,6]-*p*-cyclophane (6d). The same procedure as that for **6a** was applied to a mixture of 1,2:5,6-di-*O*-isopropylidene-3,4-bis-*O*-(4-vinylbenzoyl)-D-mannitol (**1d**) (418 mg, 0.8 mmol x 5), benzyl bromide (1mL, 8 mmol x 5), tri-*n*-butyltin hydride (220 mL, 0.8 mmol x 10), and AIBN (ca. 30 mg x 10) in dry toluene (800 mL). The crude product was roughly purified by column chromatography. Further purification was performed by preparative HPLC (CH_3CN/H_2O (vol. ratio 9/1) as eluent, 10 mL/min) to give a diastereomeric mixture **6d** as a sticky liquid (326 mg, 13.2 %). FD-HRMS m/z for $C_{37}H_{42}O_8$ calcd 614.2880, found 614.2880 (Error 0.0 ppm, 0.0 mmu).

(6*S*,7*S*)-5,8-Dioxa-4,9-dioxo-6,7-pentamethylene-1-(2-phenylethyl)-[3,6]-*p*-cyclophane (6e). The same procedure as that for **6a** was applied to a mixture of (1*S*,2*S*)-1,2-cycloheptanediyl bis(4-vinylbenzoate) (**1e**) (313 mg, 0.8 mmol x 4), benzyl bromide (1mL, 8 mmol x 4), tri-*n*-butyltin hydride (220 mL, 0.8 mmol x 8), and AIBN (ca. 30 mg x 8) in dry toluene (800 mL). The crude product was roughly purified by column chromatography. Further purification was performed by preparative HPLC (CH_3CN/H_2O (vol. ratio 9/1) as eluent, 10 mL/min) to give a diastereomeric mixture **6e** as a sticky liquid (128 mg, 8.5 %). FD-HRMS m/z for $C_{32}H_{34}O_4$ calcd 482.2457, found 482.2450 (Error -1.5 ppm, -0.7 mmu).

(6*S*,7*S*)-6,7-Bis(methoxymethyl)-5,8-dioxa-4,9-dioxo-1-(2-phenylethyl)-[3,6]-*p*-cyclophane (6f). The same procedure as that for **6a** was applied to a mixture of (1*S*,2*S*)-1,2-bis(methoxymethyl)-1,2-butanediyl bis(4-vinylbenzoate) (**1f**) (328 mg, 0.8 mmol x 4), benzyl bromide (1mL, 8 mmol x 4), tri-*n*-butyltin hydride (220 mL, 0.8 mmol x 8), and AIBN (ca. 30 mg x 8) in dry toluene (800 mL). The crude product was roughly purified by column chromatography. Further purification was performed by preparative HPLC (CH_3CN/H_2O (vol. ratio 9/1) as eluent, 10 mL/min) to give a diastereomeric mixture **6f** as a sticky liquid (181 mg, 8.6 %). FD-HRMS m/z for $C_{31}H_{34}O_6$ calcd 502.2355, found 502.2328 (Error -5.5 ppm, -2.8 mmu).

1,3-Bis(4-methoxycarbonylphenyl)-5-phenylpentane (7). ^{1}H NMR (400 MHz, $CDCl_3$) δ (ppm) = 8.03 (d, ^3J = 7.92 Hz, Ar, 2H), 7.91 (d, ^3J = 7.92 Hz, Ar, 2H), 7.27-7.05 (m, Ar, 9H), 3.92 (s, OCH_3, 3H), 3.89 (s, OCH_3, 3H), 2.66-2.59 (m, -CH-, 1H), 2.48-2.40 (m, -CH_2-Ph, 4H), 2.06-1.88 (m, -CH_2-, 4H). ^{13}C NMR (100 MHz, $CDCl_3$) δ (ppm) = 167.04 (C=O), 167.02 (C=O), 150.37 (C), 147.52 (C), 141.87 (C), 129.92

(CH, Ar), 129.66 (CH, Ar), 128.42 (C), 128.31 (CH, Ar), 128.26 (CH, Ar), 127.84 (CH, Ar), 127.82 (CH, Ar), 125.80 (CH, Ar), 51.99 (OCH_3), 51.92 (OCH_3), 45.04 (-CH-), 38.32 ($-CH_2-$), 37.95 ($-CH_2-$), 33.68 ($-CH_2$-Ph), 33.59 ($-CH_2$-Ph). UV: ε_{max} = 32900 $cm^2 \cdot mmol^{-1}$ (λ_{max} = 240.8 nm).

(*R*)-1,3-Bis(4-methoxycarbonylphenyl)-5-phenylpentane ((*R*)-7). $[\alpha]_{365}$ = -33.89°, $[\alpha]_{435}$ = -16.39°, $[\alpha]_{546}$ = -8.36°, $[\alpha]_{577}$ = -6.97°, $[\alpha]_{589}$ = -6.90° ($CHCl_3$, 21 °C, *c* 0.81). CD: λ nm ($\Delta\varepsilon$ $cm^2 \cdot mmol^{-1}$) = 246.5 (-3.89) (*c* = 7.59 x 10^{-5} $mol \cdot L^{-1}$, path length = 5 mm).

(*S*)-1,3-Bis(4-methoxycarbonylphenyl)-5-phenylpentane ((*S*)-7). $[\alpha]_{365}$ = +32.80°, $[\alpha]_{435}$ = +15.38°, $[\alpha]_{546}$ = +9.01°, $[\alpha]_{577}$ = +7.42°, $[\alpha]_{589}$ = +7.39° ($CHCl_3$, 21 °C, *c* 0.74). CD: λ nm ($\Delta\varepsilon$ $cm^2 \cdot mmol^{-1}$) = 245.9 (+4.17) (*c* = 5.84 x 10^{-5} $mol \cdot L^{-1}$, path length = 5 mm).

(6*S*,7*S*)-1-Allyl-6,7-dimethyl-5,8-dioxa-4,9-dioxo-3-(2-phenylethyl)-[3,6]-*p*-cyclophane (8a). Dry toluene (80 mL) and allyltri-*n*-butyltin (2.2 mL, 7.2 mmol) were placed into 200 mL flask. This solution was degassed by bubbling nitrogen through for 1 hr and preheated at 80 °C. To this solution, a solution of (2*S*,3*S*)-2,3-butanediyl bis(4-vinylbenzoate) (**1a**) (63 mg, 0.18 mmol) and benzyl bromide (0.21 mL, 1.8 mmol) in dry toluene (1 mL) and a portion of AIBN (ca. 10 mg) were added 10 times at intervals of 6 hrs under nitrogen atmosphere. After removal of the solvent, reaction mixture was roughly purified by column chromatography. Further purification was performed by preparative HPLC (CH_3CN/H_2O (vol ratio 9/1) as eluent, 10 mL/min) to give a stereoisomeric mixture **8a** as a sticky liquid (20.4 mg, 2.3 %).

(6*S*,8*S*)-1-Allyl-6,8-dimethyl-5,9-dioxa-4,10-dioxo-3-(2-phenylethyl)-[3,7]-*p*-cyclophane (8b). The same procedure as that for **8a** was applied to a mixture of (2*S*,4*S*)-2,4-pentanediyl bis(4-vinylbenzoate) (**1b**) (66 mg, 0.18 mmol x 10), benzyl bromide (0.22 mL, 1.8 mmol x 10), and AIBN (ca. 10 mg x 10) with allyltri-*n*-butyltin (2.2 mL, 7 mmol) in dry toluene (90 mL). The crude product was roughly purified by column chromatography. Further purification was performed by preparative HPLC (CH_3CN/H_2O (vol. ratio 9/1) as eluent, 10 mL/min) to give a stereoisomeric mixture **8b** as a sticky liquid (49.0 mg, 5.4 %). FD-HRMS m/z for $C_{33}H_{36}O_4$ calcd 496.2614, found 496.2601 (Error -2.6 ppm, -1.3 mmu).

(6*S*,9*S*)-1-Allyl-6,9-dimethyl-5,10-dioxa-4,11-dioxo-3-(2-phenylethyl)-[3,8]-*p*-cyclophane (8c). The same procedure as that for **8a** was applied to a mixture of (2*S*,5*S*)-2,4-hexanediyl bis(4-vinylbenzoate) (**1c**) (68 mg, 0.18 mmol x 10), benzyl

bromide (0.22 mL, 1.8 mmol x 10), and AIBN (ca. 10 mg x 10) with allyltri-*n*-butyltin (2.2 mL, 7 mmol) in dry toluene (90 mL). The crude product was roughly purified by column chromatography. Further purification was performed by preparative HPLC (CH_3CN/H_2O (vol. ratio 9/1) as eluent, 10 mL/min) to give a stereoisomeric mixture **8c** as a sticky liquid (37.2 mg, 4.0 %). FD-HRMS m/z for $C_{34}H_{38}O_4$ calcd 510.2770, found 510.2763 (Error -1.4 ppm, -0.7 mmu).

(6*R*,7*R*)-1-Allyl-6,7-Bis[(4*S*)-2,2-dimethyl-1,3-dioxolane-4-yl]-7-Dimethyl-5,8-dioxa-4,9-dioxo-3-(2-phenylethyl)-[3,6]-*p*-cyclophane (8d). The same procedure as that for **8a** was applied to a mixture of 1,2:5,6-di-*O*-isopropylidene-3,4-bis-*O*-(4-vinylbenzoyl)-D-mannitol (**1d**) (79 mg, 0.15 mmol x 10), benzyl bromide (0.18 mL, 1.5 mmol x 10), and AIBN (ca. 10 mg x 10) with allyltri-*n*-butyltin (1.9 mL, 6 mmol) in dry toluene (75 mL). The crude product was roughly purified by column chromatography. Further purification was performed by preparative HPLC (CH_3CN/H_2O (vol. ratio 9/1) as eluent, 10 mL/min) to give a stereoisomeric mixture **8d** as a sticky liquid (38.6 mg, 3.9 %). FD-MS ($C_{40}H_{46}O_8$): m/z (relative intensity) = 654 (100), 655 (50.3), and 656 (14.4).

4,6-Bis(4'-methoxycarbonylphenyl)-8-phenylocta-1-ene (9). FD-HRMS m/z for $C_{30}H_{32}O_4$ calcd 456.2301, found 456.2321 (Error +4.4 ppm, +2.0 mmu).

***rel*-(4*R*,6*R*)-4,6-Bis(4'-methoxycarbonylphenyl)-8-phenylocta-1-ene [*rel*-(*R*,*R*)-9].** ^{1}H NMR (400 MHz, $CDCl_3$) δ (ppm) = 7.99 (d, ^3J = 8.30 Hz, Ar, 2H), 7.96 (d, ^3J = 8.29 Hz, Ar, 2H), 7.20-6.96 (m, Ar, 9H), 5.51-5.41 (m, -CH=, 1H), 4.88-4.83 (m, $=CH_2$, 2H), 3.93(s, OCH_3, 6H), 2.39-2.20 (m, 3-CH_2, 8-CH_2, 4-CH, 6-CH, 6H), 2.09-1.95 (m, 5-CH_2, 2H), 1.90-1.75 (m, 7-CH_2, 2H). ^{13}C NMR (100 MHz, $CDCl_3$) δ (ppm) = 167.10 (C=O), 150.25 (C), 149.94 (C), 141.87 (C), 135.97 (CH), 129.84 (CH), 129.74 (CH), 128.39 (C), 128.30 (C), 128.24 (CH), 128.14 (CH), 127.95 (CH), 127.91 (CH), 125.72 (CH), 116.48 ($=CH_2$), 52.03 (CH_3), 52.01 (CH_3), 43.25 (CH), 43.20 (CH), 41.94 (3-CH_2), 41.82 (5-CH_2), 39.49 (7-CH_2), 33.63 (8-CH_2). UV ε_{max} = 32500 $cm^{-1}\cdot mmol^{-1}$ (λ_{max} = 240.8 nm).

***rel*-(4*R*,6*S*)-4,6-Bis(4'-methoxycarbonylphenyl)-8-phenylocta-1-ene [*rel*-(*R*,*S*)-9].** ^{1}H NMR (400 MHz, $CDCl_3$) δ (ppm) = 7.96 (d, ^3J = 8.29 Hz, Ar, 2H), 7.90 (d, ^3J = 8.29 Hz, Ar, 2H), 7.26-7.01 (m, Ar, 9H), 5.57-5.47 (m, -CH=, 1H), 4.90-4.86 (m, $=CH_2$, 2H), 3.913 (s, OCH_3, 3H), 3.906 (s, OCH_3, 3H), 2.67-2.59 (m, 4-CH, 1H), 2.57-2.49 (m, 6-CH, 1H), 2.43-2.24 (m, 3-CH_2 and 8-CH_2, 4H), 2.07-1.81 (m, 5-CH_2 and 7-CH_2, 4H). ^{13}C NMR (100 MHz, $CDCl_3$) δ (ppm) = 167.04 (C=O), 150.79 (C),

150.30 (C), 141.85 (C), 135.91(-CH=), 129.88 (CH), 129.70 (CH), 128.31 (CH), 128.26 (CH), 128.13 (C), 127.64 (CH), 127.59 (CH), 125.81 (CH), 116.57 (=CH_2), 52.00 (CH_3), 51.97 (CH_3), 43.38 (4-CH), 43.00 (5-CH_2), 42.73 (6-CH), 40.41 (3-CH_2), 37.32 (7-CH_2), 33.44 (8-CH_2). UV: ε_{max} = 30700 $cm^{-1}\cdot mmol^{-1}$ (λ_{max} = 240.4 nm).

(4*R*,6*R*)-4,6-Bis(4'-methoxycarbonylphenyl)-8-phenylocta-1-ene [(*R*,*R*)-9]. CD: λ nm ($\Delta\varepsilon$ $cm^2\cdot mmol^{-1}$) = 248.0 (-47.8), 229.8 (+14.5).

(4*S*,6*S*)-4,6-Bis(4'-methoxycarbonylphenyl)-8-phenylocta-1-ene [(*S*,*S*)-9]. CD: λ nm ($\Delta\varepsilon$ $cm^2\cdot mmol^{-1}$) = 248.0 (+46.1), 230.4 (-13.6).

(4*R*,6*S*)-4,6-Bis(4'-methoxycarbonylphenyl)-8-phenylocta-1-ene [(*R*,*S*)-9]. CD: λ nm ($\Delta\varepsilon$ $cm^2\cdot mmol^{-1}$) = 249.1 (-3.0), 228.9 (+5.6).

(4*S*,6*R*)-4,6-Bis(4'-methoxycarbonylphenyl)-8-phenylocta-1-ene [(*S*,*R*)-9]. CD: λ nm ($\Delta\varepsilon$ $cm^2\cdot mmol^{-1}$) = 249.8 (+3.5), 229.1 (-5.9).

3.5 References

(1) Wulff, G.; Kühneweg, B. *J. Org. Chem.* **1997**, *62*, 5785.

(2) Altomare, A.; Burla, M. C.; Camalli, M.; Cascarano, M.; Giacovazzo, C.; Guagliardi, A.; Polidori, G. *J. Appl. Cryst.* **1994**, *27*, 435.

(3) Tipson, R. S.; Cohen, A. *Carbohydr. Res.* **1968**, *7*, 232.

(4) Kaga, H.; Yamauchi, Y.; Narumi, A.; Yokota, K.; Kakuchi, T. *Enantiomer* **1998**, *3*, 203.

(5) Seebach, D.; Kalinowski, H.-O.; Bastani, B.; Crass, G.; Daum, H.; Dörr, H.; DuPreez, N. P.; Ehrig, V.; Langer, W.; Nüssler, C.; Oei, H.-A.; Schmidt, M. *Helvetica Chimica Acta* **1977**, *60*, 301.

Chapter 4

Computational Study on the Chirality Induction Mechanism

4.1 Introduction

The previous chapter clarified that the stereoselectivity in the intramolecular cyclization was depended on the dihedral angle between two 4-vinylbenzoyl groups. In addition, the stereoselectivity in the intermolecular addition of the cyclized radical was affected by the absolute configuration of the first chiral center formed through the cyclization.

The aims in this chapter are to find the driving force of the stereoselectivity and to construct the rational mechanism for chirality induction according to a numerical method used for the model reaction (Scheme 4.1).

Scheme 4.1

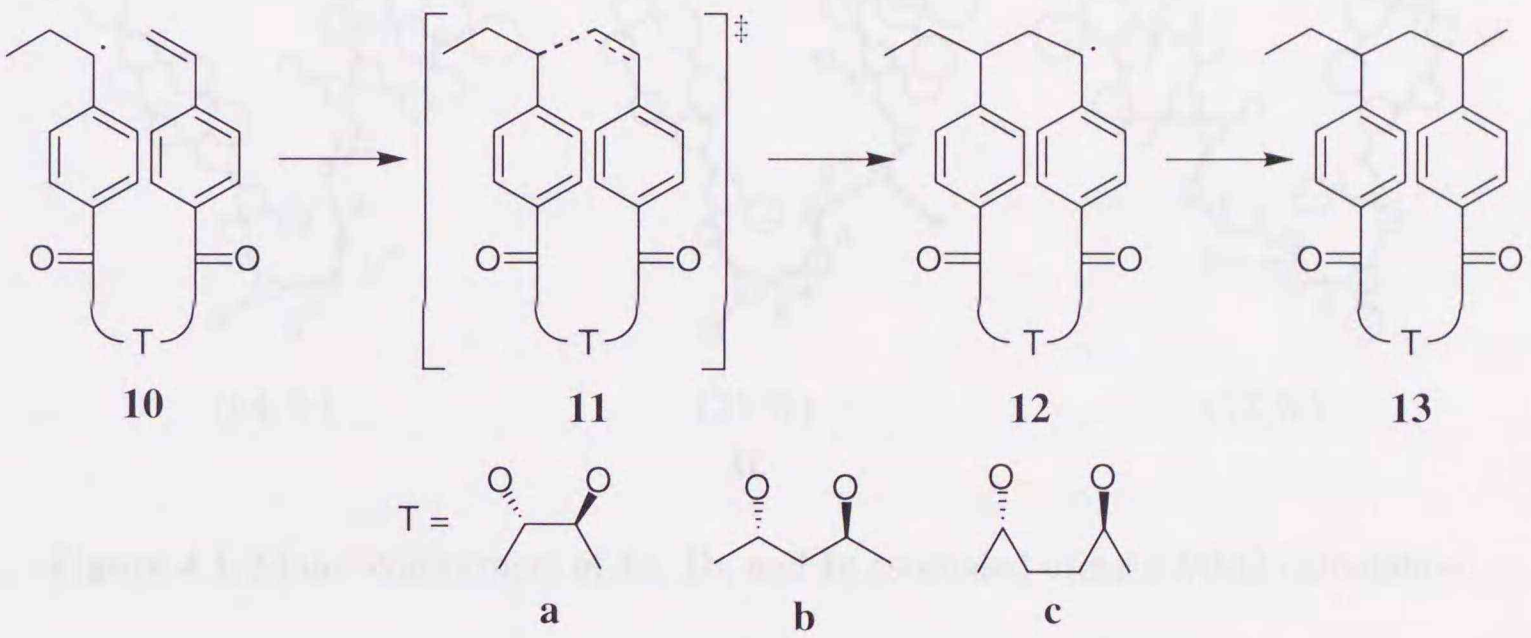

4.2 Results and Discussion

4.2.1 Search for the Minimum Energy Conformations

For the first time, the conformation of the templates must account for the following calculation. The initial structure for the MM2 calculation was assembled by specifying the skeletal carbons as all gauche form and the relative direction between the carbonyl group in ester against the methine proton in neighboring position (the details are mentioned in the procedure section). In this manner, the initial structures are numbered in 12 for **1a**, 36 for **1b**, and 108 for **1c**. The major conformers in each monomer were estimated using a MM2 calculation (Figure 4.1). Monomer **1a** predominately has a counterclockwise gauche form (hereinafter referred to as "g⁻")

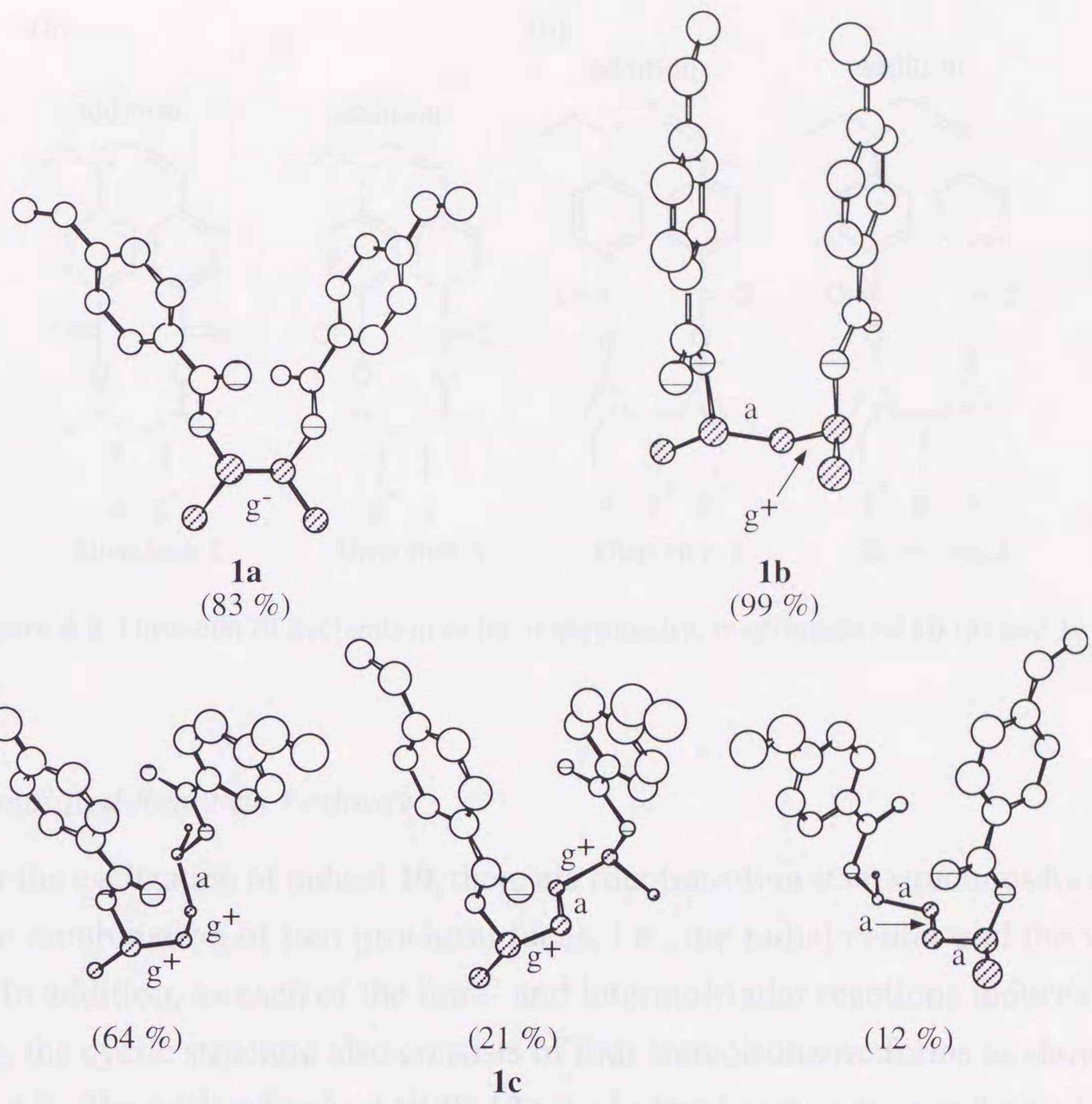

Figure 4.1. Major conformers of **1a**, **1b**, and **1c** estimated using a MM2 calculation.

in the carbon skeletal of the template, and monomer **1b** substantially has a combination of anti form ("a") and clockwise gauche form ("g^+"). For **1c**, the conformer is distributed to "ag^+g^+", "g^+ag^+", and "aaa" forms because of flexibility.

Having a high tendency for intramolecular cyclization, monomers **1a-c** should have a conformation suitable for the cyclization. For this reason, the conformers in Figure 4.1 can be applied to the conformation for **11a-c** in the transition state. The dissymmetric conformation such as "ag^+" and "ag^+g^+" yields two directions for the cyclization (Figure 4.2). Therefore, there are 4, 8, and 16 pathways for cyclizations of **10a**, **10b**, and **10c**, respectively (Scheme 4.2). For the second time, the direction of the carbonyl groups must be considered, which is controlled by the chiral template. Monomers **1a-c** have the bond vectors of the two carbonyl groups where their *Si* faces are directed toward the inside. The "aaa" conformer contains the carbonyl groups having *Re* faces.

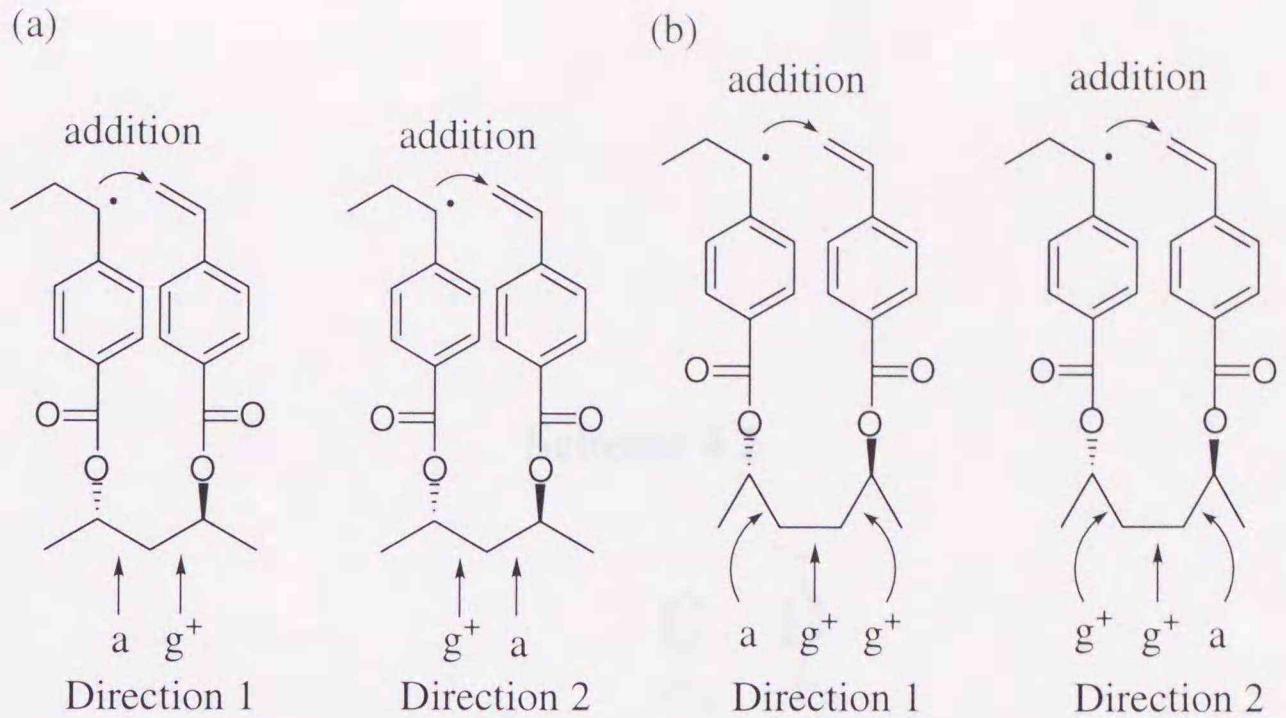

Figure 4.2. Direction of cyclization in the dissymmetric conformers of **1b** (a) and **1c** (b).

4.2.2 Simplified Reaction Pathway

For the cyclization of radical **10**, there are four transition state structures forming from the combination of two prochiral faces, i.e., the radial center and the vinyl group. In addition, as each of the intra- and intermolecular reactions induces new chirality, the cyclic structure also consists of four stereoisomeric forms as shown in Scheme 4.2. The cyclized radical (*R*,*R*)-**12a** stacks two benzene rings in the molecule (Figure 4.3). The orbital of the radical is perpendicular to the benzene ring, which situation stabilizes the radical. For the cyclized radical, hence, one of the prochiral faces on the radical center is directed to the inside of the ring and the other to the outside of the ring. As the inside direction is effectively shielded by the benzene rings, the outside direction is favorable in the addition of the cyclized radical. Hence, there is one-to-one correspondence between the cyclized radical **12** and the cyclic compound **13** on the stereochemistry. In view of cyclized radical structure, Scheme 4.2 is simplified as Scheme 4.3.

Scheme 4.2

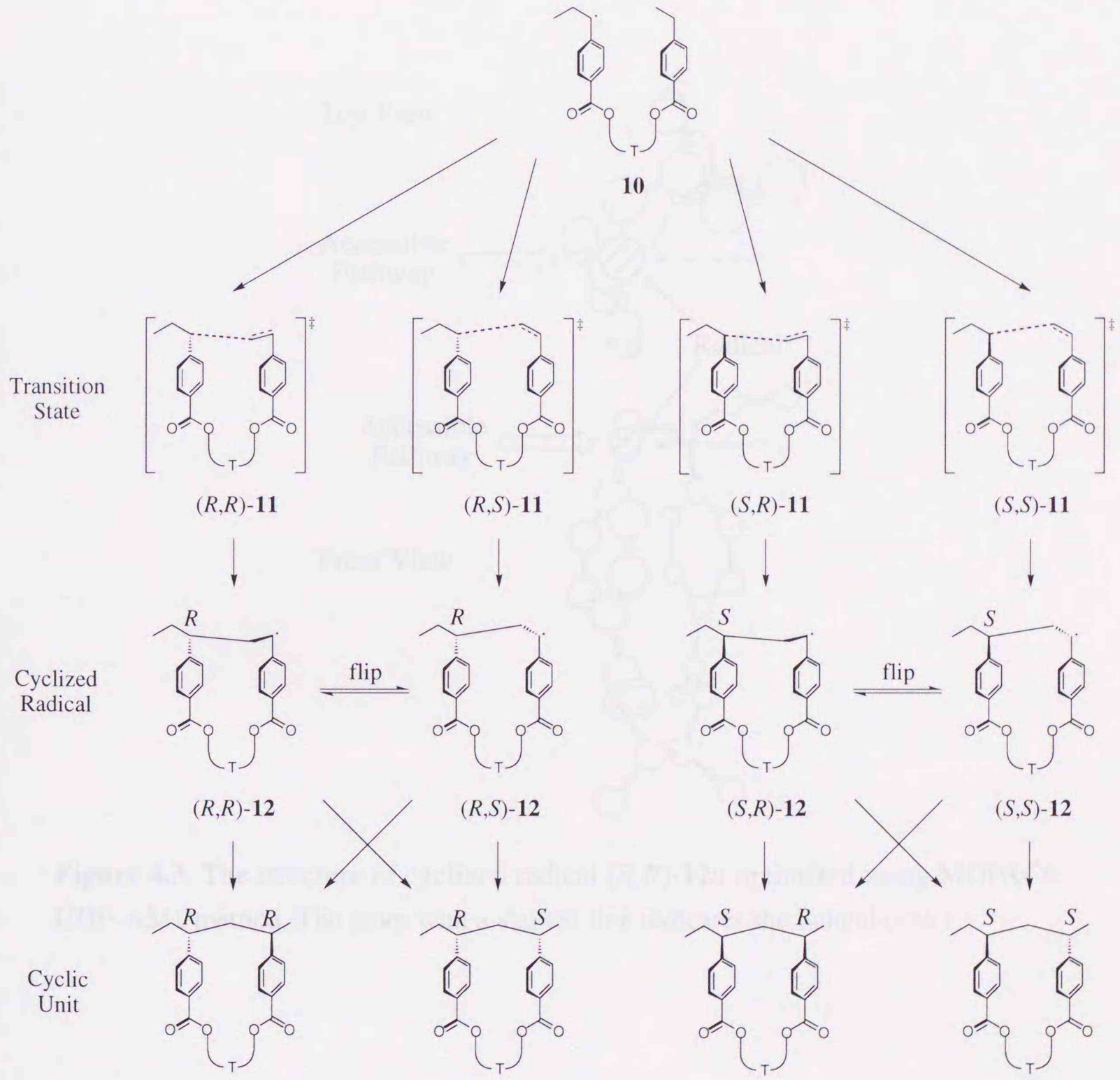
10
Transition State
(R,R)-11
(R,S)-11
(S,R)-11
(S,S)-11
Cyclized Radical
flip
flip
R
S
(R,R)-12
(R,S)-12
(S,R)-12
(S,S)-12
Cyclic Unit
(R,R)-13
(R,S)-13
(S,R)-13
(S,S)-13

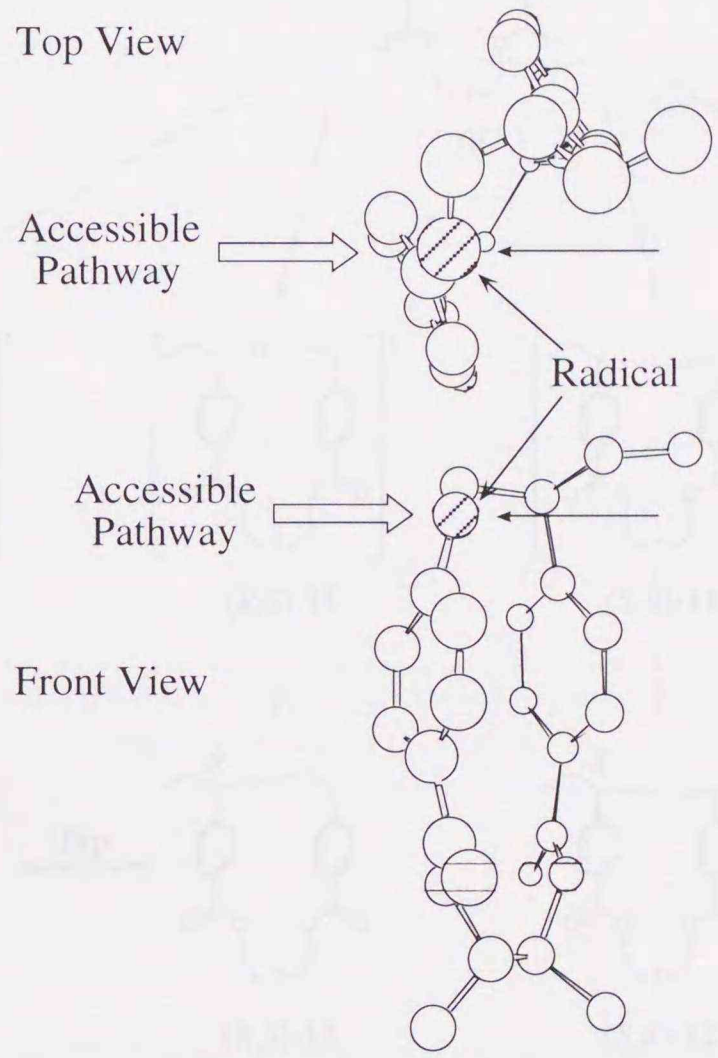

Figure 4.3. The structure of cyclized radical (*R*,*R*)-**12a** optimized using MOPAC6-UHF-AM1 method. The atom with a slanted line indicates the radical center.

Scheme 4.3

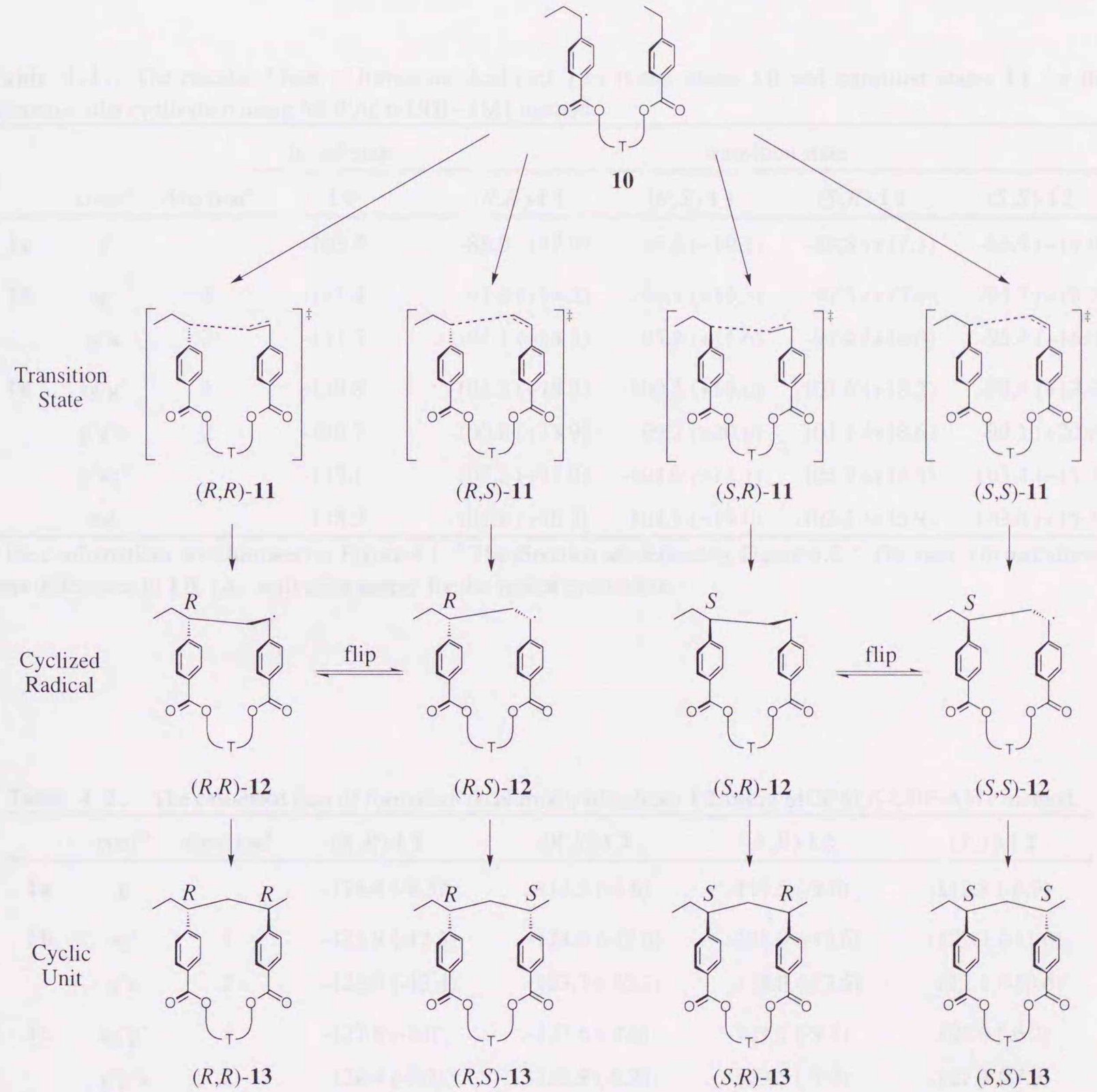
10
Transition State
(R,R)-11
(R,S)-11
(S,R)-11
(S,S)-11
Cyclized Radical
flip
flip
(R,R)-12
(R,S)-12
(S,R)-12
(S,S)-12
Cyclic Unit
(R,R)-13
(R,S)-13
(S,R)-13
(S,S)-13

4.2.3 Calculation of the Energy-Minima and the Saddle Point

The heat of formation of the energy-minima (corresponding to **10**, **12**, and **13**) and the saddle point **11** was estimated using MOPAC6-AM1 method (Tables 4.1, 4.2, and 4.3). The energy profiles for the radical reaction of **10a** are illustrated in Figure 4.4.

Table 4.1. The calculated heat of formation (kcal·mol^{-1}) of initial states **10** and transition states **11** for the intramolecular cyclization using MOPAC6-UHF-AM1 method.

			initial state	transition state			
	conf.[a]	direction[b]	**10**	(*R*,*R*)-**11**	(*R*,*S*)-**11**	(*S*,*R*)-**11**	(*S*,*S*)-**11**
1a	g^-		-105.9	-88.0 (+17.9)[c]	-86.8 (+19.1)	-88.8 (+17.1)	-86.9 (+19.0)
1b	ag^+	1	-111.4	-97.2 (+14.2)	-96.1 (+15.3)	-97.5 (+13.9)	-95.7 (+15.7)
	g^+a	2	-111.5	-97.1 (+14.3)	-95.8 (+15.6)	-97.4 (+14.0)	-95.4 (+16.0)
1c	ag^+g^+	1	-119.8	-101.3 (+18.5)	-100.2 (+19.6)	-101.6 (+18.2)	-99.9 (+19.9)
	g^+g^+a	2	-119.7	-100.8 (+18.9)	-99.7 (+20.0)	-101.1 (+18.6)	-99.1 (+20.6)
	g^+ag^+		-119.1	-105.2 (+13.9)	-104.0 (+15.1)	-105.7 (+13.4)	-103.4 (+15.7)
	aaa		-118.2	-102.8 (+16.3)	-104.1 (+15.0)	-103.2 (+15.9)	-103.8 (+15.3)

[a] The confomations are illustrated in Figure 4.1. [b] The direction are defined by Figure 4.2. [c] The values in parenthesis were differences to **10**, i.e., activation energy for the radical cyclization.

Table 4.2. The calculated heat of formation (kcal·mol^{-1}) of radicals **12** using MOPAC6-UHF-AM1 method.

	conf.[a]	direction[b]	(*R*,*R*)-**12**	(*R*,*S*)-**12**	(*S*,*R*)-**12**	(*S*,*S*)-**12**
1a	g^-		-114.4 (-8.5)[c]	-114.5 (-8.6)	-115.5 (-9.6)	-112.8 (-6.9)
1b	ag^+	1	-123.9 (-12.5)	-124.0 (-12.6)	-125.0 (-13.6)	-122.4 (-11.0)
	g^+a	2	-123.9 (-12.4)	-123.7 (-12.2)	-125.0 (-13.5)	-122.1 (-10.6)
1c	ag^+g^+	1	-127.8 (-8.0)	-127.6 (-7.8)	-129.1 (-9.3)	-126.0 (-6.2)
	g^+g^+a	2	-128.4 (-8.7)	-128.9 (-9.2)	-129.5 (-9.8)	-127.3 (-7.6)
	g^+ag^+		-132.1 (-13.0)	-132.4 (-13.3)	-133.4 (-14.3)	-130.7 (-11.6)
	aaa		-129.9 (-11.7)	-132.0 (-13.8)	-131.5 (-13.3)	-130.8 (-12.6)

[a] The confomations are illustrated in Figure 4.1. [b] The direction are defined by Figure 4.2. [c] The values in parenthesis were differences to **10**, i.e., heat of reaction for the radical cyclization.

Table 4.3. The calculated heat of formation (kcal·mol^{-1}) of **13** using MOPAC6-AM1 method.

	conf.[a]	direction[b]	(*R*,*R*)-**13**	(*R*,*S*)-**13**	(*S*,*R*)-**13**	(*S*,*S*)-**13**
1a	g^-		-139.4 (-33.5)[c]	-141.3 (-35.4)	-141.2 (-35.3)	-139.3 (-33.4)
1b	ag^+	1	-148.7 (-37.3)	-150.6 (-39.2)	-150.5 (-39.1)	-148.6 (-37.2)
	g^+a	2	-148.7 (-37.2)	-150.6 (-39.1)	-150.5 (-39.0)	-148.6 (-37.1)
1c	ag^+g^+	1	-152.2 (-32.4)	-154.2 (-34.4)	-154.2 (-34.4)	-152.3 (-32.5)
	g^+g^+a	2	-151.9 (-32.2)	-154.1 (-34.4)	-154.2 (-34.5)	-152.2 (-32.5)
	g^+ag^+		-156.4 (-37.3)	-158.4 (-39.3)	-158.3 (-39.2)	-156.5 (-37.4)
	aaa		-155.4 (-36.3)	-157.3 (-38.2)	-157.4 (-38.3)	-155.4 (-36.3)

[a] The confomations are illustrated in Figure 4.1. [b] The direction are defined by Figure 4.2. [c] The values in parenthesis were differences to **10**.

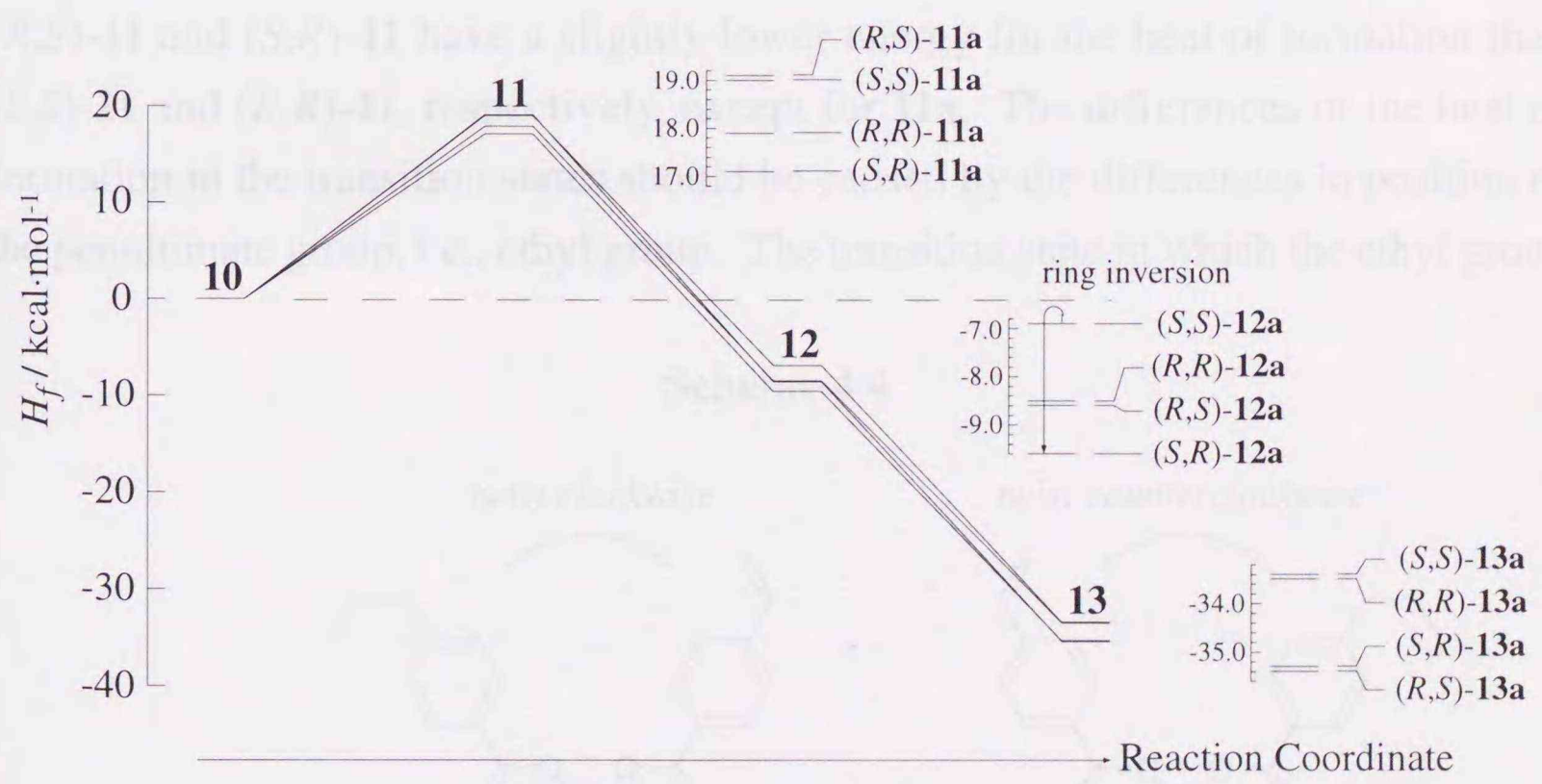

Figure 4.4. Energy profile for the radical addition of **10a**.

The chirality induction mechanism for intramolecular cyclization can be explain on the basis of the stereoelectronic effect during the radical addition. Houk et. al. estimated the theoretical transition structure for the radical addition on the basis of the ab initio calculation.[1] According to their study, the angle with which the radical attacks the carbon-carbon double bond is fairly constant in the range from 102 to 109° (Figure 4.5). For the radical cyclization of monomers **1a**-**c**, only one side of the

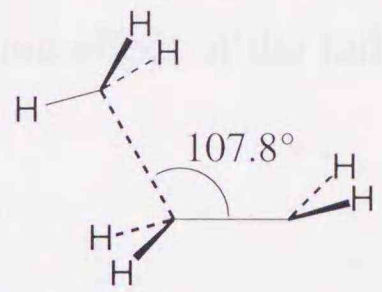

Figure 4.5. Calculated geometry of the transition state for the addition of methyl radical to ethylene.

prochiral faces of the vinyl group, therefore, is accepted for the attack of radical because of chiral twist of the two 4-vinylbenzoyl groups (Scheme 4.4). In the transition state of cyclization, the clockwise twist selects (*R*,*S*)-**11** and/or (*S*,*S*)-**11**, while the counterclockwise twist selects (*R*,*R*)-**11** and/or (*S*,*R*)-**11**. Table 4.1 indicated that (*R*,*S*)-**11** and (*S*,*R*)-**11** have a slightly lower energy for the heat of formation than (*S*,*S*)-**11** and (*R*,*R*)-**11**, respectively, except for **11a**. The differences of the heat of formation in the transition states should be caused by the differences in position of the penultimate group, i.e., ethyl group. The transition state in which the ethyl group

Scheme 4.4

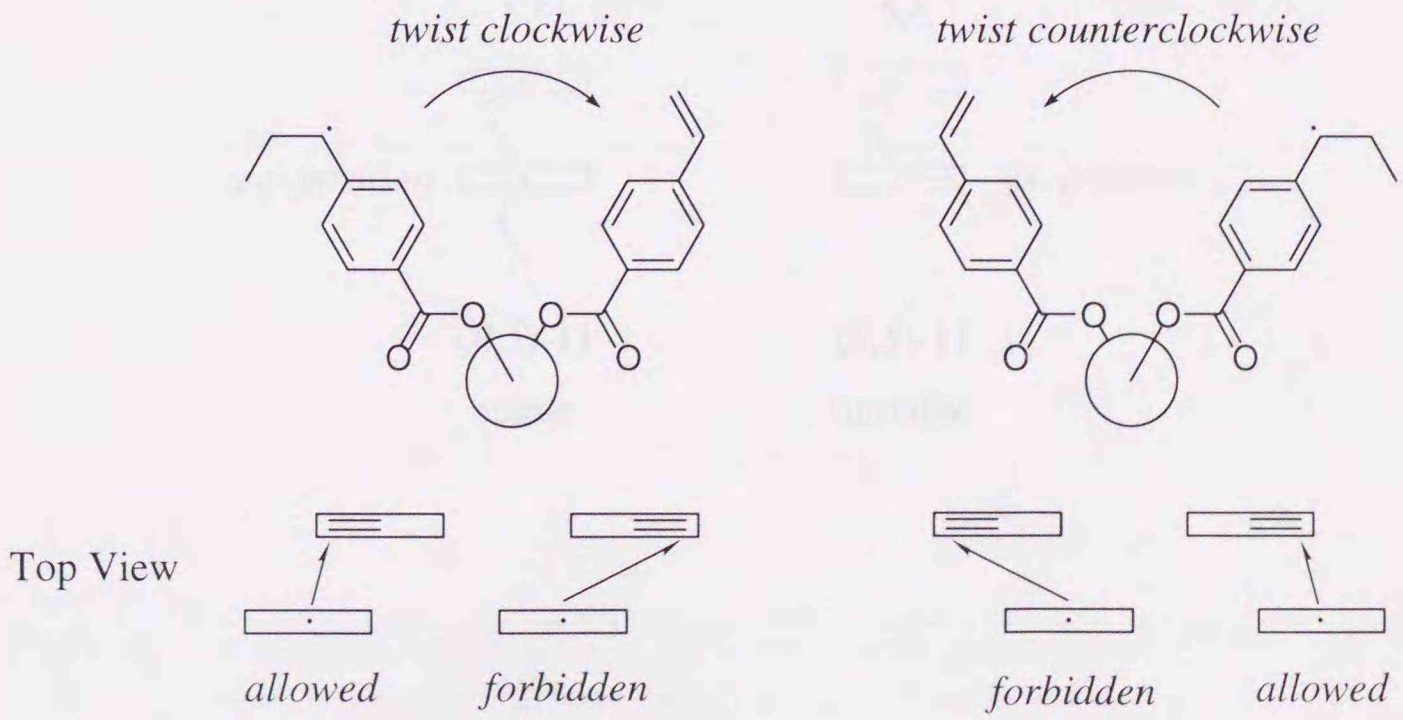

is situated in *pseudo-equatorial* position is more stable than that in *pseudo-axial* position (Scheme 4.5). Table 4.4 lists the calculated stereoselectivity in the intramolecular cyclization on the basis of the heat of formation for the transition state **11**. These results indicated that the positive twist of two 4-vinylbenzoyl groups induces the first chirality with (*R*)-configuration, and *vise versa* for the negative twist, which fairly agree with the results in chapter 2. Hence, the chirality induction in the intramolecular cyclization is arised by the chiral twist of bis(4-vinylbenzoate) accompanying the stereoelectronic effect of the radical addition and the steric effect of the penultimate group.

Scheme 4.5

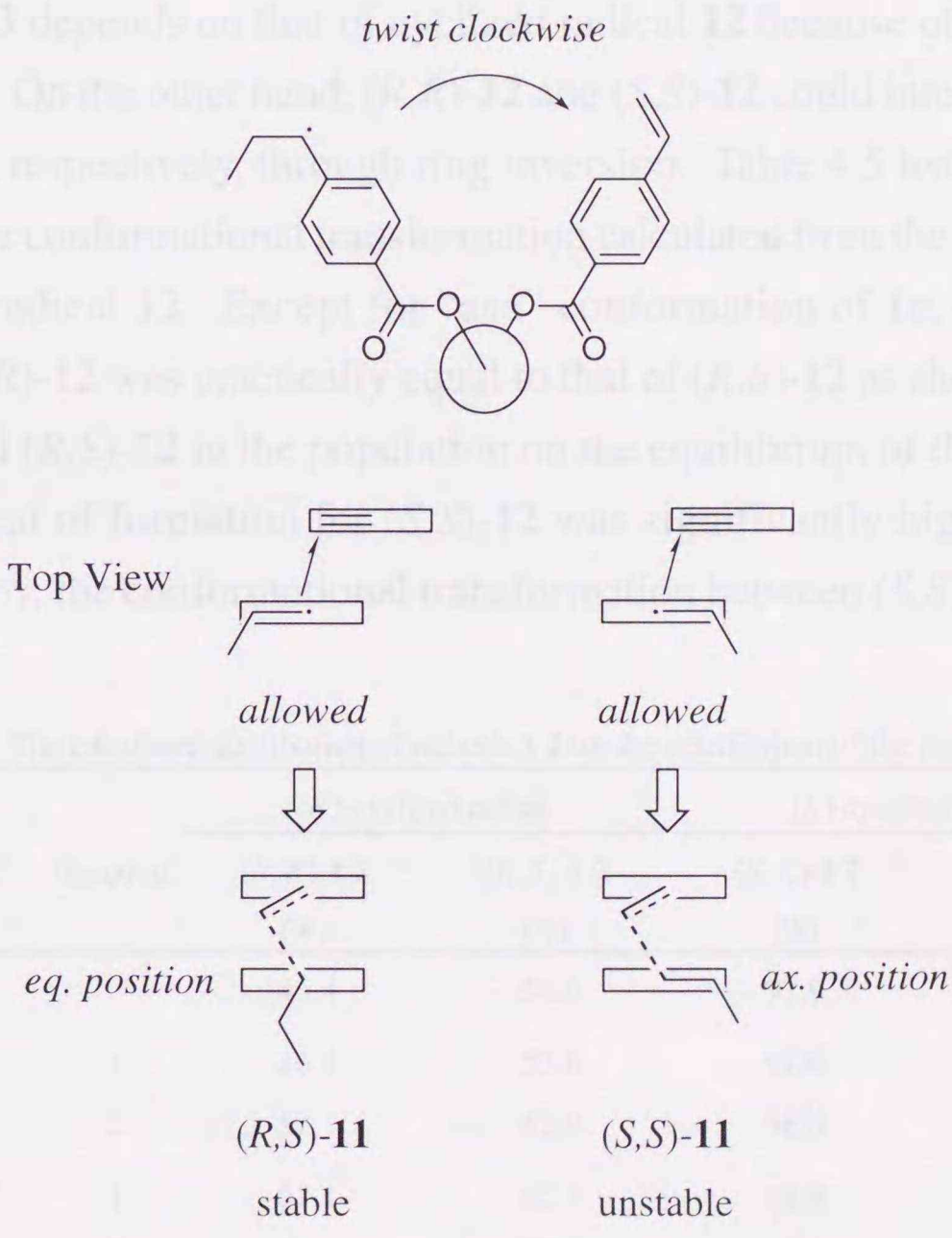

Table 4.4. The calculated extent of stereoselectivity for the intramolecular cyclization[a].

			positive chirality		negative chirality	
	conf.[b]	direction[c]	(*R*,*S*)-**11** (%)	(*S*,*S*)-**11** (%)	(*R*,*R*)-**11** (%)	(*S*,*R*)-**11** (%)
1a	g^-		46.4	53.6	24.2	75.8
1b	ag^+	1	63.9	36.1	39.5	60.5
	g^+a	2	63.9	36.1	39.5	60.5
1c	ag^+g^+	1	60.5	39.5	39.5	60.5
	g^+g^+a	2	70.2	29.8	39.5	60.5
	g^+ag^+		70.2	29.8	32.9	67.1
	aaa		60.5	39.5	36.1	63.9

[a] The Boltzmann distribution calculated on the basis of the heat of formation of transition state **11** at 80 ℃. [b] The conformations are illustrated in Figure 4.1. [c] The directions are defined by Figure 4.2.

For the intermolecular addition of the cyclized radical, the stereochemical distribution of **13** depends on that of cyclized radical **12** because of their one-to-one correspondence. On the other hand, (*R*,*R*)-**12** and (*S*,*S*)-**12** could interconvert to (*R*,*S*)-**12** and (*S*,*R*)-**12**, respectively, through ring inversion. Table 4.5 lists the equilibrium distribution of the conformational transformation calculated from the heat of formation of the cyclized radical **12**. Except for "aaa" conformation of **1c**, since the heat of formation of (*R*,*R*)-**12** was practically equal to that of (*R*,*S*)-**12** as shown in Table 4.2, (*R*,*R*)-**12** equaled (*R*,*S*)-**12** in the population on the equilibrium of the ring inversion. However, the heat of formation for (*S*,*S*)-**12** was significantly higher than that for (*S*,*R*)-**12**. Thereby, the conformational transformation between (*S*,*S*)-**12** and (*S*,*R*)-**12**

Table 4.5. The calculated distribution of radicals **12** on the equilibrium of the ring inversion[a]

			(*R*)-cyclized radical		(*S*)-cyclized radical	
	conf.[b]	direction[c]	(*R*,*R*)-**12** (%)	(*R*,*S*)-**12** (%)	(*S*,*R*)-**12** (%)	(*S*,*S*)-**12** (%)
1a	g^-		46.4	53.6	97.9	2.1
1b	ag^+	1	46.4	53.6	97.6	2.4
	g^+a	2	57.1	42.9	98.4	1.6
1c	ag^+g^+	1	57.1	42.9	98.8	1.2
	g^+g^+a	2	32.9	67.1	95.8	4.2
	g^+ag^+		39.5	60.5	97.9	2.1
	aaa		4.7	95.3	73.0	27.0

[a] The Boltzmann districution calculated on the basis of the heat of formation of radicals **12** at 80 ℃ [b] The conformations are illustrated in Figure 4.1. [c] The directions are defined by Figure 4.2.

strongly shifted toward (*S*,*R*)-**12** to suppress the formation of (*S*,*S*)-**13**. Consequently, the cyclized radical **12** having the (*R*)-configuration exhibited the poor stereoselectivity in intermolecular addition, whereas the cyclized radical **12** having the (*S*)-configuration exhibited the excellent stereoselectivity. These results satisfactorily agreed with the experimental results in chapter 3.

In order to estimate the stereoelectronic effect on the stability of the cyclized radical, the heat of formation for (-,*R*)-**14** and (-,*S*)-**14** as shown in Scheme 4.6 was calculated using the MOPAC6-UHF-AM1 method (Table 4.6). Because the heat of formation for (-,*R*)-**14** is lower than that of (-,*S*)-**14** except for "aaa" conformation of **1c**, the stereoelectronic effect of the radical gives a priority to (-,*R*)-**14** over (-,*S*)-**14**.

Scheme 4.6

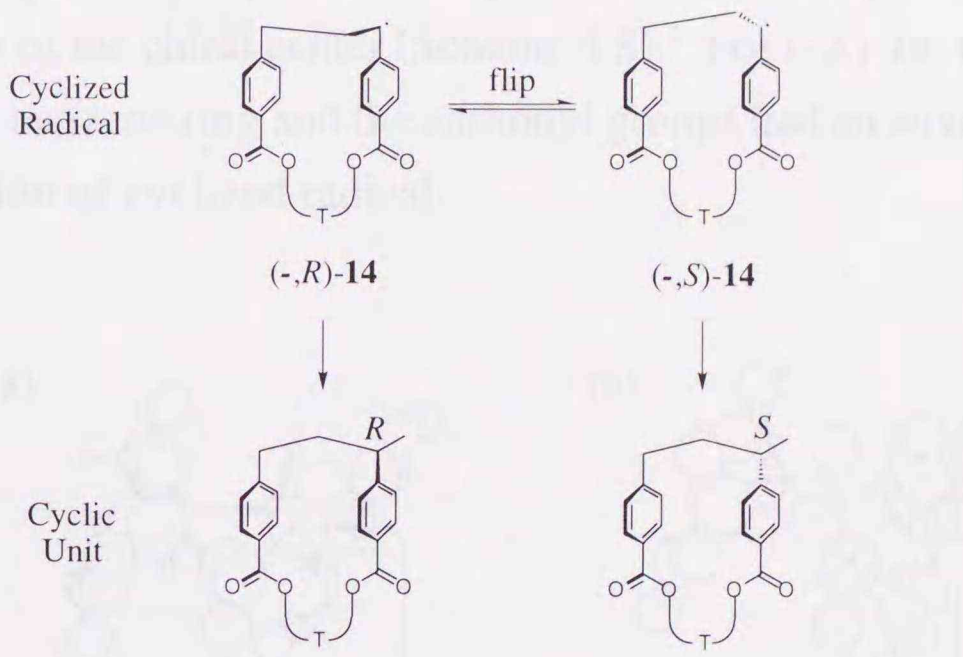

Table 4.6. The calculated heat of formation (kcal·mol^{-1}) and the torsion angle θ (deg) of **14** using MOPAC6-UHF-AM1 method.

			heat of formation (kcal·mol^{-1})		torsion angle θ^c (deg)	
	conf.[a]	direction[b]	(-,*R*)-**14**	(-,*S*)-**14**	(-,*R*)-**14**	(-,*S*)-**14**
1a	g^-		-106.0	-104.5	+22.2	+37.0
1b	ag^+	1	-115.4	-114.0	+13.7	+33.3
	g^+a	2	-115.4	-113.8	+20.6	+40.2
1c	ag^+g^+	1	-119.5	-117.6	+14.0	+33.7
	g^+g^+a	2	-119.9	-118.9	+3.5	+13.4
	g^+ag^+		-123.7	-122.4	+11.6	+25.3
	aaa		-121.6	-122.4	-21.6	+3.6

[a] The conformations are illustrated in Figure 4.1. [b] The directions are defined by Figure 4.2. [c] The torsion angle θ is defined by Figure 4.6.

The promotive factor in the heat of formation for **14** should become a driving force of the stereoselectivity in the intermolecular addition. For the cyclized radical **14**, the rotation around a single bond as shown in Figure 4.6 lowers the stabilization energy based on the conjugation. Table 4.6 lists the torsion angle θ for cyclized radical **14**. Except for "aaa" conformation of **14**, the torsion angle θ of (-,*R*)-**14** was smaller than that of (-,*S*)-**14**. On the other hand, the reverse took place in the "aaa" conformer. These results agreed very closely with those obtained by the heat of formation. The torsional strain in the cyclized radical, which is essentially concerned with the heat of formation, should be closely connected with the stereoselectivity in the intermolecular addition of the cyclized radical. Since the orbital of the radical is perpendicular to the benzene ring, the direction of the benzene ring is controlled by the direction of the radical orbital as shown in Scheme 4.7. On the other hand, the direction of the carbonyl group is preferentially faced to form eclipsed conformation with a hydrogen atom of the chiral center (Scheme 4.8).[2] For (-,*S*)-**14**, the conflict of direction between the benzene ring and the carbonyl groups had an adverse influence on the heat of formation of cyclized radical.

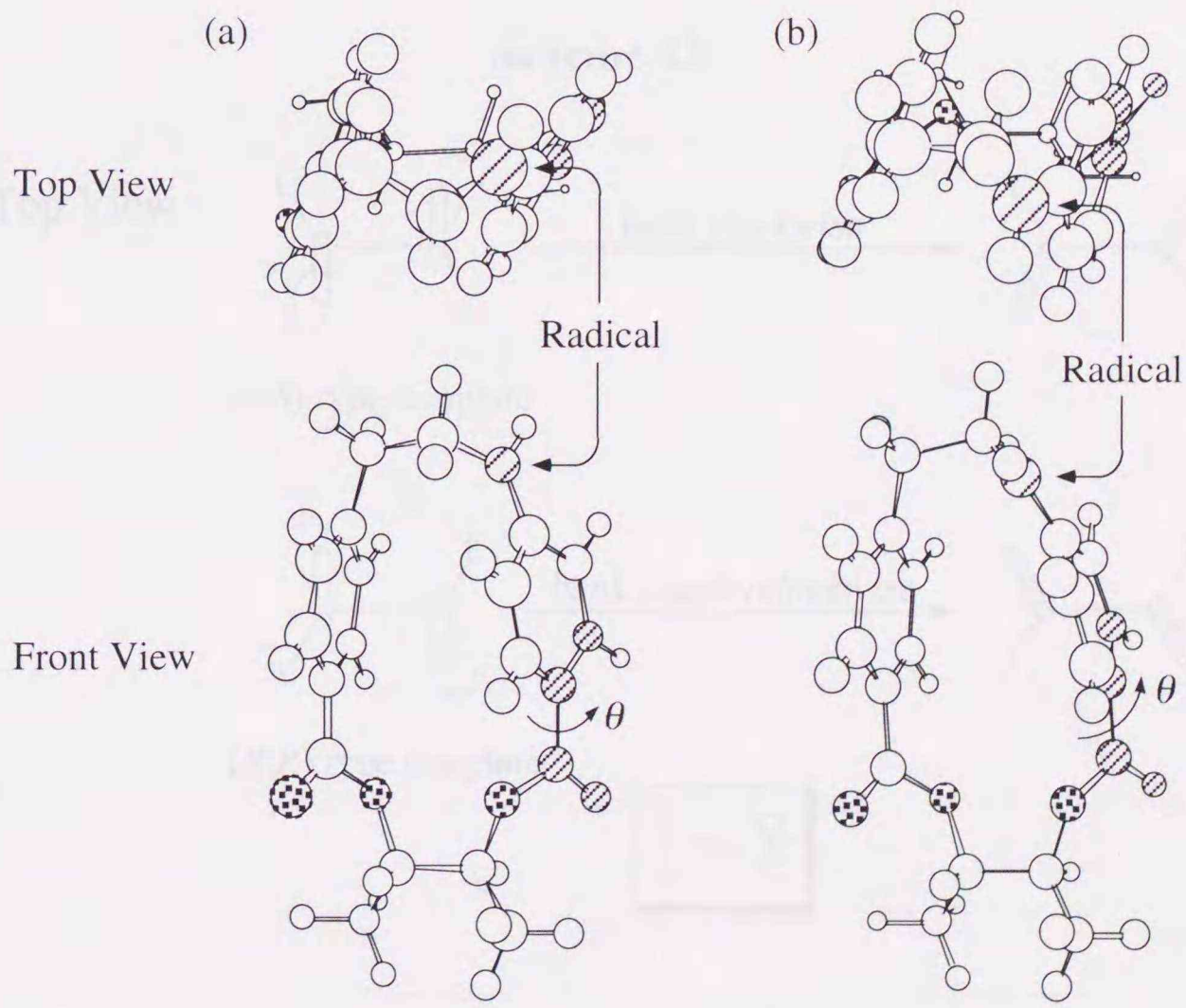

Figure 4.6. The structures of cyclized radicals (-,*R*)-**14a** (a) and (-,*S*)-**14a** (b) estimated using MOPAC6-UHF-AM1 method. The torsion angles θ are listed in Table 4.6.

Scheme 4.7

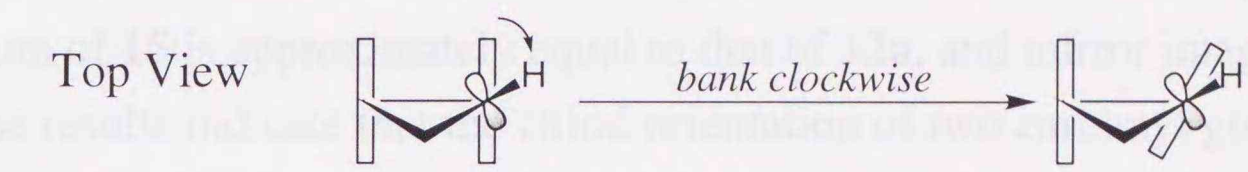

(-,*R*)-**14**

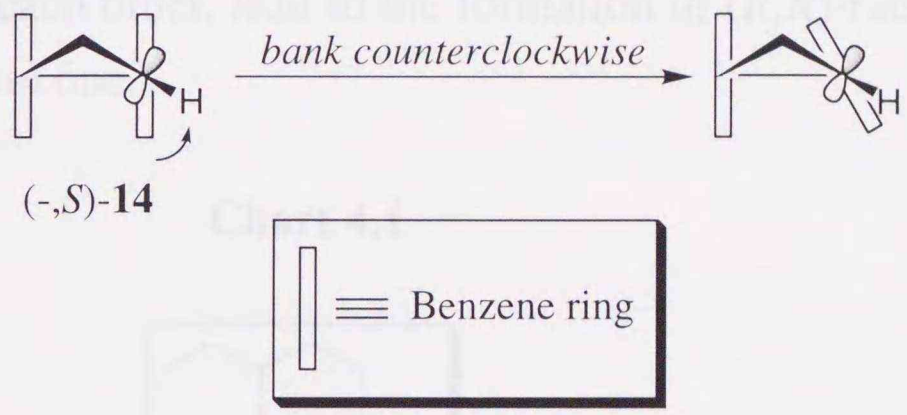

(-,*S*)-**14**

Scheme 4.8

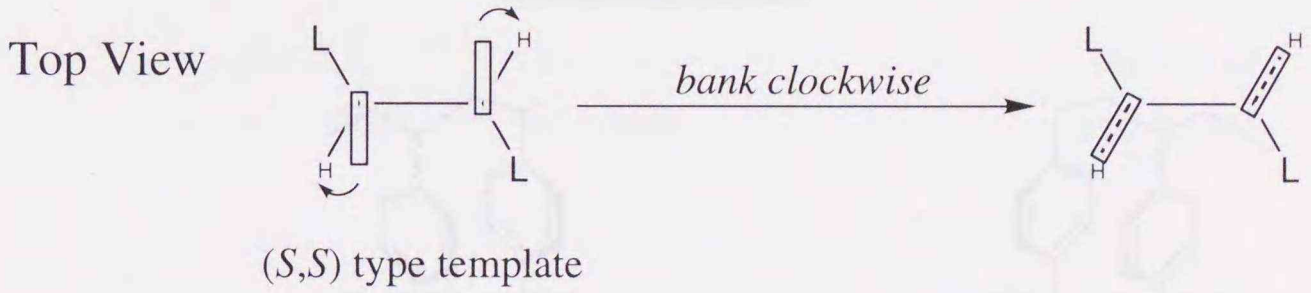

(*S*,*S*) type template

(*R*,*R*) type template

In order to the estimate the effect of the direction of the carbonyl groups, the heat of formation of **15** and **16** as shown in Chart 4.1 were calculated using MOPAC6-UHF-AM1 method. For both of **15** and **16**, the bond vectors of the two carbonyl groups are opposite in direction. However, **15** takes a conformation where their *Si* faces are directed toward the inside similar to that of **12a**, and *vise versa* for **16**. The results are listed in Table 4.7. The calculated distribution of the ring inversion equilibrium of **15** is approximately equal to that of **12a**, and mirror image to that of **16**. These results indicate that the chiral orientation of two carbonyl groups due to chiral template exhibits the stereoselctivity in the intermolecular addition of the cyclized radical. The conformer **15**, in which the *Si* face for the carbonyl groups of the 4-vinylbenzoate face each other, lead to the formation of (*R*,*R*)-racemo cyclic unit rather that (*S*,*S*)-racemo one.

Chart 4.1

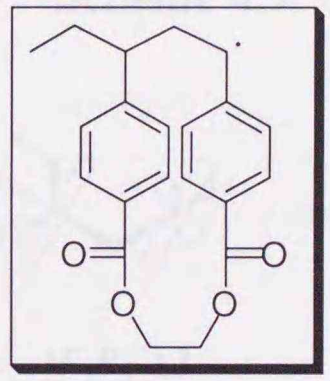

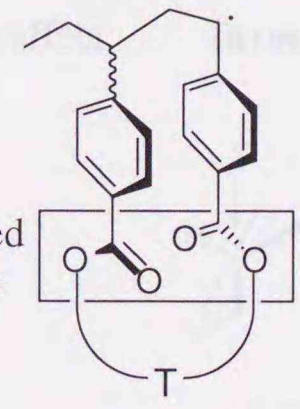

15

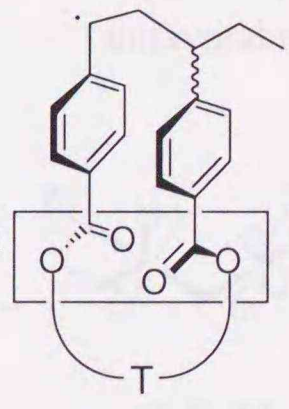

16

Table 4.7. The calculated heat of formation (kcal·mol^{-1}) of radicals **15** and **16** using MOPAC6-AM1 method.

	(*R*)-cyclized radical		(*S*)-cyclized radical	
	(*R*,*R*)-	(*R*,*S*)-	(*S*,*R*)-	(*S*,*S*)-
15	-106.0 (46.4 %)[a]	-106.1 (53.6 %)	-107.1 (97.6 %)	-104.5 (2.4 %)
16	-104.5 (2.4 %)	-107.1 (97.6 %)	-106.1 (53.6 %)	-106.0 (46.4 %)

[a] The values in parenthesis were partition percentage on ring inversion equilibrium at 80 ℃.

The stereoselectivity in the addition of the cyclized radical can be explained by considering the stereoelectronic effect of the radical and the steric effect of the penultimate group (Scheme 4.9). For (*R*,*R*)-**12** and (*R*,*S*)-**12**, the stereoelectronic effect selects (*R*,*R*)-**12** rather than (*R*,*S*)-**12**, whereas the steric effect selects (*R*,*S*)-**12** rather than (*R*,*R*)-**12**. The conflict, therefore, lowered the stereoselectivity in the addition of the cyclized radical. For (*S*,*S*)-**12** and (*S*,*R*)-**12**, on the other hand, both of the stereoelectronic and the steric effects selects (*S*,*R*)-**12** rather than (*S*,*S*)-**12**. Hence the cooperative effect resulted in the excellent stereoselection for the (*S*)-cyclized radical.

Scheme 4.9

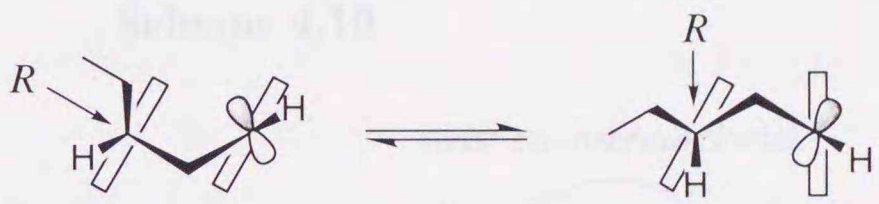

	(*R*,*R*)-**12**	(*R*,*S*)-**12**
Steric effect	unfavorable	**favorable**
Stereoelectronic effect	**favorable**	unfavorable

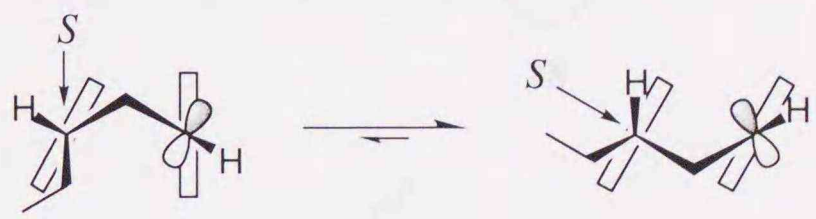

	(*S*,*S*)-**12**	(*S*,*R*)-**12**
Steric effect	unfavorable	**favorable**
Stereoelectronic effect	unfavorable	**favorable**

4.3 Summary for Chirality Induction Mechanism

Chiral template biases two conformational elements, i.e., chiral twist of two 4-vinylbenzoyl groups and chiral orientation of two carbonyl groups (Scheme 4.10). With the stereoelectoronic effect of radical addition and the steric effect of penultimate group in the transition state, the conformation **17** in which two 4-vinylbenzoyl groups twist clockwise preferentially forms (*R*)-configuration in the intramolecular cyclization, and *vise versa* for **18**. For the intermolecular addition of cyclized radical, the stereoselectivity is explicable on the basis of the ring inversion equilibrium of the cyclized radical. Because of the stereoelectronic effect of the radical on the conformation of the benzene ring and the steric effect of the penultimate group, the conformation **19** in which two carbonyl groups direct each *Si* face toward inside leads to the formation of (*R*,*R*)-configuration unit than (*S*,*S*)-configuration one, *vise versa* for **20**.

Scheme 4.10

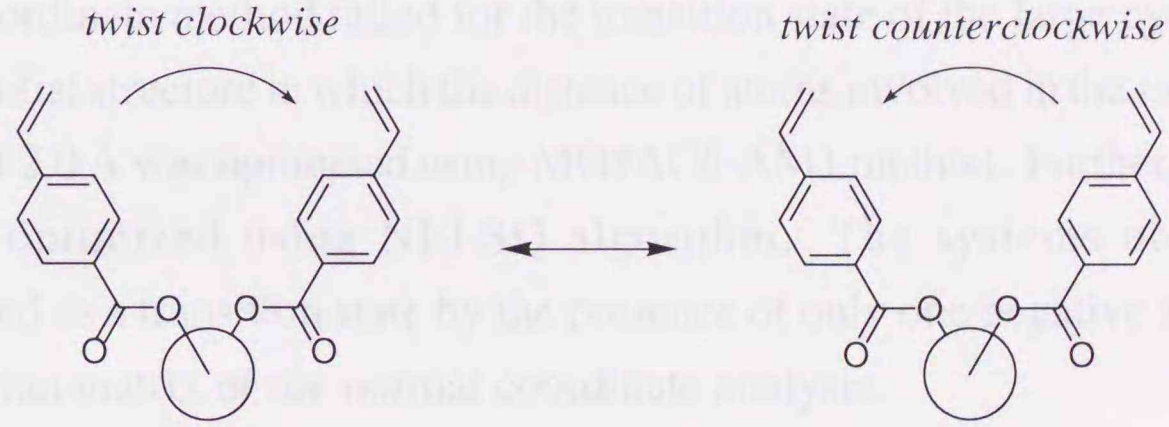

17 **18**

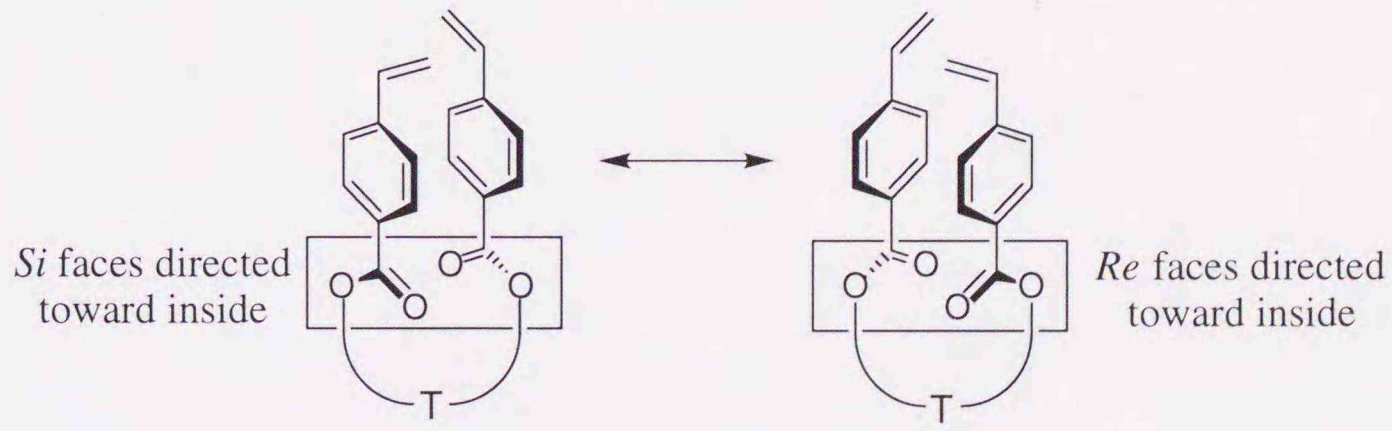

19 **20**

4.4 Procedures

The molecular mechanics and the semiempirical molecular orbital calculation were carried out using MM2[3] and MOPAC6-AM1[4] method (implemented in MacGAMESS ver 6[5]). All the open-shell systems were treated with the unrestricted Hartree-Fock procedure (MOPAC6-UHF-AM1[4]).

Conformer distribution was calculated as follows: The set of initial structures for the MM2 calculation consisted of conformers having the staggered forms of carbons in the template and was assembled by consideration of all combinations that could face the prochiral carbonyl groups in the monomer (i.e., *Re-Re*, *Re-Si*, *Si-Re*, *Si-Si* faces). In this manner, the number of initial structures obtained is 12 for **1a**, 36 for **1b**, and 108 for **1c**. The optimization of the initial structure using MM2 calculation gave a set of equilibrium structures and its steric energy. Then, relative free energy of a conformer was estimated using the steric energy as the enthalpy term and the symmetry number as the entropy term. The conformer distribution was calculated according to the Boltzmann distribution using the free energy at 353 K.

The saddle points were calculated as follows: In most case, attempts using the reaction coordinate method failed for the transition state of the large cyclic structure. Then, the initial structure in which the distance of atoms involved in the radical addition was fixed at 2.0 Å was optimized using MOPAC6-AM1 method. Further, this structure was fully optimized using NLLSQ algorithm. The systems obtained were characterized as a transition state by the presence of only one negative force constant in the Hessian matrix of the normal coordinate analysis.

4.5 References

(1) Houk, K. N.; Paddon-Row, M. N.; Spellmeyer, D. C.; Rondan, N. G.; Nagase, S. *J. Org. Chem.* **1986**, *51*, 2874.

(2) Methineson, A. McL. *Tetrahedron Lett.* **1965**, 4137.

(3) Allinger, N. A. *J. Am. Chem. Soc.* 1977, 99, 8127.

(4) Dewer, M. J. S.; Zoebisch, E. G.; Healy, E. F.; Stewart, J. J. P. *J. Am. Chem. Soc.* **1985**, *107*, 3902.

(5) Schmidt, M. W.; Baldridge, K. K.; Boatz, J. A.; Elbert, S. T.; Gordon, M. S.; Jensen, J. H.; Koseki, S.; Matsunaga, N.; Nguyen, K. A.; Su, S. J.; Windus, T. L.; Dupuis, M.; Montgomery, J. A. *J. Comput. Chem.* **1993**, *14*, 1347.

Chapter 5

Effect of the Total Monomer Concentration on the Chirality Induction

5.1 Introduction

The chirality induction mechanism described in the chapter 4 requires the equilibrium on the ring inversion of the cyclized radical. As for the ring inversion of radical species, Fessenden et. al. reported a kinetic study of the ring inversion of cyclohexyl radical using ESR spectroscopy.[1] According to their study, the activation energy for ring inversion of cyclohexyl radical is 4.9 kcal·mol^{-1}. This value is low enough for concurrent occurrence in the polymerization system by comparison with the activation energy of propagation in radical polymerization.[2] The rate of ring inversion is independent of total monomer concentration, whereas other competitive elemental reactions are proportional to total monomer concentration. Therefore, the examination of the effect of the total monomer concentration on chirality induction would clarify whether ring inversion functions or not.

In this chapter, the cyclocopolymerization of (2*S*,3*S*)-2,3-butanediyl, (2*S*,4*S*)-2,4-pentanediyl, and (2*S*,5*S*)-2,5-hexanediyl bis(4-vinylbenzoate) (**1a**, **1b**, and **1c**, respectively) with styrene were carried out at several total monomer concentrations in the range of 0.05 to 0.09 mol·L^{-1} (Scheme 5.1). The effect of the total monomer concentration was discussed on the basis of the specific rotation of the template-free polymer.

Scheme 5.1

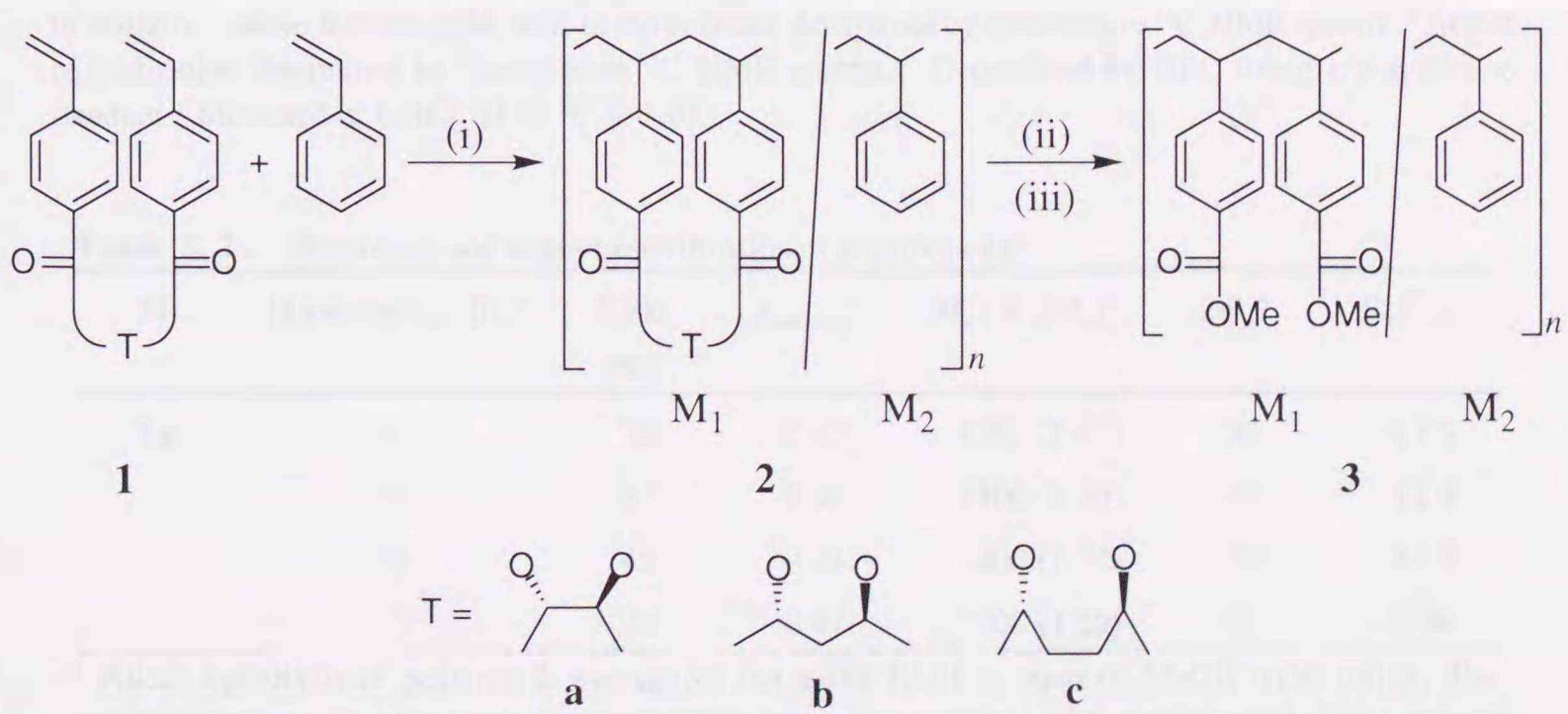

Conditions: (i) AIBN, toluene, 60 °C; (ii) KOH, MeOH, reflux; (iii) CH_2N_2, Et_2O

5.2 Results and Discussion

5.2.1 Molecular Weight Dependency of Chiroptical Property

The cyclocopolymerization of (2*S*,3*S*)-2,3-butanediyl bis(4-vinylbenzoate) (**1a**, M_1) with styrene (M_2) were carried out under the condition of the $[\mathbf{1}+\text{styrene}]_0/[\text{AIBN}]_0$ molar ratio of 31, 15, 10, and 5. The results are listed in Table 5.1. The mole fraction of M_1 unit (f_1) and the extent of cyclization (f_c) of the resulting polymer **2a** were substantially constant at the value of 0.28 and 0.96, respectively, while the degree of polymerization on the basis of the monomer unit (DP_n) decreased from 26 to 15 with a decrease of the $[\mathbf{1}+\text{styrene}]_0/[\text{AIBN}]_0$ molar ratio. In order to estimate the molecular weight dependency of the chiroptical property of the template-free polymer **3**, the removal of the chiral template from **2a** was carried out by the same procedure described in chapter 2. Table 5.2 lists the results of hydrolysis and methyl esterification. The

Table 5.1. Cyclocopolymerizations of (2*S*,3*S*)-2,3-butanediyl bis(4-vinylbenzoate) (**1a**, M_1) with styrene (M_2)[a]

M_1	$[\mathbf{1}+\text{styrene}]_0$ / $[I]_0$[b]	Time (h)	Yield (%)	f_1[c]	f_c[d]	M_n (M_w/M_n)[e]	DP_n	$[\alpha]^{23}_{435}$[f]
1a	31	12.5	16	0.27	0.96	4500 (1.48)	26	+251
	15	12.0	17	0.31	0.96	3500 (1.37)	20	+237
	10	11.5	17	0.26	0.96	3300 (1.37)	19	+229
	5	7.0	10	0.29	0.94	2600 (1.28)	15	+231

[a] Solvent, toluene; $[\mathbf{1}+\text{styrene}]_0 = 0.1\ \text{mol}\cdot\text{L}^{-1}$; Initiator, AIBN; temp, 60 °C. [b] The molar ratio of monomer to initiator. [c] Mole fraction of M_1 unit in the polymer determined by quantitative ^{13}C NMR spectra. [d] Extent of cyclization determined by quantitative ^{13}C NMR spectra. [e] Determined by GPC using a polystyrene standard. [f] Measured in $CHCl_3$ at 23 °C (*c* 1.0).

Table 5.2. Hydrolysis and methyl esterification of polymers **2a**[a]

M_1	$[\mathbf{1}+\text{styrene}]_0$ / $[I]_0$[b]	Yield (%)	f_{benzoate}[c]	M_n (M_w/M_n)[d]	DP_n[e]	$[\alpha]^{23}_{435}$[f]
1a	31	72	0.45	4200 (1.41)	32	-11.8
	15	47	0.45	3400 (1.30)	26	-11.9
	10	45	0.44	3400 (1.27)	26	-11.2
	5	24	0.47	2700 (1.20)	21	-10.8

[a] Alkali hydrolysis of polymer **2** was carried out using KOH in aqueous MeOH under reflux. The resulting polymer was treated with diazomethane in benzene-ether to yield the polymer **3**. [b] The ratio of monomer to initiator [c] Mole fraction of methyl benzoate unit in the polymer **3** determined by ^1H NMR spectra. [d] Determined by GPC using a polystyrene standard. [e] Degree of polymerization on the basis of the vinyl groups. [f] Measured in $CHCl_3$ at 23 °C (*c* 1.0).

peaks due to chiral template disappeared in the ^{1}H NMR spectrum, indicating that the removal of the chiral template was completely performed. The degree of polymerization on the basis of the vinyl group (DP_n') decreased from 32 to 21 with a decrease of the [**1**+styrene]$_0$/[AIBN]$_0$ molar ratio in the polymerization. The specific rotation ([α]$_{435}$, *c* 0.1, $CHCl_3$) of **2a** practically constant within the range from -11.8 to -10.8°. As long as the DP_n' ranges from 32 to 21, therefore, the DP_n' has no influence on the chiroptical property of the polymer **3**.

5.2.2 Effect of the Monomer Concentration on the Chirality Induction

The cyclocopolymerizations of **1a**, **1b**, and **1c** (M_1) with styrene (M_2) were carried out under the condition of the [**1**+styrene]$_0$ ranging from 0.09 to 0.05 mol·L^{-1}, and the results are listed in Table 5.3. The mole fraction of M_1 unit (f_1) and the extent of cyclization (f_c) of the resulting polymers **2a-c** were practically constant. The decrease of the [**1**+styrene]$_0$ values caused to decrease the number-average molecular weight (M_n) from 3200 to 2500 for **2a**, from 3300 to 2700 for **2b**, and from 3300 to 2300 for **2c**. The effect of the decrease in the [**1**+styrene]$_0$ is similar to that in the [**1**+styrene]$_0$/

Table 5.3. Cyclocopolymerizations of (2*S*,3*S*)-2,3-butanediyl, (2*S*,4*S*)-2,4-pentanediyl, and (2*S*,5*S*)-2,5-hexanediyl bis(4-vinylbenzoate)s (**1a**, **1b**, and **1c**, respectively, M_1) with styrene (M_2)[a]

M_1	[**1**+styrene]$_0$[b] (mol·L^{-1})	Time (h)	Yield (%)	f_1[c]	f_c[d]	M_n (M_w/M_n)[e]	DP_n	[α]$^{23}_{435}$[f]
1a	0.09	16	22	0.27	0.96	3200 (1.50)	19	+244
	0.08	22	20	0.27	0.96	3200 (1.40)	19	+234
	0.07	28	22	0.26	0.97	2900 (1.42)	17	+236
	0.06	38	24	0.29	0.97	2800 (1.36)	16	+239
	0.05	48	23	0.24	0.97	2500 (1.40)	15	+246
1b	0.09	9	14	0.28	1.00	3300 (1.43)	19	+236
	0.06	24	17	0.25	1.00	2900 (1.30)	17	+252
	0.05	30	18	0.25	1.00	2700 (1.30)	16	+248
1c	0.09	16	24	0.24	0.96	3300 (1.49)	19	+190
	0.08	22	22	0.23	0.96	3000 (1.45)	18	+190
	0.07	28	29	0.24	0.96	2800 (1.44)	16	+192
	0.06	38	27	0.25	0.98	2700 (1.40)	16	+194
	0.05	48	33	0.21	0.98	2300 (1.48)	14	+197

[a] Solvent, toluene; [**1**+styrene]$_0$/[AIBN]$_0$ = 15; mole fraction of **1** in feed (F_1), 0.1; temp, 60 °C. [b]. Total monomer concentration. [c] Mole fraction of M_1 unit in the polymer determined by ^{1}H and quantitative ^{13}C NMR spectra. [d] Extent of cyclization determined by quantitative ^{13}C NMR spectra. [e] Determined by GPC using a polystyrene standard. [f] Measured in $CHCl_3$ at 23 °C (*c* 1.0).

$[AIBN]_0$ ratio on the degree of polymerization of polymer **2**. However, the decrease in the $[\mathbf{1}+\text{styrene}]_0$ influenced on the ^{13}C NMR spectra of **2a**, while the decrease in the $[\mathbf{1}+\text{styrene}]_0/[AIBN]_0$ ratio has no influence on those. Figure 5.1 shows the expanded ^{13}C NMR spectra of **2a** within the region of the methyl carbon of the template, indicating that the change in the $[\mathbf{1}+\text{styrene}]_0$ leads to the monotonous change in the distribution of the cyclic structure.

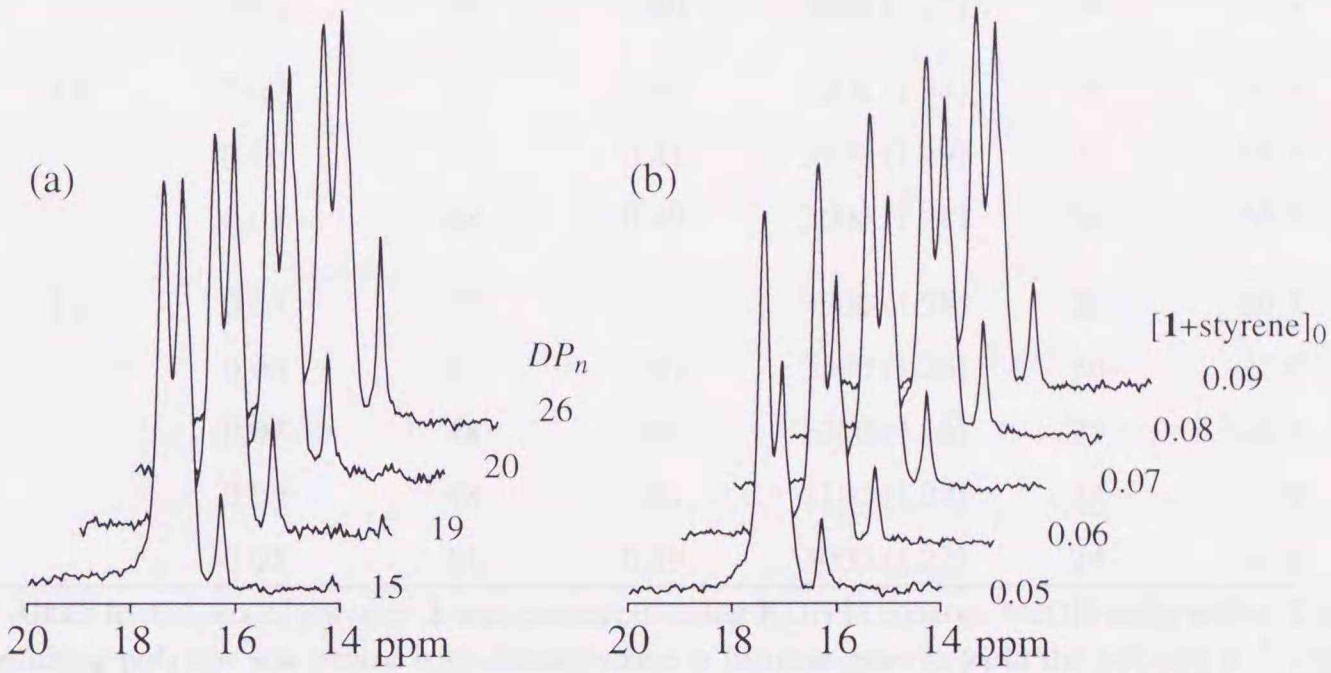

Figure 5.1. The molecular weight dependency (a) and the total monomer concentration dependency (b) of expanded ^{13}C NMR spectra of polymers **2a** (template methyl region).

The quantitative removal of the chiral template from **2a**-**c** was carried by the same procedure described in chapter 2, and the results are listed in Table 5.4. With the decrease in the $[\mathbf{1}+\text{styrene}]_0$, the absolute value of specific rotation ($[\alpha]_{435}$, *c* 0.1, $CHCl_3$) increased from 13.0 to 19.5 for **3a**, from 52.5 to 55.9 for **3b**, and from 26.5 to 32.6 for **3c** (Figure 5.2). Because the DP_n' values of **3a**-**c** falls in the range from 32 to 21, these changes in the chiroptical property are attributable to the effect of the total monomer concentration ($[\mathbf{1}+\text{styrene}]_0$).

5.2.3 Ring Inversion of the Cyclized Radical

The optical rotatory power of polymer **3** increased with a decrease of the total monomer concentration without change in values of f_1 and f_c. These results mean that the change in the total monomer concentration leads to the change in the optical purity of the cyclic unit, i.e., chirality induction efficiency. Because the intramolecular cyclization is independent from the monomer concentration, the change in optical rotatory power is attributable to that in stereoselectivity in the intermolecular addition

Table 5.4. Hydrolysis and methyl esterification of polymers **2a-c**[a]

M_1	[**1**+styrene]$_0$[b] (mol·L^{-1})	Yield (%)	$f_{benzoate}$[c]	M_n (M_w/M_n)[d]	DP_n[e]	$[\alpha]^{23}_{435}$[f]
1a	0.09	29	0.43	3400 (1.36)	26	-13.0
	0.08	20	0.40	3400 (1.28)	27	-13.7
	0.07	38	0.40	3200 (1.28)	25	-15.8
	0.06	25	0.41	3400 (1.21)	27	-17.4
	0.05	30	0.40	3000 (1.22)	24	-19.5
1b	0.09	20	0.45	3700 (1.34)	28	-52.5
	0.06	70	0.41	3100 (1.29)	24	-55.7
	0.05	48	0.39	3000 (1.28)	24	-55.9
1c	0.09	45	0.42	3600 (1.28)	28	-26.5
	0.08	45	0.43	3300 (1.26)	26	-27.6
	0.07	48	0.41	3200 (1.26)	25	-28.6
	0.06	48	0.41	3100 (1.24)	24	-30.4
	0.05	51	0.39	3000 (1.23)	24	-32.6

[a] Alkali hydrolysis of polymer **2** was carried out using KOH in aqueous MeOH under reflux. The resulting polymer was treated with diazomethane in benzene-ether to yield the polymer **3**. [b] The total monomer concentration in the polymerization [c] Mole fraction of methyl benzoate unit in the polymer **3** determined by ^{1}H NMR spectra. [d] Determined by GPC using a polystyrene standard. [e] Degree of polymerization on the basis of the vinyl group. [f] Measured in $CHCl_3$ at 23 ℃ (*c* 1.0).

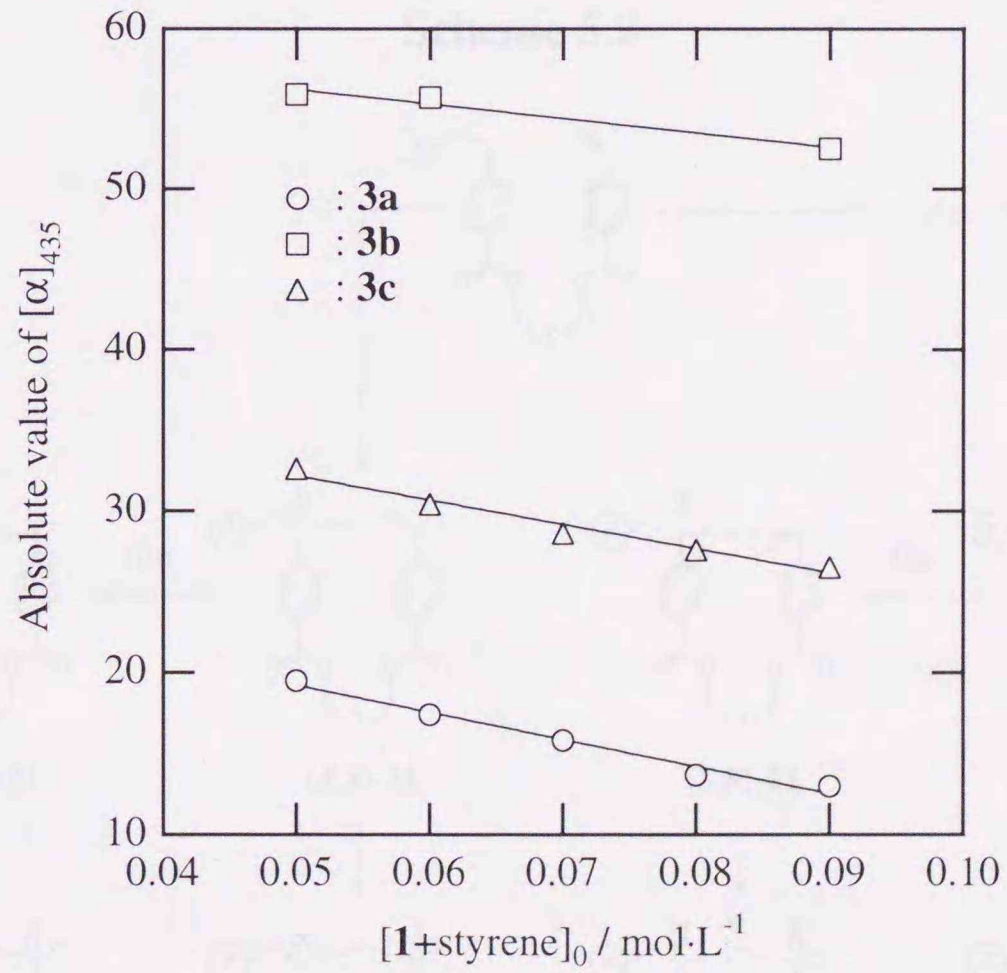

Figure 5.2. Specific rotations ($[\alpha]_{435}$, *c* 0.1, $CHCl_3$) of polymers **3a** (○), **3b** (□), and **3c** (△).*versus* the total monomer concentration ([**1**+styrene]$_0$) in the polymerization.

of the cyclized radical. According to the chirality induction mechanism described in chapter 4, the stereoselectivity in the intermolecular addition of the cyclized radical depends on the equilibrium for the ring inversion of the cyclized radical. Therefore, these results mean that the cyclocopolymerization proceeded under nonequilibrium situation on the ring inversion of the cyclized radical.[3] The enhancement of the chirality induction is explained as follows (see Scheme 5.2). (1) The bis(4-vinylbenzoate) monomer having positive chirality preferentially forms the cyclized radicals (*R*,*S*)-**21** and (*S*,*S*)-**21** by the stereoelectronic effect of radical addition. (2) In order to reach the equilibrium condition, the cyclized radicals (*R*,*S*)-**21** and (*S*,*S*)-**21** are transformed into (*R*,*R*)-**21** and (*S*,*R*)-**21**, respectively, through the ring inversion until the cyclized radical attacks to other monomers. (3) Because the rate of the intermolecular addition of the cyclized radical is proportional to the monomer concentration, the decrease in the total monomer concentration extends the life time of the cyclized radical to enhance the chirality induction efficiency, i.e. the excess amount of the (*R*,*R*)-cyclic unit over the (*S*,*S*)-cyclic unit.

Scheme 5.2

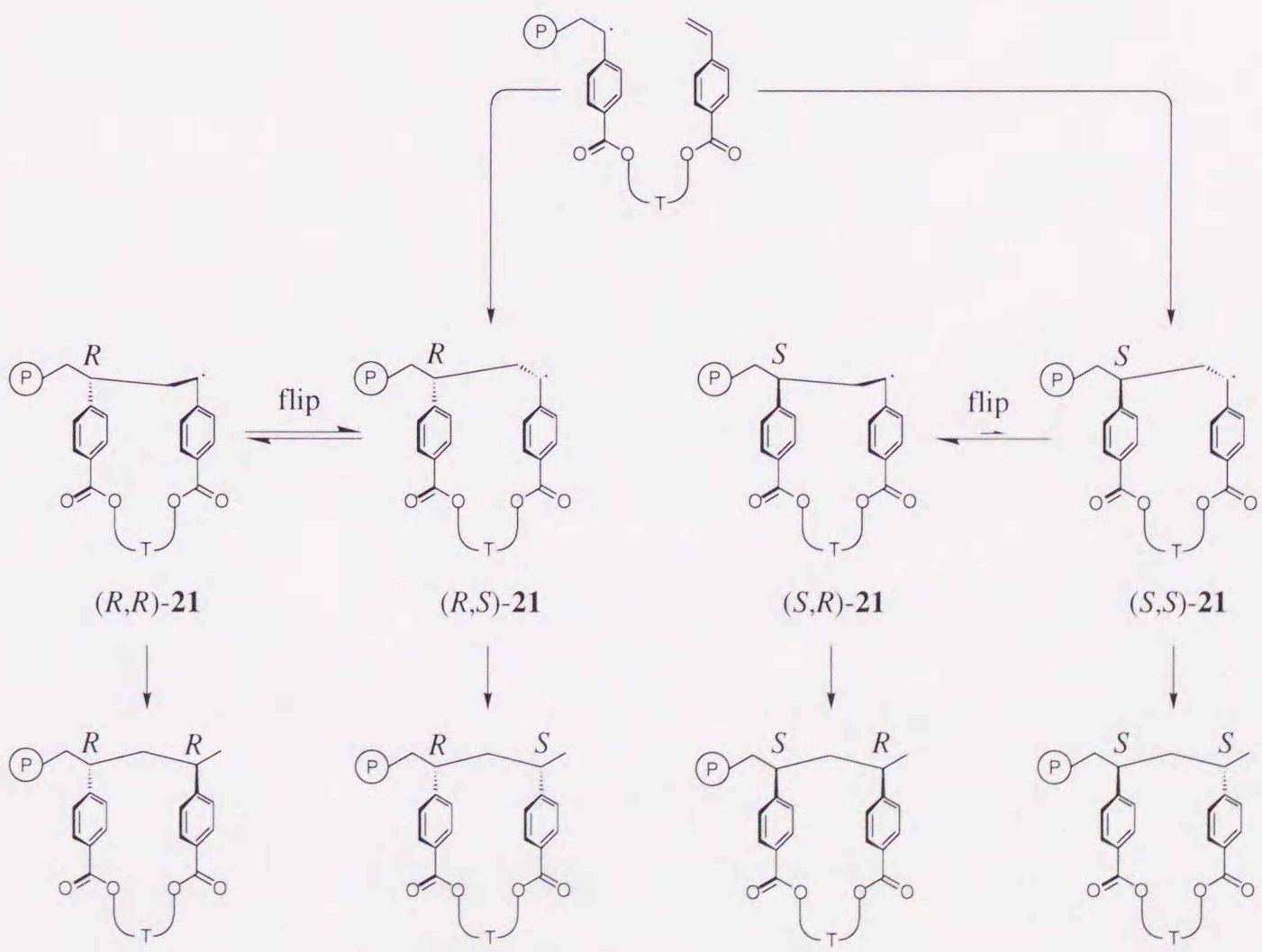

5.3 Conclusions

The cyclocopolymerization of (2*S*,3*S*)-2,3-butanediyl, (2*S*,4*S*)-2,4-pentanediyl, and (2*S*,5*S*)-2,5-hexanediyl bis(4-vinylbenzoate)s (**1a**, **1b**, and **1c**, respectively) with styrene were carried out under the condition of the $[\mathbf{1}+\text{styrene}]_0$ ranging of 0.09 to 0.05 mol·L^{-1}. For the template-free polymer **3a**-**c**, the optical rotatory power increased with a decrease in the total monomer concentration ($[\mathbf{1}+\text{styrene}]_0$). The effect of the total monomer concentration was explicable by the chirality induction mechanism described in chapter 4.

5.4 Experimental Section

Measurements. ^{1}H and ^{13}C NMR spectra were recorded using JEOL JNM-EX270 and JNM-A400II instruments. Quantitative ^{13}C NMR spectra were obtained at 30 °C in $CDCl_3$ (100 mg·mL^{-1}; delay time 7.0 seconds; inverse gated decoupling). The molecular weight of the resulting polymers was measured by gel permeation chromatography (GPC) in tetrahydrofuran on a Jasco GPC system (GPC-900) equipped with three polystyrene gel columns (Shodex KF-804L). The number-average molecular weight (M_n) was calculated on the basis of a polystyrene calibration. Optical rotations were measured with a Jasco DIP-1000 digital polarimeter.

Materials. Toluene was refluxed over sodium benzophenone ketyl and distilled just before use. 2,2'-Azobis(2-methylpropionitrile) (AIBN) was recrystallized from methanol. (2*S*,3*S*)-2,3-Butanediyl, (2*S*,4*S*)-2,4-pentanediyl, and (2*S*,5*S*)-2,5-hexanediyl bis(4-vinylbenzoate) (**1a**, **1b**, and **1c**, respectively) were synthesized according to procedures similar to those described in chapter 2.

Cyclocopolymerization. The polymerization was carried out according to the similar procedure as that described in chapter 2.

Poly[(methyl 4-vinylbenzoate)-*co*-styrene] (3). The similar procedures as those described in chapter 2 were applied.

5.5 References

(1) Ogawa, S.; Fessenden, R. W.; *J. Chem. Phys.* **1964**, *41*, 994.

(2) 6.9 kcal·mol^{-1} for the polymerization of styrene, cite in Hughes, J.; North, A. M.; *J. Chem. Soc., Faraday. Trans.* 1966, 62, 1866.

(3) The same nonequilibrium situation was observed in the radical polymerization of bulky esters of methacrylate such as triphenylmethyl methacrylate. Nakano, T.; Matsuda, A.; Okamoto, Y. *Polym. J.* **1996**, *28*, 556.

Chapter 6

Conformational Effect of Monomer on the Chirality Induction

6.1 Introduction

As described in chapter 4, the computational study indicated that the chirality induction is controlled by the direction of carbonyl groups as well as the chiral twist of two 4-vinylbenzoyl groups. For bis(4-vinylbenzoate) of 1,2-diols, Chart 6.1 shows the conformations formed by the combination of the direction of the carbonyl groups and the chiral twist of two 4-vinylbenzoyl groups. In general, most monomers having 1,2-diol template take conformer **22**. Thus, it is interesting to confirm the chirality induction of the monomer being the conformer **23** (i.e., conformational effect of monomers). Yamamoto et. al. reported that the stable conformation of dibenzoyl L-tartaric acid was different from that of dibenzoate of (2*S*,3*S*)-2,3-butanediol in spite of their same configuration on the chiral center.[1] Thus, the tartaric acid derivatives are well suitable as templates to confirm the conformational effect of monomer.

Chart 6.1

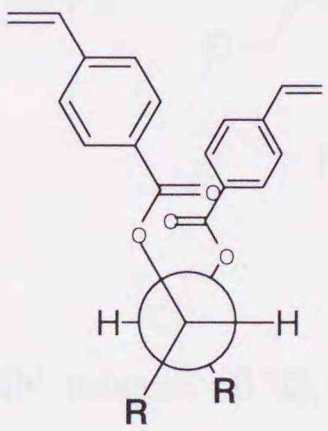

22

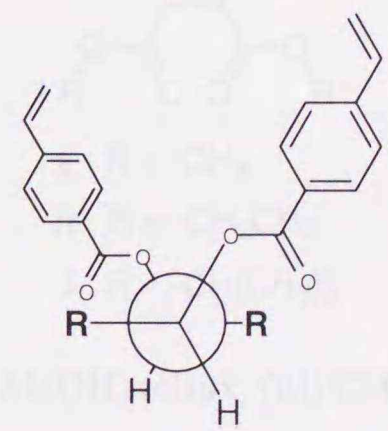

23

In this chapter, the cyclocopolymerization of methyl, ethyl, and isopropyl 2,3-bis-*O*-(4-vinylbenzoyl)-L-tartarate (**1g**, **1h**, and **1i**, respectively) and (2*S*,3*S*)-1,4-dimethoxy-2,3-butanediyl bis(4-vinylbenzoate) (**1f**, i.e., the decarbonyl analog of **1g**) with styrene were carried out (Scheme 6.1). The conformational effect was discussed on the basis of the CD spectral analysis of monomer conformations and the comparison of the chiroptical property of the template-free polymers.

Scheme 6.1

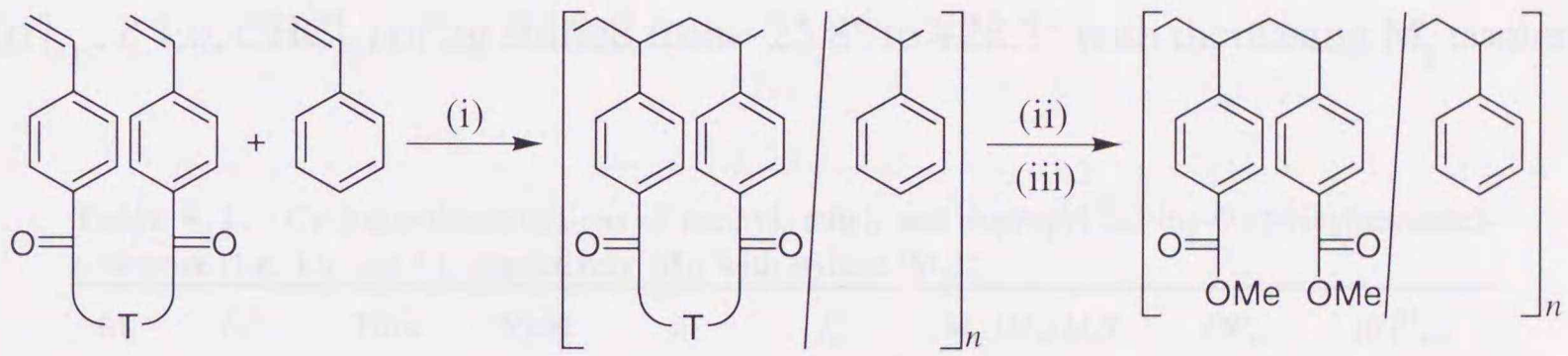

M_1 M_2 M_1 M_2

1 **2** **3**

T = **f**

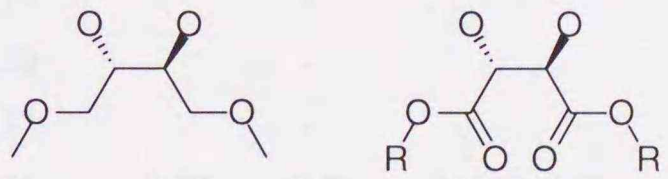

g : R = -CH_3

h : R = -CH_2CH_3

i : R = -$CH(CH_3)_2$

Conditions: (i) AIBN, toluene, 60 °C; (ii) KOH, MeOH, reflux; (iii) CH_2N_2, Et_2O-benzene

6.2 Results and Discussion

*6.2.1 Cyclocopolymerizations of Monomers **1g-i** with Styrene*

The cyclocopolymerizations of methyl 2,3-bis-*O*-(4-vinylbenzoyl)-L-tartarate (**1g**, M_1) with styrene (M_2) were carried out using AIBN in toluene at 60 °C, and the results are listed in Table 6.1. For a mole fractions of less than 0.5 in the feed of **1g**, the obtained polymers were soluble in organic solvents. The extent of cyclization (f_c), which was estimated by quantitative ^{13}C NMR spectroscopy, varied from 0.74 to 0.80 for copolymer **2g**. The number-average molecular weights (M_ns) of **2g** increased from 3200 to 14800 with an increase in the mole fraction of **1g** in the feed. As the content of the M_1 unit in the polymer was higher than that in the feed, the copolymerization reactivity of **1g** was higher than that of styrene. The specific rotation ($[\alpha]_{435}$, *c* 1.0, $CHCl_3$) of **2g** shifted from -25.8° to +28.3° with increasing M_2 content.

Table 6.1. Cyclocopolymerizations of methyl, ethyl, and isopropyl 2,3-bis-*O*-(4-vinylbenzoate)-L-tartarate (**1 g**, **1 h**, and **1 i**, respectively, M_1) with styrene (M_2).[a]

M_1	F_1[b]	Time (h)	Yield (%)	f_1[c]	f_c[d]	M_n (M_w/M_n)[e]	DP_n	$[\alpha]^{23}_{435}$[f]
1 g	0.9	2.0	14	-	-	-	-	-
	0.8	2.5	17	-	-	-	-	-
	0.7	3.0	20	-	-	-	-	-
	0.6	3.5	27	-	-	-	-	-
	0.5	5.5	21	0.87	0.74	14800 (8.87)	37	-25.8
	0.4	5.5	15	0.72	0.76	7300 (2.60)	21	-39.5
	0.3	6.9	23	0.50	0.80	9200 (1.94)	34	+1.0
	0.2	9.0	21	0.39	0.78	5400 (2.04)	23	+23.3
	0.1	17.0	18	0.26	0.79	3200 (2.12)	17	+28.3
1 h	0.2	9.0	26	0.37	0.88	5800 (1.96)	24	+4.3
	0.1	17.0	18	0.27	0.87	3600 (1.88)	18	+12.5
1 i	0.2	9.0	24	0.37	0.88	6900 (1.81)	28	-15.9
	0.1	17.0	24	0.21	0.87	4000 (1.88)	21	-4.4

[a] Solvent, toluene; $[\mathbf{1}+\text{styrene}]_0 = 0.1$ mol·L^{-1}; $[\text{AIBN}]_0 = 6.1$ mmol·L^{-1}; temp, 60 °C. [b] Mole fraction of **1** in the monomer feed. [c] Mole fraction of M_1 unit in the polymer determined by ^1H and quantitative ^{13}C NMR spectra. [d] Extent of cyclization determined by quantitative ^{13}C NMR spectra. [e] Determined by GPC using a polystyrene standard. [f] Measured in $CHCl_3$ at 23 °C (*c* 1.0).

The quantitative removal of the chiral template from **2g** was carried out using methanolic KOH, followed by methyl esterification using diazomethane. The results are listed in Table 6.2. The peaks due to L-tartaric acid disappeared in the ^{1}H NMR spectrum (Figure 6.1), thus indicating that the template-free polymer was poly[(methyl 4-vinylbenzoate)-*co*-styrene] (**3g**). The specific rotation ($[\alpha]_{435}$, *c* 1.0, $CHCl_3$) of **3g** slightly increased from +0.2° to -2.9° with an increase in the M_2 content in the copolymer. Polymer **3g** was optically active though it had an lower optical rotatory power.

Table 6.2. Hydrolysis and methyl esterification of polymers **2g-i**.[a]

M_1	f_1[b]	Yield (%)	M_n (M_w/M_n)[c]	$[\alpha]^{23}_{435}$[d]
1a	(0.9)[e]	-	18700 (1.50)	-0.5
	(0.8)	-	14200 (1.73)	+0.2
	(0.7)	-	11900 (2.49)	0.0
	(0.6)	-	8000 (2.08)	-0.6
	0.87	83	7500 (1.98)	-0.7
	0.72	61	6000 (1.93)	-0.8
	0.50	74	5100 (2.14)	-0.8
	0.39	43	3200 (2.28)	-1.3
	0.26	38	2700 (1.88)	-2.9
1b	0.37	59	3600 (2.17)	-0.7
	0.27	56	2400 (1.92)	-1.1
1c	0.37	71	4600 (1.84)	-0.1
	0.21	43	3100 (1.73)	-0.8

[a] Alkali hydrolysis of polymer **2** was carried out using KOH in aqueous MeOH under reflux. The resulting polymer was treated with diazomethane in benzene-ether to yield the polymer **3**. [b] Mole fraction of M_1 unit in the polymer **2**. [c] Determined by GPC using a polystyrene standard. [d] Measured in $CHCl_3$ at 23 °C (*c* 1.0). [e] The values in parenthesis were mole fraction of **1** in the feed.

The cyclocopolymerizations of ethyl and isopropyl 2,3-bis-*O*-(4-vinylbenzoyl)-L-tartarates (**1h** and **1i**, respectively) with styrene were examined to elucidate the effect of the alkyl group of an alcohol for tartarates on the chirality induction. These results are listed in Table 6.1. The f_cs for **2h** and **2i** were slightly higher than that for **2g**. The cyclization tendency was improved by increasing the size of the alkyl group on the alcohols. The specific rotations for **2h** and **2i** showed a change from a minus sign to a plus sign, which is similar to those for **2g**. The specific rotations of **3h** were -0.7° and -1.1° and for **3i** were -0.1° and -0.8°, which were lower than those of **3g** (-1.3° and -2.9°) as listed in Table 6.2. The alkyl group on the alcohols in the tartarates had only a marginal effect on the chirality induction.

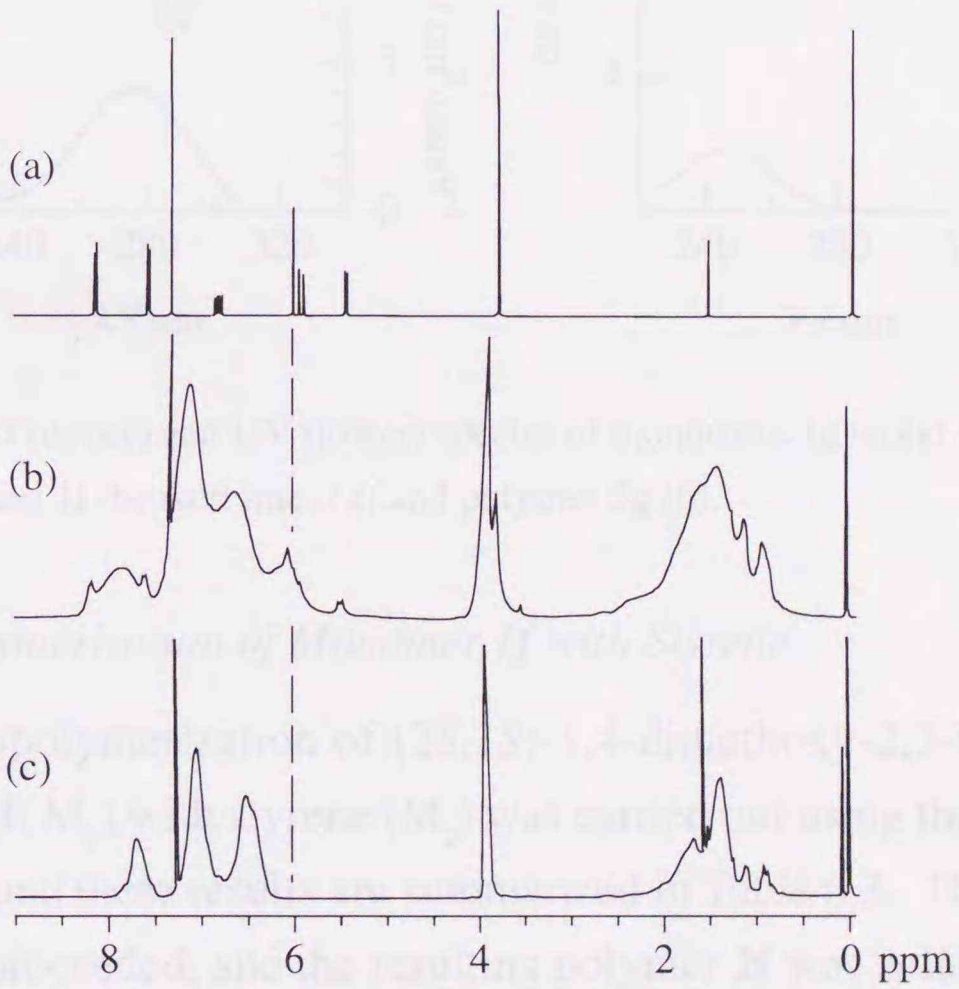

Figure 6.1. ^{1}H NMR spectra of monomer **1g** (a), polymer **2g** (b), and polymer **3g** (c).

Figure 6.2 shows the CD and UV spectra of monomers **1g-i** and polymer **3g** in HFIP. A negative Cotton effect at 287 nm and a positive Cotton effect at 262 nm due to the exciton coupling between two 4-vinylbenzoate chromophores are observed. According to the CD exciton chirality method, two 4-vinylbenzoyl groups twist counterclockwise for **1g-i**. Although monomers **1g-i** had a chiral twist of the two 4-vinylbenzoyl groups, copolymer **3g** did not exhibited a splitting Cotton effect in their CD spectra in contrast to that derived from (2*S*,3*S*)-2,3-butanediyl bis(4-vinylbenzoate) (**1a**). These results indicate that chirality induction depends on other conformational elements in addition to the chiral twist of the two 4-vinylbenzoyl groups.

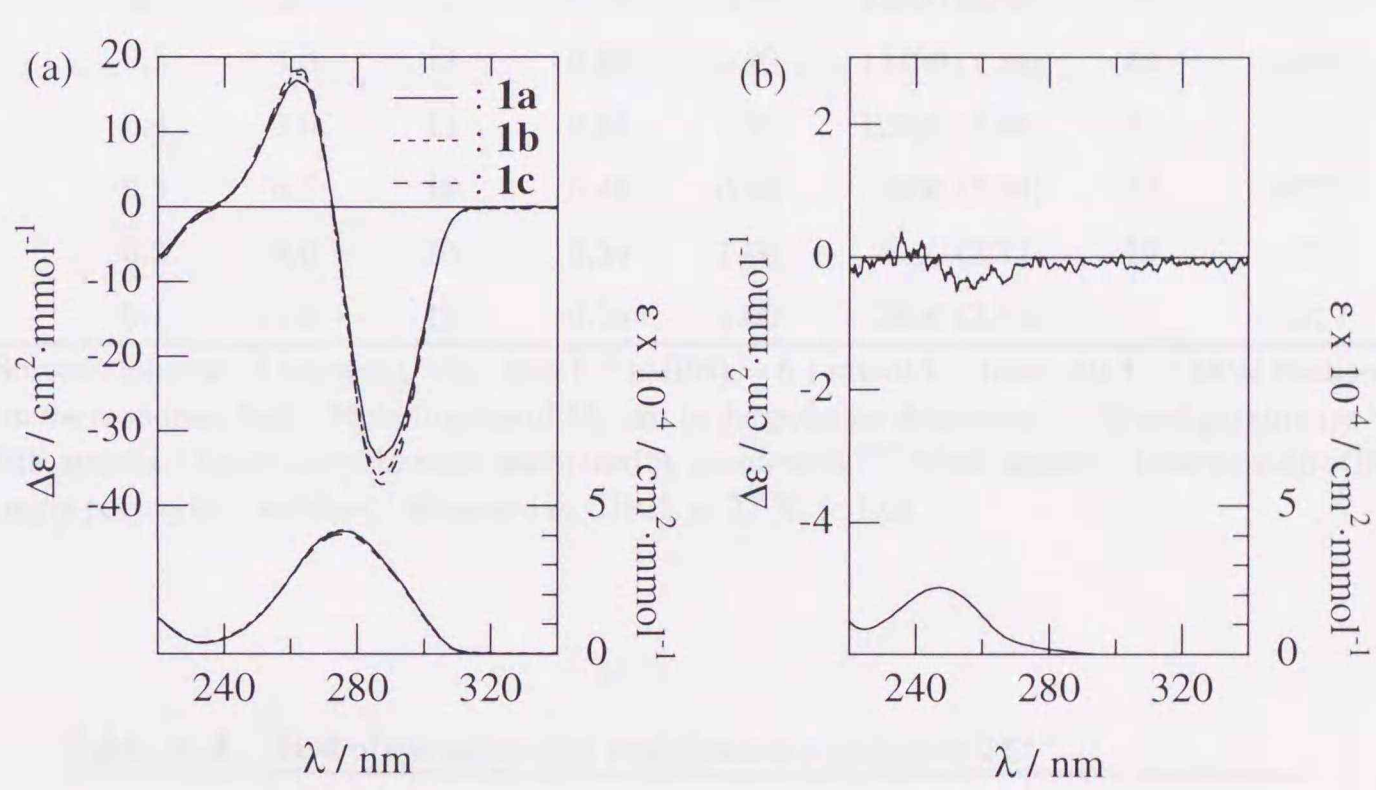

Figure 6.2. CD (upper) and UV (lower) spectra of monomers **1g** (solid line), **1h** (short broken line), and **1i** (broken line) (a) and polymer **3g** (b).

*6.2.2 Cyclocopolymerization of Monomer **1f** with Styrene*

The cyclocopolymerization of (2*S*,3*S*)-1,4-dimethoxy-2,3-butanediyl bis(4-vinylbenzoate) (**1f**, M_1) with styrene (M_2) was carried out using the same conditions as that for **1g**/St, and these results are summarized in Table 6.3. The polymerization homogeneously proceeded, and the resulting polymer **2f** was soluble in chloroform and tetrahydrofuran. The M_n of **2f** increased from 2600 to 18000 with an increase in the mole fraction of **1f** in the feed. The f_c for **2f** ranged from 0.90 to 1.00, and was higher than that for **2g**. In contrast to **2g**, **2f** showed a specific rotation ($[\alpha]_{435}$, *c* 1.0, $CHCl_3$) which was almost constant at +270° for every composition.

Table 6.3. Cyclocopolymerizations of (2*S*,3*S*)-1,4-dimethoxy-2,3-butanediyl bis(4-vinylbenzoate) (**1f**, M_1) with styrene (M_2).[a]

M_1	F_1[b]	Time (h)	Yield (%)	f_1[c]	f_c[d]	M_n (M_w/M_n)[e]	DP_n	$[\alpha]^{23}_{435}$[f]
1a	0.9	2.0	21	0.92	0.90	14600 (1.62)	38	+270
	0.8	2.0	17	0.90	0.91	15300 (1.41)	40	+263
	0.7	2.5	20	0.83	0.91	14000 (1.49)	39	+264
	0.6	2.5	12	0.74	0.90	18000 (1.43)	54	+275
	0.5	3.0	13	0.64	0.92	13400 (1.54)	45	+287
	0.4	3.0	11	0.61	0.95	12200 (1.48)	42	+264
	0.3	6.5	19	0.48	0.98	5800 (2.20)	23	+277
	0.2	9.0	20	0.39	1.00	4300 (2.32)	19	+258
	0.1	18.0	18	0.24	1.00	2600 (2.30)	15	+217

[a] Solvent, toluene; $[\mathbf{1}+\text{styrene}]_0 = 0.1$ mol·L^{-1}; $[\text{AIBN}]_0 = 6.1$ mmol·L^{-1}; temp, 60 °C. [b] Mole fraction of **1** in the monomer feed. [c] Mole fraction of M_1 unit in the polymer determined by ^{1}H and quantitative ^{13}C NMR spectra. [d] Extent of cyclization determined by quantitative ^{13}C NMR spectra. [e] Determined by GPC using a polystyrene standard. [f] Measured in $CHCl_3$ at 23 °C (*c* 1.0).

Table 6.4. Hydrolysis and methyl esterification of polymers **2f**.[a]

M_1	f_1[b]	Yield (%)	M_n (M_w/M_n)[c]	$[\alpha]^{23}_{435}$[d]
1f	0.92	43	11800 (1.47)	-2.3
	0.90	50	12000 (1.48)	-2.8
	0.83	41	10700 (1.53)	-4.5
	0.74	53	11500 (1.75)	-4.5
	0.64	42	11100 (1.50)	-5.8
	0.61	48	10700 (1.41)	-6.3
	0.48	65	5800 (1.88)	-11.0
	0.39	74	3600 (2.23)	-16.9
	0.24	39	3300 (1.77)	-21.9

[a] Alkali hydrolysis of polymer **2** was carried out using KOH in aqueous MeOH under reflux. The resulting polymer was treated with diazomethane in benzene-ether to yield the polymer **3**. [b] Mole fraction of M_1 unit in the polymer **2**. [c] Determined by GPC using a polystyrene standard. [d] Measured in $CHCl_3$ at 23 °C (*c* 1.0).

The specific rotation ($[\alpha]_{435}$, *c* 1.0, $CHCl_3$) of **3f** significantly increased from -2.3° to -21.9° with increasing M_2 content (Table 6.4). The optical rotatory power of **3f** was significantly higher than those of **3g-i**, indicating that the (2*S*,3*S*)-1,4-dimethoxy-2,3-butanediol template corresponding to the decarbonyl templates of L-tartaric acid has a higher ability for chirality induction. Figure 6.3 shows the CD and UV spectra of monomer **1f** and polymer **3f**. The CD spectrum of **1f** showed a positive Cotton effect at 287 nm and a negative Cotton effect at 262 nm, indicating that the two 4-vinylbenzoyl groups twist clockwise. On the other hand, a negative Cotton effect at 252 nm and a positive Cotton effect at 236 nm are observed for **3f**. According to the CD exciton chirality method, two adjacent methyl benzoate units twist counterclockwise, suggesting that the preferential configuration of methyl benzoate

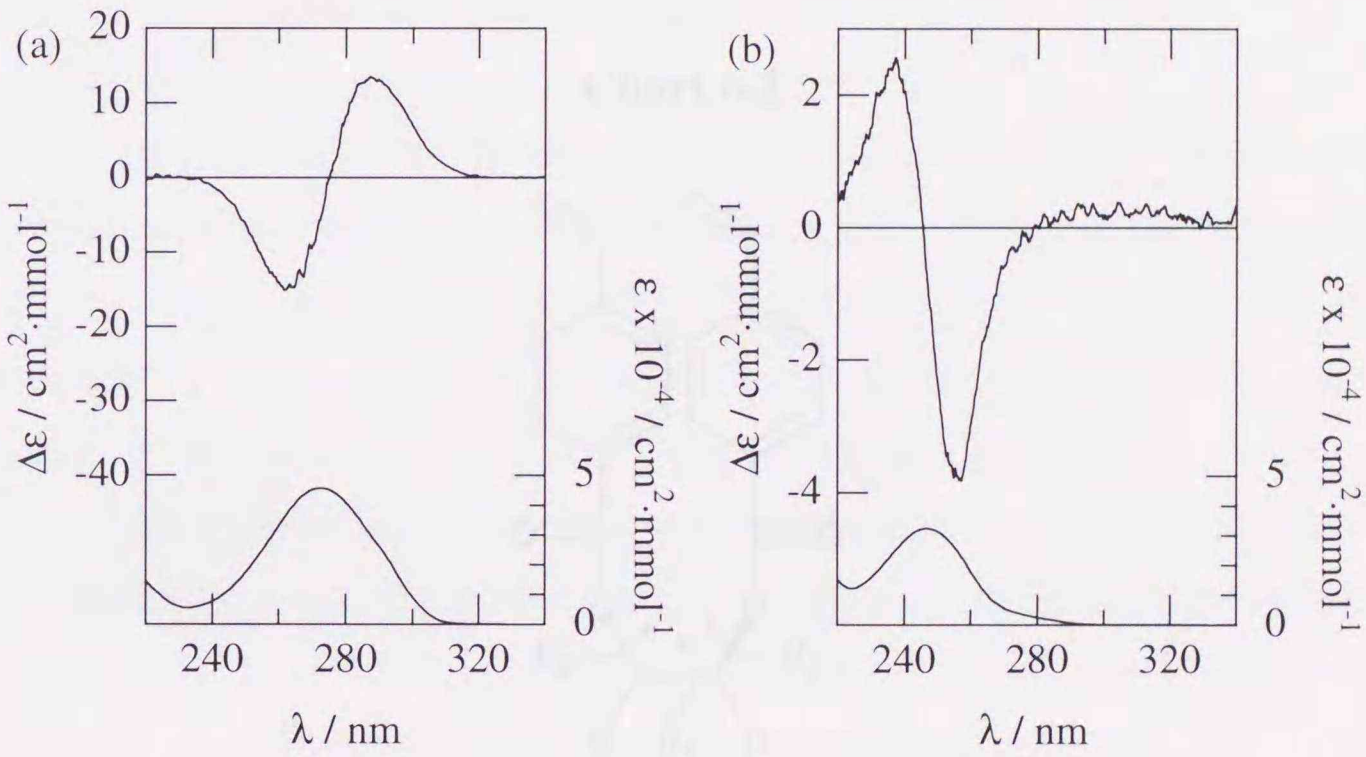

Figure 6.3. CD (upper) and UV (lower) spectra of monomer **1f** (a) and polymer **3f** (b).

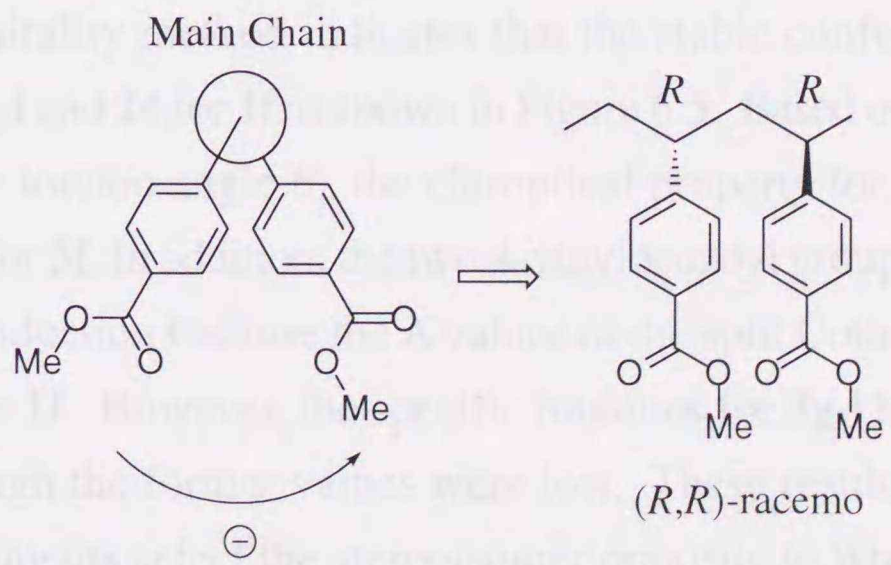

Figure 6.4. Schematic conclusion of CD spectrum of polymer **3f**.

diad is (*R*,*R*)-racemo. For the cyclocopolymerization of **3f** with styrene, hence, the positive chirality of the 4-vinylbenzoyl groups formed benzoate diad with an (*R*,*R*)-racemo configuration, which fairly agrees with the results for **1a**/St in chapter 2 (Figure 6.4).

6.2.3 Conformational Effect of Monomer on Chirality Induction

In general, the chiral template controls the chiral alignment of the two 4-vinylbenzoyl groups, resulting in a chirality induction in the main chain. Chiral alignment of two 4-vinylbenzoyl groups is constructed with two conformational elements, i.e., the chiral twist of the 4-vinylbenzoyl groups (torsion angle θ_1) and orientation of the carbonyl group of 4-vinylbenzoyl groups (torsion angles θ_2 and θ_3) (Chart 6.2). Here, **1g-i** have a torsion angle θ_1 with the sign opposite to that for **1f**

Chart 6.2

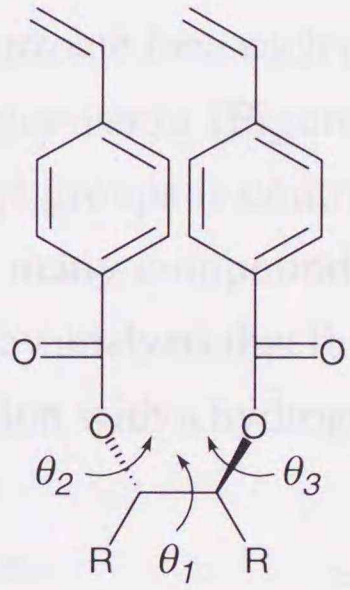

because of the dipole-dipole repulsion between the two carbonyl groups of L-tartarate. The CD exciton chirality method indicates that the stable conformation for torsion angle θ_1 is **25** for **1g-i** and **24** for **1f** as shown in Figure 6.5. Based on the stereochemical selection due to the torsion angle θ_1, the chiroptical property for **3g-i** is presumed to be opposite to that for **3f**. In addition, the two 4-vinylbenzoyl groups of **1g-i** adequately twist for chirality induction because the A values of the split Cotton effect for **1g-i** are greater than that for **1f**. However, the specific rotations for **3g-i** had the same sign as those for **3f**, although the former values were low. These results suggest that other conformational elements select the stereoisomer opposite to what the torsion angle θ_1 for **1g-i** induces.

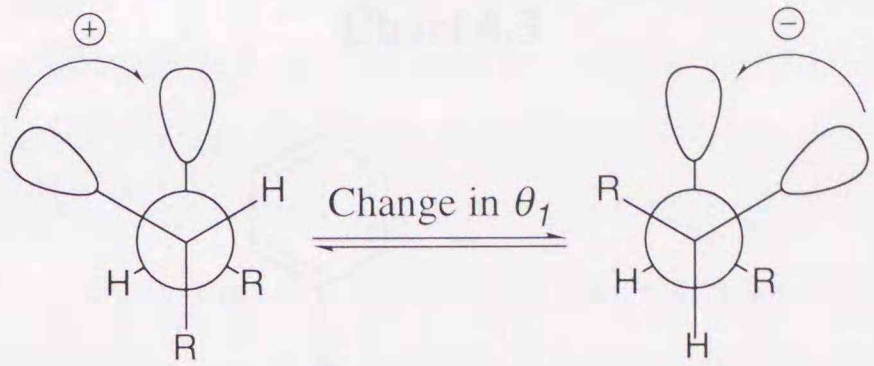

24 **25**

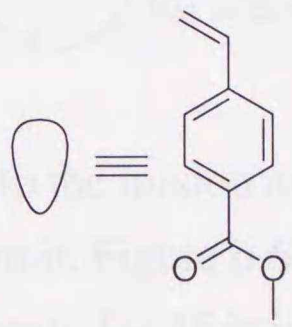

Figure 6.5. Conformations on the torsion angle θ_1.

As described in chapter 4, the conformer **26**, in which the *Si* planes for the carbonyl groups of the 4-vinylbenzoate face each other, leads to the formation of an (*R*,*R*)-racemo cyclic unit and *vice versa* (Figure 6.6). In general, the carbonyl orientation of the 4-vinylbenzoyl groups is controlled by the configuration of the alcohol moiety in the ester. In many compounds having an ester moiety, it was confirmed by a single crystal X-ray analysis that the carbonyl groups of esters have a preference for the syn conformation with a hydrogen atom of the alkyl residue from

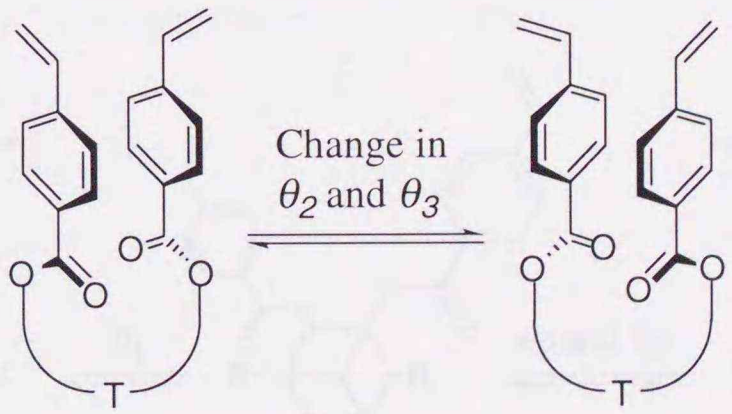

Si planes face each other — **26** — (*R*,*R*)-racemo

Re planes face each other — **27** — (*S*,*S*)-racemo

Figure 6.6. Conformations on torsion angles θ_2 and θ_3.

Chart 6.3

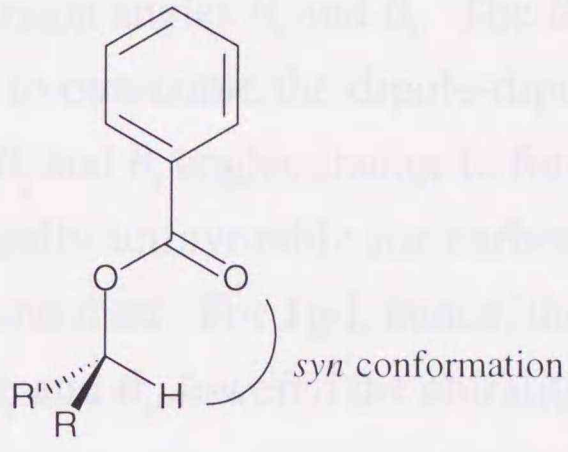

syn conformation

alcohols (Chart 6.3).[2] With regard to the torsion angles θ_2 and θ_3, the sterically stable conformations for **1f-i** are **26** shown in Figure 6.6. The preferential formation of the (*R*,*R*)-racemo diad of 4-vinylbenzoate for **1f** is in fair agreement with the chirality induction through the control based on the carbonyl direction as shown in chapter 4. The specific rotations for **1g-i** indicate that **3g-i** predominately have an (*R*,*R*)-racemo configuration of the 4-vinylbenzoate diad, which can be elucidated on the basis of the carbonyl direction. However, the optical activity for **3g-i** is too low in comparison with that for **3f**. Therefore, during the polymerization of **1g-i**, the torsion angle θ_1 has an influence on the torsion angles θ_2 and θ_3, namely, carbonyl direction.

Figure 6.7 illustrates the combination of the torsion angle θ_1 and the torsion angles θ_2 and θ_3. Conformer **22** for **1f** consists of conformation **24** for θ_1 and **26** for θ_2 and θ_3. The conformer has an advantage during the cyclization because the two 4-vinylbenzoyl groups situate close to each other. On the other hand, Conformer **23** for

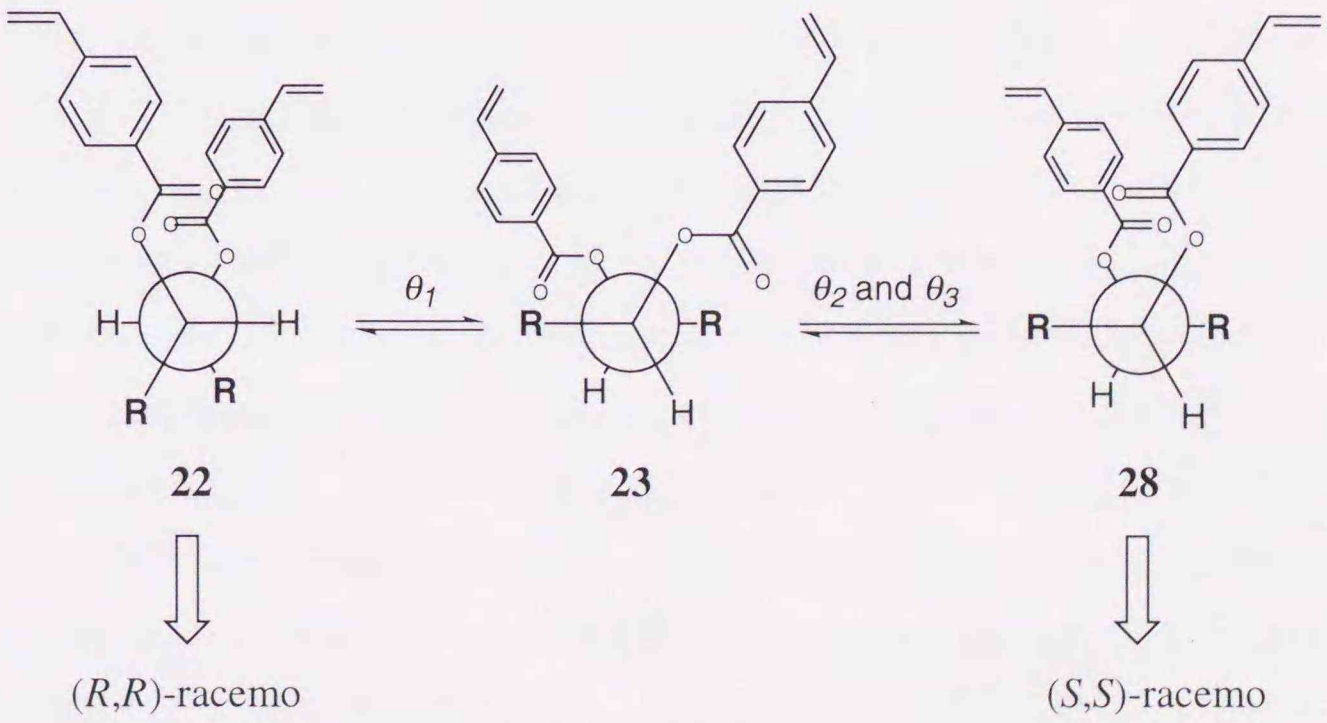

Figure 6.7. Effect of the combination of the torsion angles θ_1, θ_2, and θ_3.

1g-i, which consist of conformation **25** for θ_1 and **26** for θ_2 and θ_3, separates the two groups. Hence, the cyclization of the 4-vinylbenzoyl groups for **1g-i** requires a change in the torsion angle θ_1 or torsion angles θ_2 and θ_3. The θ_1 angle, in which the change requires activation energy to overcome the dipole-dipole repulsion, is maintained and, alternatively, those of θ_2 and θ_3 angles change to form the conformation **28**. The conformation that is sterically unfavorable for carbonyl orientation leads to the formation of the (*S*,*S*)-racemo diad. For **1g-i**, hence, the unsuitable combination of the torsion angles θ_1, and θ_2 and θ_3, lowered the chirality induction ability.

6.3 Conclusions

The cyclocopolymerization of methyl, ethyl, and isopropyl 2,3-bis-*O*-(4-vinylbenzoyl)-L-tartarate (**1g**, **1h**, and **1i**, respectively) with styrene were carried out to examine the conformational effect of monomer. After removal of the template, the resulting polymer **3g-i** shows an extremely low specific rotation in contrast with that of the polymer **3f** synthesized from the cyclocopolymerization of (2*S*,3*S*)-1,4-dimethoxy-2,3-butandiyl bis(4-vinylbenzoate) (**1f**), which is the decarbonyl analog of **1g**, with styrene. From the CD spectral analysis, two 4-vinylbenzoyl groups twisted counterclockwise for **1g-i** and clockwise for **1f**. The stable conformations of **1g-i** are different from that of **1f** and separate the two 4-vinylbenzoyl groups, thus lowering the ability for chirality induction because of the unsuitable combination of the torsion angles θ_1, θ_2, and θ_3 for the cyclization. Hence, the appropriate selection of these torsion angles should be considered for the design of an effective chiral template to form an optically active polymer due to main chain chirality.

6.4 Experimental Section

Measurements. ^{1}H and ^{13}C NMR spectra were recorded using JEOL JNM-EX270 and JNM-A400II instruments. Quantitative ^{13}C NMR spectra were obtained at 30 °C in $CDCl_3$ (100 mg·mL^{-1}; delay time 7.0 seconds; inverse gated decoupling). The molecular weight of the resulting polymers was measured by gel permeation chromatography (GPC) in tetrahydrofuran on a Jasco GPC system (GPC-900) equipped with three polystyrene gel columns (Shodex KF-804L). The number-average molecular weight (M_n) was calculated on the basis of a polystyrene calibration. Optical rotations were measured with a Jasco DIP-1000 digital polarimeter. CD spectra were measured in 1,1,1,3,3,3-hexafluoro-2-propanol (HFIP) with a 5 mm path length using a Jasco J-720 spectropolarimeter.

Materials. Dry toluene was purchased from the Kanto Chemical Co. and used without further purification. 2,2'-Azobis(2-methylpropionitrile) (AIBN) was recrystallized from methanol. HFIP was donated by the Central Glass Co. and used without further purification. Methyl, ethyl, and isopropyl L-tartarates were synthesized from L-tartaric acid and the corresponding alcohol using a typical acidic esterification procedure. (2*S*,3*S*)-1,4-dimethoxy-2,3-butanediyl bis(4-vinylbenzoate) (**1f**) was synthesized according to procedure similar to that described in chapter 3.

Methyl 2,3-Bis-*O*-(4-vinylbenzoyl)-L-tartarate (1g). A solution of methyl L-tartarate (4.7 g, 26.1 mmol) in dry pyridine (210 mL) was cooled to 5 °C. To this solution, 4-vinylbenzoyl chloride (12.7 g, 76.6 mmol) was gradually added so that the temperature of the solution did not rise over 10 °C. The reaction mixture was stirred for 24 hrs at room temperature. The mixture was cooled to 0 °C in an ice bath, and water was then added. The resulting mixture was extracted with three portions of 160 mL of diethyl ether. The extract was successively washed with 0.5 M aqueous HCl, 5 % aqueous NaOH, and water, then dried over anhydrous sodium sulfate. After removal of the solvent under reduced pressure, chromatography on silica gel (Kiesel Gel 60) with hexane/diethyl ether (vol. ratio 1/1) gave **1g** as a sticky liquid. Yield 7.7 g (17.6 mmol, 67.5 %). $[\alpha]_{435}$ = -323°, $[\alpha]_D$ = -115° ($CHCl_3$, 23 °C, *c* 1.0). ^{1}H NMR (270 MHz, $CDCl_3$): δ (ppm) = 8.06 (d, ^{3}J = 8.3 Hz, 4H, Ar), 7.50 (d, ^{3}J = 8.5 Hz, 4H, Ar), 6.77 (dd, $^{3}J_{trans}$ = 17.6 Hz, $^{3}J_{cis}$ = 11.0 Hz, 2H, =CH-), 6.00 (s, 2H, OCH), 5.89 (d, $^{3}J_{trans}$ = 17.6 Hz, 2H, $=CH_2$), 5.42 (d, $^{3}J_{cis}$ = 11.0 Hz, 2H, $=CH_2$), 3.77 (s, 6H, CH_3). ^{13}C NMR (67.5 MHz, $CDCl_3$): δ (ppm) = 166.4 (C=O), 142.9, 130.5, 127.7, 126.3 (Ar),

135.9 (=CH-), 117.1 (=CH_2), 71.5 (OCH), 53.1 (CH_3). Anal. Calcd for $C_{24}H_{22}O_8$ (438.4): C 65.75; H 5.06. Found: C 65.68; H 5.20.

Ethyl 2,3-Bis-*O*-(4-vinylbenzoyl)-L-tartarate (1h). The same procedure as that for **1a** was applied to a mixture of ethyl L-tartarate (1.1 g, 5.4 mmol), 4-vinylbenzoyl chloride (2.5 g, 15 mmol) and 30 mL of pyridine. The crude product was purified by column chromatography on silica gel (Kiesel Gel 60) with hexane/ diethyl ether (vol. ratio 7/3) to give **1h** as a sticky liquid. Yield 2.3 g (4.9 mmol, 90.7 %). $[\alpha]_{435}$ = -333°, $[\alpha]_D$ = -117° ($CHCl_3$, 23 °C, *c* 1.0). ^{1}H NMR (270 MHz, $CDCl_3$): δ (ppm) = 8.07 (d, ^3J = 8.3 Hz, 4H, Ar), 7.49 (d, ^3J = 8.3 Hz, 4H, Ar), 6.77 (dd, $^3J_{trans}$ = 17.5 Hz, $^3J_{cis}$ = 10.9, 2H, =CH-), 6.00 (s, 2H, OCH), 5.89 (d. $^3J_{trans}$ = 17.5 Hz, 2H, =CH_2), 5.41 (d, $^3J_{cis}$ = 11.2 Hz, 2H, =CH_2), 4.29 - 4.19 (m, 4H, -CH_2-), 1.19 (t, ^3J = 7.1 Hz, 6H, -CH_3). ^{13}C NMR (67.5 MHz, $CDCl_3$): δ (ppm) = 165.8 (C=O, benzoate), 165. 0 (C=O, tartarate), 142.8, 130.4, 127.7, 126.3 (Ar), 135.91 (=CH-), 117.0 (=CH_2), 71.6 (OCH), 62.3 (CH_2), 14.1 (CH_3). Anal. Calcd for $C_{26}H_{26}O_8$ (466.5): C 66.94; H 5.62. Found: C 66.80; H 5.68.

Isopropyl 2,3-Bis-*O*-(4-vinylbenzoyl)-L-tartarate (1i). The same procedure as that for **1a** was applied to a mixture of isopropyl L-tartarate (1.2 g, 5.1 mmol), 4-vinylbenzoyl chloride (2.7 g, 16 mmol) and 30 mL of pyridine. The crude product was purified by column chromatography on silica gel (Kiesel Gel 60) with hexane/ diethyl ether (vol. ratio 7/3) to give **1i** as a sticky liquid. Yield 2.0 g (4.0 mmol, 78.4 %). $[\alpha]_{435}$ = -330°, $[\alpha]_D$ = -114° ($CHCl_3$, 23 °C, *c* 1.0). ^{1}H NMR (270 MHz, $CDCl_3$): δ (ppm) = 8.07 (d, ^3J = 8.3 Hz, 4H, Ar), 7.49 (d, ^3J = 8.3 Hz, 4H, Ar), 6.77 (dd, $^3J_{trans}$ = 17.7 Hz, $^3J_{cis}$ = 11.1, 2H, =CH-), 5.99 (s, 2H, OCH), 5.89 (d. $^3J_{trans}$ = 17.5 Hz, 2H, =CH_2), 5.41 (d, $^3J_{cis}$ = 10.9 Hz, 2H, =CH_2), 5.08 (m, 2H, $CHMe_2$), 1.25 (d, ^3J = 6.3 Hz, 6H, CH_3), 1.08 (d, ^3J = 6.3 Hz, 6H, CH_3). ^{13}C NMR (67.5 MHz, $CDCl_3$): δ (ppm) = 165.3 (C=O, benzoate), 165.0 (C=O, tartarate), 142.7, 130.4, 127.8, 126.2 (Ar), 135.9 (=CH-), 116.9 (=CH_2), 71.6 (OCH), 70.3 ($CHMe_2$), 21.6 (CH_3), 21.5 (CH_3). Anal. Calcd for $C_{28}H_{30}O_8$ (494.5): C 68.00; H 6.11. Found: C 67.84; H 6.16.

Cyclocopolymerization. The polymerization was carried out according to the similar procedure as that described in chapter 2.

Poly[(methyl 4-vinylbenzoate)-*co*-styrene] (3). The similar procedures as those described in chapter 2 were applied.

6.5 References

(1) Yamamoto, Y.; Fushimi, M.; Oda, J.; Inouye, Y. *Agr. Biol. Chem.* **1975**, *39*, 2223.

(2) Methineson, A. McL. *Tetrahedron Lett.* **1965**, 4137.

Chapter 7

Asymmetric Cyclocopolymerization of 1,2:5,6-Di-O-isopropylidene-3,4-Di-O-methacryloyl-D-Mannitol with Styrene

7.1 Introduction

In the previous chapters, the asymmetric cyclocopolymerization of bis(4-vinylbenzoate) having a chiral template with styrene was discussed, especially, about the chirality induction mechanism. This polymerization system has an advantage in that the CD exciton chirality method for the stereochemical analysis can be applied to the template-free polymer. However, the template-free polymer is unsuitable for the structural analysis using NMR spectroscopy, which is powerful tool for the estimation of the microstructure of polymers, i.e, monomer sequence and tacticity. Hence, it is interesting to explore the asymmetric cyclocopolymerization system to give a template-free polymer which can be applicable to the NMR spectral analysis.

In this chapter, the cyclocopolymerization of the 1,2:5,6-di-*O*-isopropylidene-3,4-di-*O*-methacryloyl-D-mannitol with styrene carried out (Scheme 7.1). The origin of chirality was discussed on the basis of the specific rotation and the NMR spectral analysis of the template-free copolymer, i.e., poly[(methyl methacrylate)-*co*-styrene].

Scheme 7.1

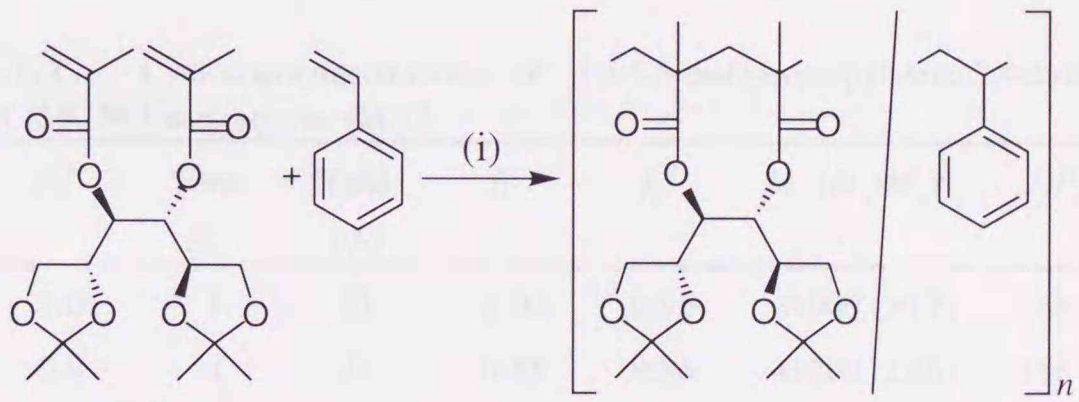

29 **30**

M_1 M_2

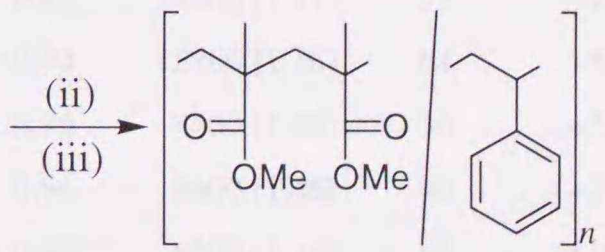

31

M_1 M_2

Conditions: (i) AIBN, toluene, 60 °C; (ii) KOH, MeOH, reflux; (iii) CH_2N_2, Et_2O

7.2 Results and Discussion

7.2.1 Cyclocopolymerizations

The copolymerizations of 1,2:5,6-di-*O*-isopropylidene-3,4-di-*O*-methacryloyl-D-mannitol (**29**, M_1) with styrene (M_2) were carried out using AIBN in toluene at 60 °C, and the results are listed in Table 7.1. The polymerization system was homogeneous, and the resulting polymer **30** was soluble in chloroform and tetrahydrofuran. The number average molecular weight (M_n) of **30** ranged from 4300 to 34900. The ^{1}H NMR spectra showed that the polymers **30** contained a small amount of residual double bonds (Figure 7.1). The extent of cyclization (f_c), which was estimated from peaks at 5.6 and 6.2 ppm due to the methacrylic groups, was varied from 1.00 to 0.86 with an increase in the mole fraction of **29** in the feed. For the cyclocopolymerization, the intramolecular cyclization of the divinyl monomer is generally inhibited by incorporation of the comonomer. Table 7.2 shows the effect of the comonomer on the cyclization in the cyclocopolymerization of **29** with styrene. The f_c value was only slightly influenced by incorporation of the comonomer.

Table 7.1. Cyclocopolymerizations of 1,2:5,6-di-*O*-isopropylidene-3,4-di-*O*-methacryloyl-D-mannitol (**29**, M_1) with styrene (M_2).[a]

M_1	F_1[b]	Time (h)	Yield (%)	f_1[c]	f_c[d]	M_n (M_w/M_n)[e]	DP_n	$[\alpha]^{23}_{435}$[f]
29	1.0[g]	5	53	1.00	0.95	34900 (20.7)	88	+77.9
	0.9	4	27	0.85	0.86	41200 (2.66)	116	+52.5
	0.8	6	27	0.74	0.89	26600 (1.86)	83	+39.5
	0.7	5	18	0.62	0.91	17600 (1.52)	61	+32.0
	0.6	7	18	0.56	0.92	14800 (1.41)	55	+26.4
	0.5	9	20	0.48	0.94	15700 (1.16)	64	+23.9
	0.4	12	19	0.43	0.95	8400 (1.46)	36	+22.8
	0.3	12	19	0.37	0.96	8600 (1.45)	40	+20.9
	0.2	10	14	0.31	0.96	8500 (1.35)	43	+19.3
	0.1	14	14	0.21	1.00	6100 (1.39)	37	+16.9
	0.05	27	19	0.13	1.00	4300 (1.64)	30	+12.6

[a] Solvent, toluene; [**29**+styrene]$_0$ = 0.2 mol·L^{-1}; [AIBN]$_0$ = 6.1 mmol·L^{-1}; temp, 60 °C. [b] Mole fraction of **29** in the monomer feed. [c] Mole fraction of M_1 unit in the polymer determined by ^{1}H NMR spectra. [d] Extent of cyclization determined by ^{1}H NMR spectra. [e] Determined by GPC using a polystyrene standard. [f] Measured in $CHCl_3$ at 23 °C (*c* 1.0). [g] [**29**]$_0$ = 0.1 mol·L^{-1}

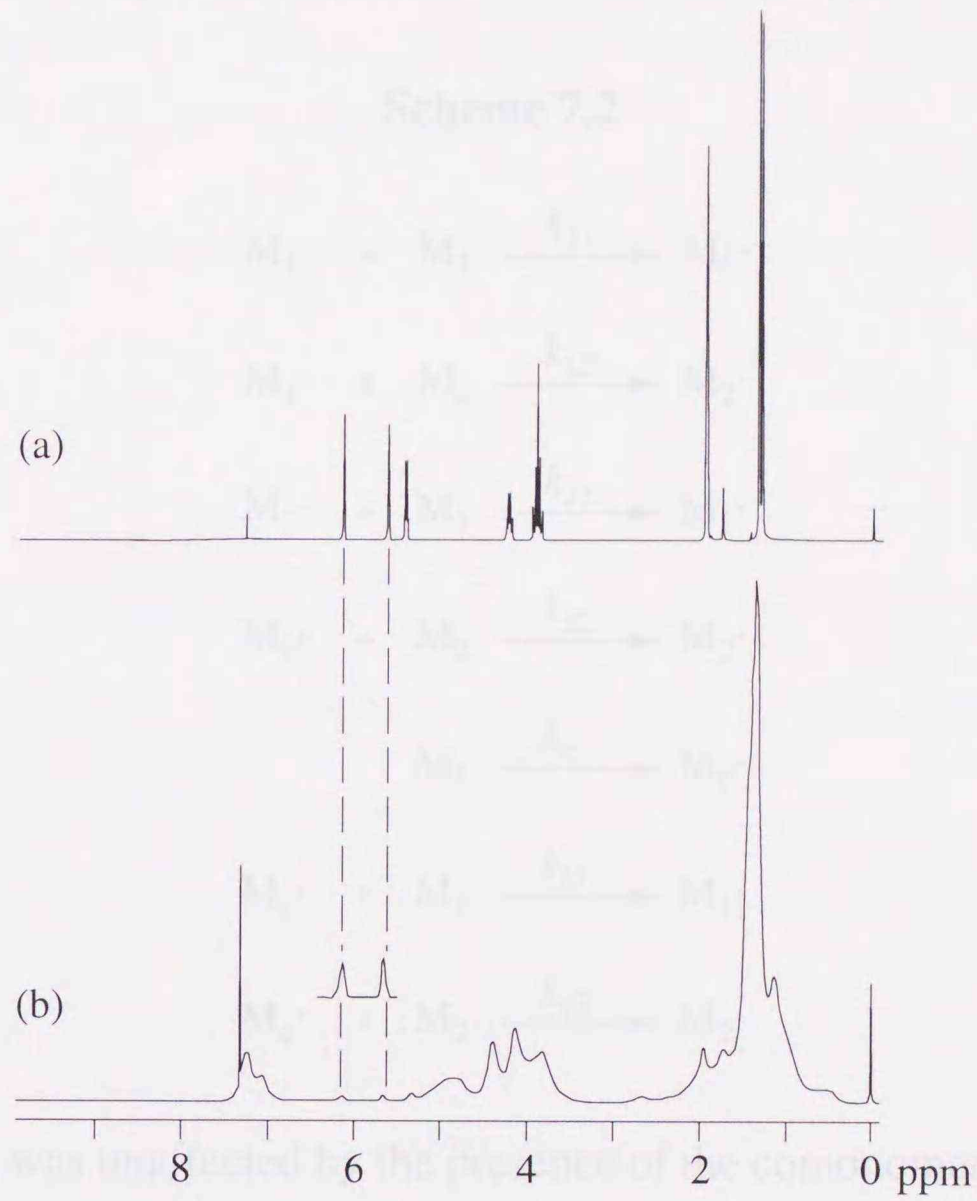

Figure 7.1. ^{1}H NMR spectra of monomer **29** (a) and polymer **30** ($f_1 = 0.74, f_c = 0.89$) (b).

Table 7.2. Effect of comonomer (M_2) on the cyclopolymerization tendency of monmer **29**[a]

$[M_1]$ / mol·L^{-1}	$[M_2]$ / mol·L^{-1}	f_c[b]
0.10	0.10	0.94
0.10	0.00	0.95

[a] Solvent, toluene; $[AIBN]_0 = 6.1$ mmol·L^{-1}; temp, 60 °C. [b] Extent of cyclization determined by ^{1}H NMR spectra.

In order to further clarify the effect of the comonomer, the kinetics of the cyclocopolymerization are discussed. The set of elementary reactions in the cyclocopolymerization is summarized in Scheme 7.2. Since the intramolecular

Scheme 7.2

$$M_1\cdot + M_1 \xrightarrow{k_{11}} M_1\cdot$$

$$M_1\cdot + M_2 \xrightarrow{k_{12}} M_2\cdot$$

$$M_2\cdot + M_1 \xrightarrow{k_{21}} M_1\cdot$$

$$M_2\cdot + M_2 \xrightarrow{k_{22}} M_2\cdot$$

$$M_1\cdot \xrightarrow{k_c} M_c\cdot$$

$$M_c\cdot + M_1 \xrightarrow{k_{c1}} M_1\cdot$$

$$M_c\cdot + M_2 \xrightarrow{k_{c2}} M_2\cdot$$

cyclization of **29** was unaffected by the presence of the comonomer (i.e., $k_{12} = 0$), the expression of Roovers and Smets[1] can be applied to the polymer composition relationship.

$$\frac{d[M_1]}{d[M_2]} = \frac{2[M_1]}{[M_2]} \cdot \frac{2r_c[M_1]+[M_2]}{2[M_1]+r_2[M_2]}\left(1+\frac{2[M_1]}{K_c}\right) \qquad (7.1)$$

$$\frac{1}{f_c} = \frac{d[M_1]}{d[M_c]} = 1+\frac{2[M_1]}{K_c} \qquad (7.2)$$

$$\frac{d[M_c]}{d[M_2]} = \frac{[M_1]}{[M_2]} \cdot \frac{r'_1[M_1]+[M_2]}{[M_1]+r'_2[M_2]} \qquad (7.3)$$

where $r_c = k_{c1}/k_{c2}$, $r_2 = k_{21}/k_{22}$, $r'_1 = 2r_c$, $r'_2 = r_2/2$, $K_c = k_c/k_{11}$, and $d[M_c] = f_c \cdot d[M_1]$. The experimental data are plotted according to eq. 7.2 (Figure 7.2). A good straight line was found; the slope gave $K_C = 2.3$ mol·L^{-1} and a intercept of 1.0, thereby indicating that the comonomer simply acts as a diluent for the intramolecular cyclization of **29**. The K_C value of **29** is comparable to 4.0 mol·L^{-1} for ethylene glycol dimethacrylate[2]

and 3.4 mol·L^{-1} for diethylene glycol dimethacrylate[3] during the homopolymerization, thus indicating that **29** has a high tendency for cyclopolymerization. The Kelen-Tüdös plots for the data in Table 7.1 according to eq. 7.3 gave $r'_1 = 0.35$ and $r'_2 = 0.36$. The parameters r'_1 and r'_2 are the monomer reactivity ratios without consideration of the bifunctionality of **29**.

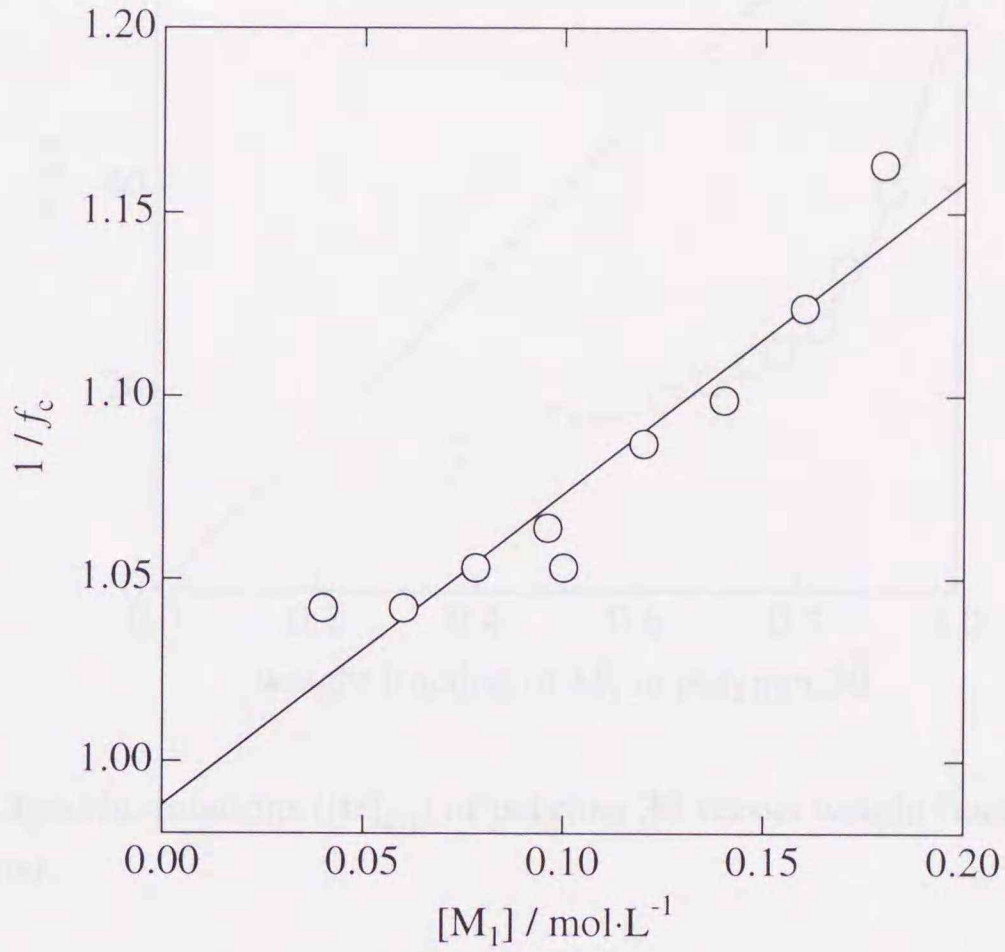

Figure 7.2. Representation of the experimental data according to eq 7.2 in **29**/St.

*7.2.2. Chiroptical Properties of Polymers **30** and **31***

The specific rotation ($[\alpha]_{435}$) of polymer **30** showed a deviation from a linear dependence on the weight fraction of M_1 units (Figure 7.3). This result means that the polymer **30** exhibited the optical activity due to the new chirality except the chiral template.

The removal of the chiral template from **30** was carried out using KOH in aqueous MeOH. The hydrolyzed polymer was then treated with diazomethane to yield polymer **31**. However, since the characteristic peaks due to the template were slightly found in the ^{13}C NMR spectra of **31**, the removal of the chiral template from **30** was not completely performed.

In spite of the slight residue of the chiral template, the sign of the specific rotation was changed from plus for polymer **30** to minus for polymer **31** (Table 7.3). Then the

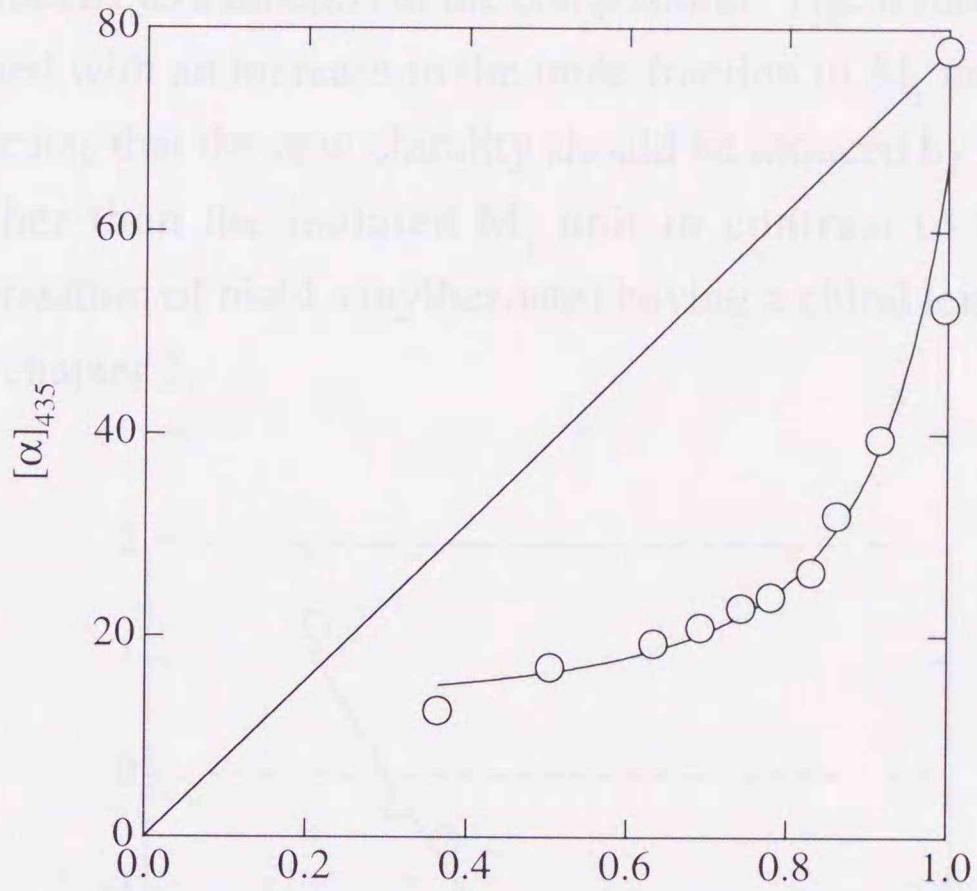

Figure 7.3. Specific rotations ($[\alpha]_{435}$) of polymer **30** versus weight fraction of M_1 unit in the polymer.

Table 7.3. Hydrolysis and methyl esterification of polymer **30**.[a]

M_1	f_1[b]	Yield (%)	M_n (M_w/M_n)[c]	$[\alpha]^{23}_{435}$[d]
29	1.00	21	25400 (2.56)	-
	0.85	57	23200 (2.15)	-4.3
	0.74	52	18100 (1.69)	-4.0
	0.62	72	17600 (1.52)	-2.6
	0.56	48	11800 (1.32)	-1.4
	0.48	14	6400 (1.87)	-2.5
	0.43	46	9500 (1.39)	-2.4
	0.37	-	7300 (2.06)	-0.6
	0.31	41	7500 (1.27)	-0.3
	0.21	56	4200 (1.56)	+1.3

[a] Alkali hydrolysis of polymer **30** was carried out using KOH in aqueous MeOH under reflux. The resulting polymer was treated with diazomethane in benzene-ether to yield the polymer **31**. [b] Mole fraction of M_1 unit in the polymer **30**. [c] Determined by GPC using a polystyrene standard. [d] Measured in $CHCl_3$ at 23 ℃ (*c* 1.0).

new chirality exhibited the optical rotation of minus sign, getting over the optical activity due to the slight residue of the chiral template. Figure 7.4 showed the specific rotation of polymer **31** as a function of the composition. The absolute value of specific rotation increased with an increase in the mole fraction of M_1 units in the polymer. This result indicates that the new chirality should be induced by the M_1 diad and/or triad units rather than the isolated M_1 unit in contrast to the results in the cyclocopolymerization of bis(4-vinylbezoate) having a chiral template with styrene as described in chapter 2.

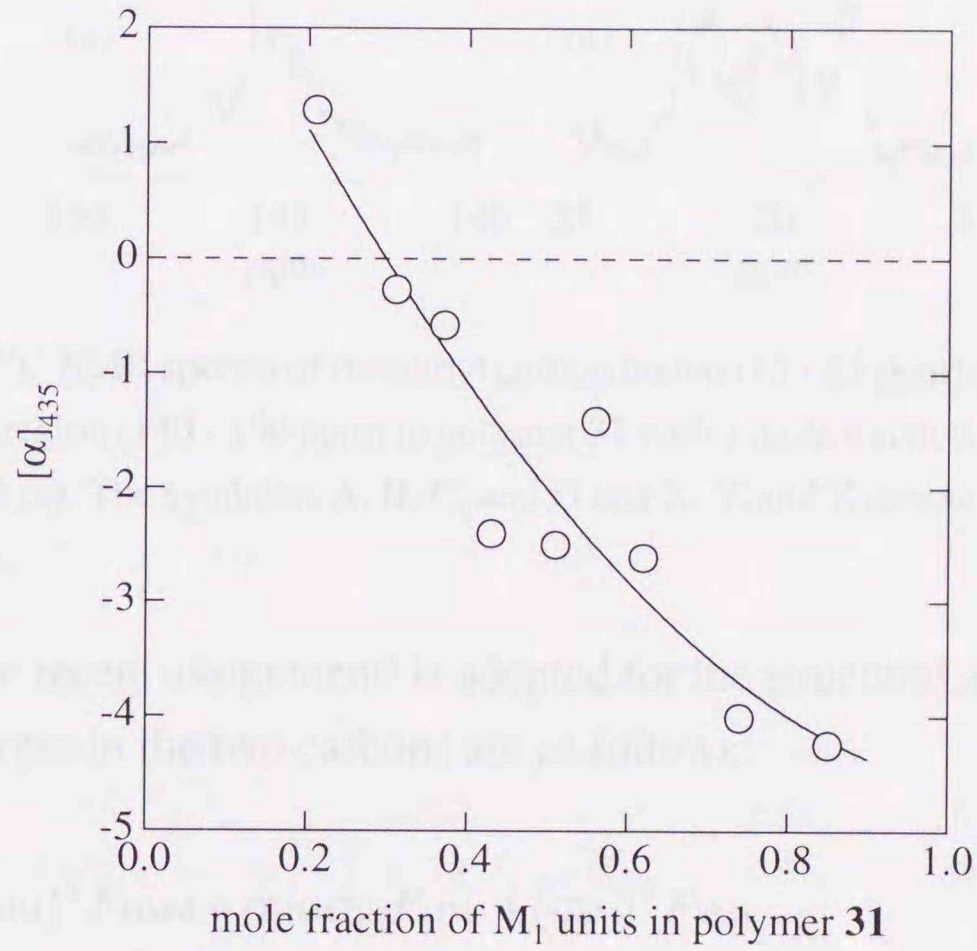

Figure 7.4. Specific rotations ($[\alpha]_{435}$) of polymer **31** versus mole fraction of M_1 unit in the polymer.

*7.2.3. Sequential Analysis of Polymer **31***

Polymer **31** is poly[(methyl methacrylate)-*co*-styrene] (poly(MMA-*co*-St)) of which the structural analysis has already been established by ^1H and ^{13}C NMR spectral methods.[4-6] Figure 7.5 shows the ^{13}C NMR spectra of the aromatic ipso-carbon and the α-methyl carbon in polymer **31**. The ipso-carbon region was divided into three peaks, X, Y, and Z, and the α-methyl carbon region divided into four peaks, A, B, C, and D. Since the assignments of these peaks are slightly different in the three articles,

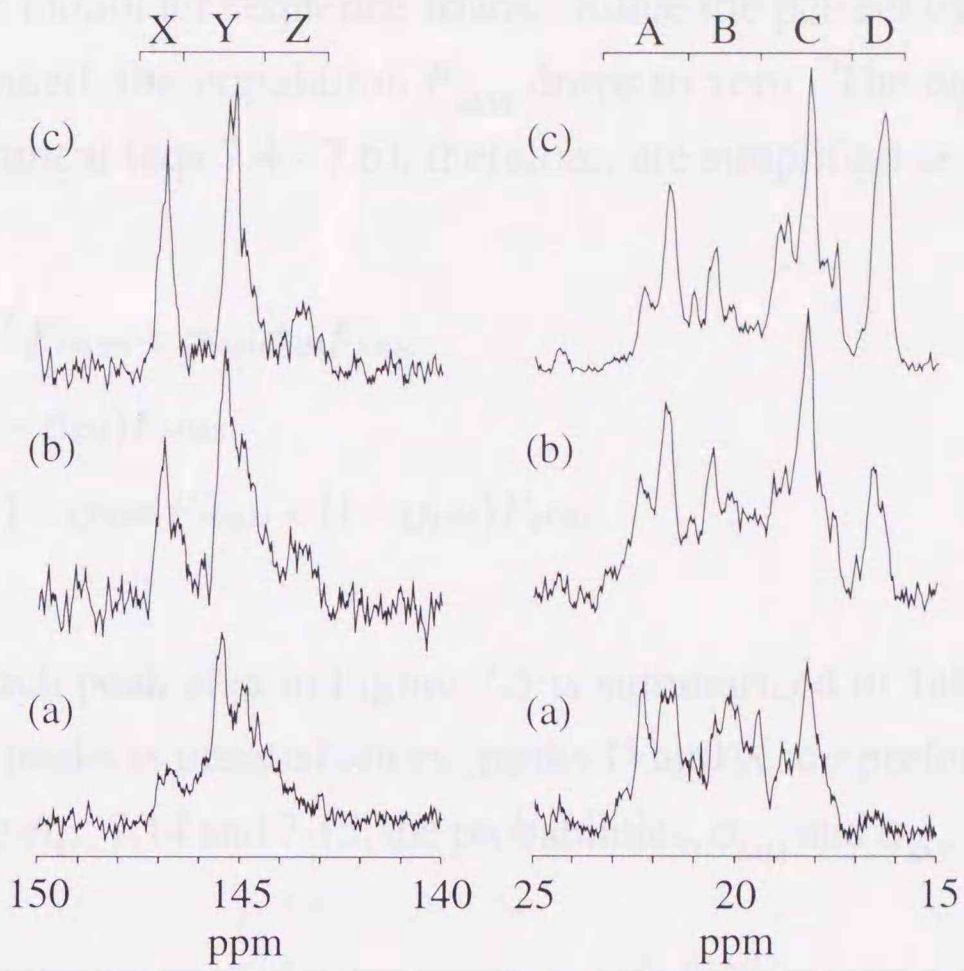

Figure 7.5. ^{13}C NMR spectra of α-methyl carbon region (15 - 25 ppm) and the aromatic ipso-carbon region (140 - 150 ppm) in polymer **31** with a mole fraction of 0.21 (a), 0.51 (b), and 0.62 (c). The symboles A, B, C, and D and X, Y, and Z denote the divisions of both regions.

Germann's more recent assignment[6] is adopted for the structural analysis of polymer **31**. The peak areas in the two carbons are as follows:

$$S_A = (\sigma_{MM})^2 F_{MMM} + \sigma_{MM}\sigma_{SM}F_{MMS} + (\sigma_{SM})^2 F_{SMS} \quad (7.4)$$

$$S_B = \sigma_{MM}(1-\sigma_{SM})F_{MMS} + 2\sigma_{SM}(1-\sigma_{SM})F_{SMS} + (1-\sigma_{SM})^2 F_{SMS} \quad (7.5)$$

$$S_C = 2\sigma_{MM}(1-\sigma_{MM})F_{MMM} + (1-\sigma_{MM})F_{MMS} + (1-\sigma_{SM})^2 F_{SMS} \quad (7.6)$$

$$S_D = (1-\sigma_{MM})^2 F_{MMM} \quad (7.7)$$

$$S_X = (1-\sigma_{SM})^2 F_{MSM} \quad (7.8)$$

$$S_Y = F_{SSS+}(1-\sigma_{SM})F_{SSM} + 2\sigma_{SM}(1-\sigma_{SM})F_{MSM} \quad (7.9)$$

$$S_Z = \sigma_{SM}F_{SSM+}(\sigma_{SM})^2 F_{MSM} \quad (7.10)$$

where the symbols, M and S, denote the MMA and the St units, respectively, the set of S_A, S_B, S_C, and S_D and the set of S_X, S_Y, and S_Z are peak area ratios for α-methyl and ipso-carbon regions, respectively, and σ_{MM} and σ_{SM} are the probability that two adjacent monomer units have a meso configuration, F_{MMM}, F_{MMS}, F_{MSM}, and F_{SSM} are the

population of the monomer sequence triads. Since the perfect cyclization of **29** is reasonably presumed, the population F_{SMS} drops to zero. The equations based on Germann's assignment (eqs 7.4 - 7.6), therefore, are simplified as follows:

$$S_A = (\sigma_{MM})^2 F_{MMM} + \sigma_{MM}\sigma_{SM}F_{MMS} \tag{7.11}$$

$$S_B = \sigma_{MM}(1-\sigma_{SM})F_{MMS} \tag{7.12}$$

$$S_C = 2\sigma_{MM}(1-\sigma_{MM})F_{MMM} + (1-\sigma_{MM})F_{MMS} \tag{7.13}$$

The fraction of each peak area in Figure 7.5 is summarized in Table 7.4. Although the separation of peaks is unsatisfactory, peaks D and X are preferably used for the analysis. By using eqs. 7.14 and 7.15, the probabilities, σ_{MM} and σ_{SM}, may be estimated.

Table 7.4. Summary of the ratios of peak areas in ^{13}C NMR spectra of polymer **31**.[a]

	α-methyl				ipso-C		
f_1	S_A	S_B	S_C	S_D	S_X	S_Y	S_Z
0.85	0.155	0.109	0.416	0.320	0.391	0.490	0.118
0.74	0.157	0.104	0.425	0.314	0.359	0.541	0.100
0.62	0.197	0.169	0.419	0.216	0.278	0.562	0.160
0.56	0.242	0.186	0.434	0.139	0.258	0.629	0.114
0.48	0.315	0.282	0.336	0.066	0.198	0.683	0.119
0.43	0.335	0.243	0.354	0.069	0.204	0.667	0.130
0.37	0.317	0.334	0.294	0.056	0.208	0.623	0.170
0.31	0.375	0.310	0.295	0.020	0.114	0.638	0.248
0.21	0.407	0.346	0.243	0.005	0.094	0.856	0.050

[a] The peak areas are defined as shown in Figure 7.5.

The populations, F_{MMM} and F_{MSM}, are calculated from the reactivity ratios, $r'_1 = 0.35$ and $r'_2 = 0.36$, in the terminal model. The number-average chain length (N) of polymer **31** is derived from the mole fraction (f_1) of the M_1 units and the chain length (N') in polymer **30**:

$$N = 2f_1N' + (1-f_1)N' = (1+f_1)N' \tag{7.14}$$

As the M_1 units in **30** are converted to the MM diad unit in **31**, the diad units M_1M_1, M_1M_2, and M_2M_2 produce the sequences MMMM, MMS, and SS, respectively.

There is an exact correspondence between the number (n'_{12}) of M_1M_2 diad in **30** and the number (n_{MMS}) of MMS triad in **31**:

$$n_{MMS} = (N-2)F_{MMS} = (N'-1)F'_{12} = n'_{12} \tag{7.15}$$

For the larger values of N and N', the population F_{MMS} is then:

$$F_{MMS} = \frac{N'}{N}F'_{12} = \frac{1}{1+f_1}F'_{12} \tag{7.16}$$

The sequence $M_1M_2M_1$ quantitatively corresponds to the sequence MSM. Thus,

$$n_{MSM} = (N-2)F_{MMS} = (N'-2)F'_{121} = n'_{121} \tag{7.17}$$

For the larger values of N and N', the population F_{MSM} is given as

$$F_{MSM} = \frac{N'}{N}F'_{121} = \frac{1}{1+f_1}F'_{121} \tag{7.18}$$

In a similar manner one obtains

$$F_{SSM} = \frac{1}{1+f_1}F'_{221} \tag{7.19}$$

$$F_{SSS} = \frac{1}{1+f_1}F'_{222} \tag{7.20}$$

The population F'_{12} of the diad M_1M_2 and populations F'_{121}, F'_{221}, and F'_{222} of the triads $M_1M_2M_1$, $M_2M_2M_1$, and $M_2M_2M_2$ are given by the probabilities P'_{11}, P'_{12}, P'_{21}, and P'_{22} forming the diads M_1M_1, M_1M_2, M_2M_1, and M_2M_2, that is,

$$F'_{12} = \frac{2P'_{21}P'_{12}}{P'_{12}+P'_{21}} \tag{7.21}$$

$$F'_{121} = \frac{P'_{21}P'_{12}P'_{21}}{P'_{12}+P'_{21}} \tag{7.22}$$

$$F'_{221} = \frac{2P'_{12}P'_{22}P'_{21}}{P'_{12} + P'_{21}} \tag{7.23}$$

$$F'_{222} = \frac{P'_{12}P'_{22}P'_{22}}{P'_{12} + P'_{21}} \tag{7.24}$$

The probabilities are given by

$$P'_{12} = \frac{[M_2]}{r'_1[M_1] + [M_2]} = 1 - P'_{11} \tag{7.25}$$

$$P'_{21} = \frac{[M_1]}{[M_1] + r'_2[M_2]} = 1 - P'_{22} \tag{7.26}$$

Figure 7.6 shows the triad populations which were calculated by using eqs. 7.14 - 7.26. Figure 7.7 shows the probabilities σ_{MM} and σ_{SM} which were estimated on the basis of the calculated populations F_{MMM} and F_{MSM} and the peak areas S_D and S_X using eqs. 7.7 and 7.8, respectively. The values of σ_{MM} and σ_{SM} changed with composition in the polymer **31**.

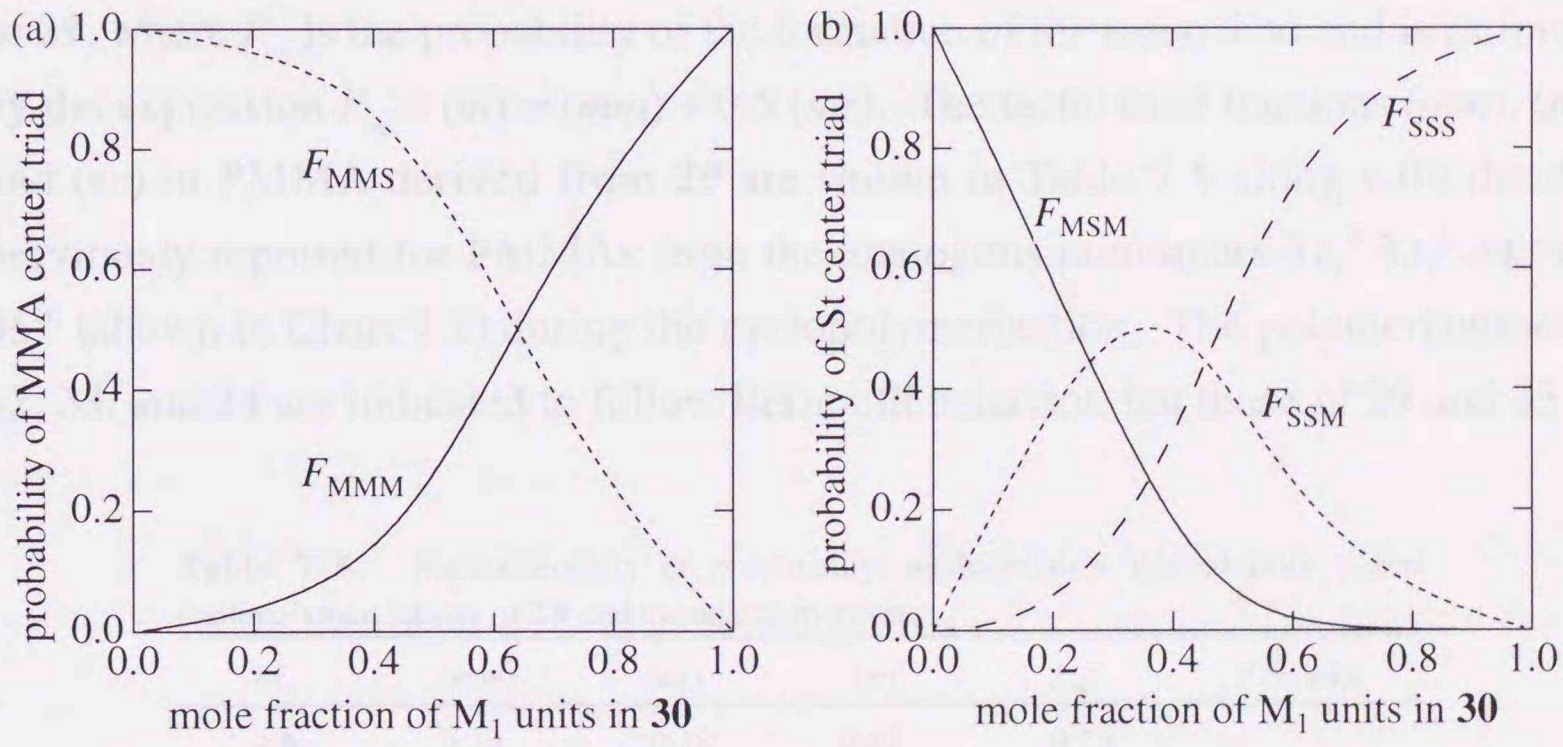

Figure 7.6. Populations of MMA center triads (a) and St center triads (b) calculated by using the reactivity ratios, $r'_1 = 0.35$ and $r'_2 = 0.36$, versus mole fraction of M_1 units in polymer **30**.

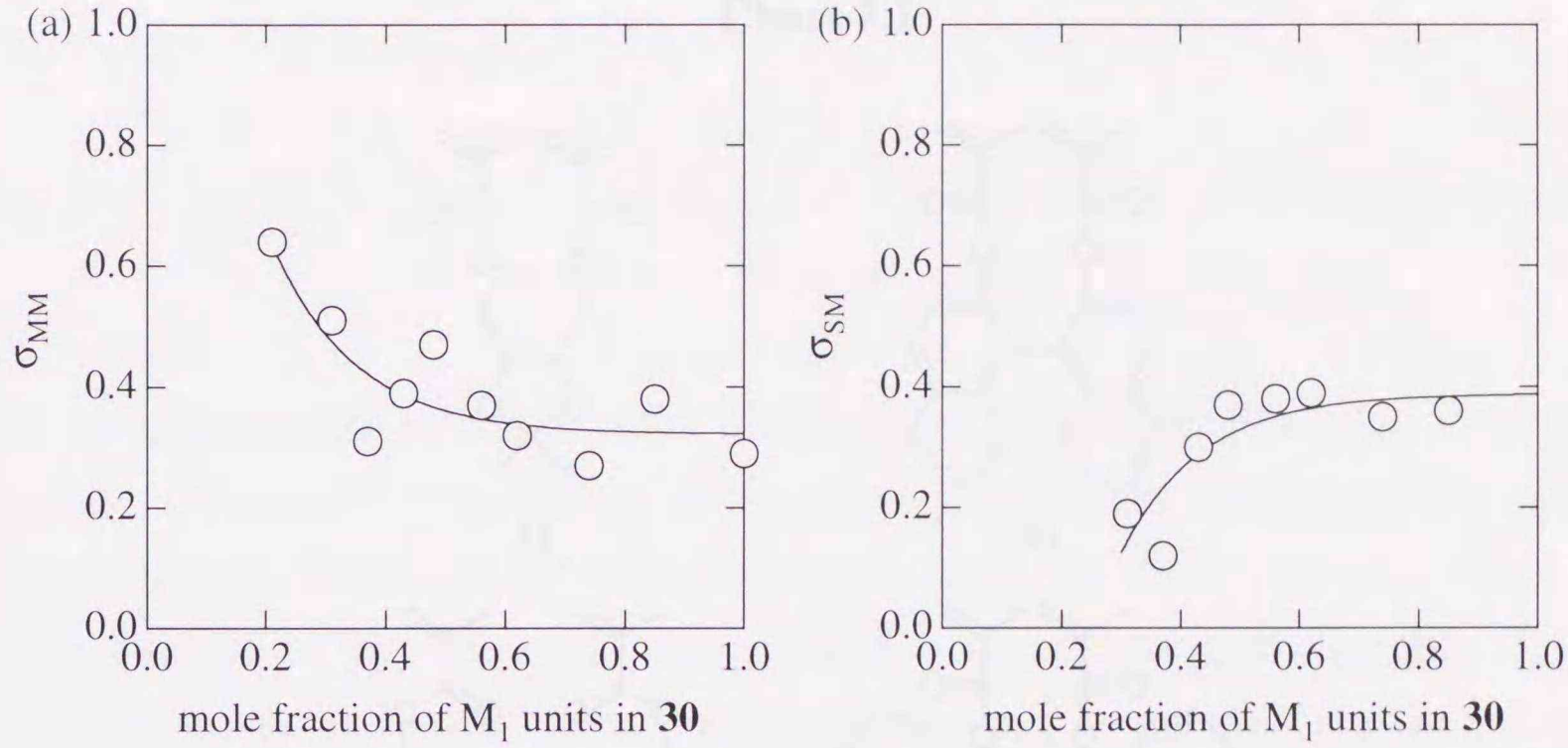

Figure 7.7. Probabilities σ_{MM} (a) and σ_{SM} (b) estimated by using eqs 7.7 and 7.8 versus mole fraction of M_1 units in polymer **30**.

*7.2.4. Origin of Chirality in Polymer **31***

As shown in Figure 7.7, the σ_{MM} value decreases with an increase in the mole fraction of M_1 unit in polymer **31**. The extrapolated value of σ_{MM} to the M_1 fraction of 1.0 agrees with the P_m value of 0.29 in PMMA derived from the homopolymerization of **29**, where P_m is the probability of the formation of the meso diad and is estimated by the expression $P_m = (m) = (mm) + 0.5\ (mr)$. The tactic triad fractions (*mm*), (*mr*), and (*rr*) in PMMA derived from **29** are shown in Table 7.5 along with the data previously reported for PMMAs from the analogous monomers **32**,[7] **33**,[8] **34**,[9] and **35**[10] (shown in Chart 7.1) during the cyclopolymerization. The polymerizations of **32**, **33**, and **34** are indicated to follow Bernoulli behavior, but those of **29** and **35** are

Table 7.5. Stereochemistry of poly(methyl methacrylate)s derived from radical cyclopolymerizations of **29** and the analog monomers.

M_1	(*mm*)	(*mr*)	(*rr*)	P_m [a]	Remarks
29	0.20	0.18	0.62	0.29	
32	0.12	0.49	0.39	0.37	T. Kakuchi[b]
33	0.14	0.51	0.36	0.39	T. Nakano[c]
34	0.20	0.52	0.28	0.46	H. Gueniffey[d]
35	0.84	0.10	0.06	0.89	T. Nakano[e]

[a] Calculated by use of the expression $P_m = (mm) + 0.5\ (mr)$. [b] Data from ref 7. [c] Data from ref 8. [d] Data from ref 9. [e] Data from ref 10.

Chart 7.1

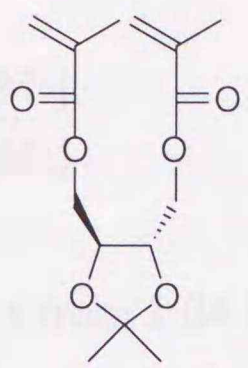

32

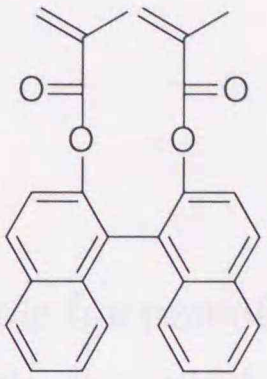

33

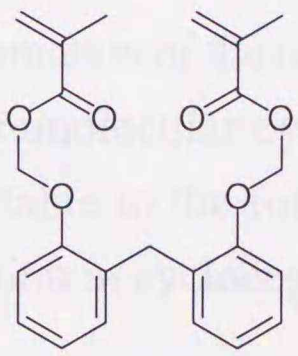

34

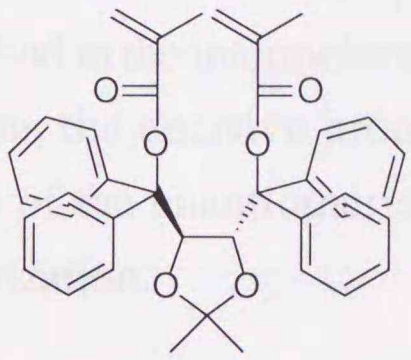

35

like the first-order Markov model. It is characteristic of PMMA derived from **29** that the fraction of tactic triad *rr* is significantly high in contrast to the extremely high fraction of tactic triad *mm* in PMMA from **35**.

The probability σ_{MM} is composed of two distinctive probabilities σ'_{MM} and σ''_{MM}, which mean the probabilities of meso addition in the intramolecular cyclization of **29** to form M_1 unit and in the intermolecular addition to form M_1M_1 diad, respectively. The contribution of the σ''_{MM} against observable σ_{MM} increases with an increase of the mole fraction of M_1 unit and will be asymptotic to 0.5 in PMMA. The decrease in σ_{MM} with an increase of M_1 unit in **31**, therefore, implies $\sigma'_{MM} > \sigma''_{MM}$. The probability of the formation of the racemo MM diad is higher in the intermolecular reaction than in the intramolecular cyclization.

As described in chapter 2, the specific rotation of the template-free polymer **3** derived form bis(4-vinylbenzoate) with styrene increased with an increase in the weight fraction of the isolated M_1 unit (i.e., isolated benzoate diad). Therefore, the chirality induction is caused to the formation of the enantiomeric racemo diad in the intramolecular cyclization. On the contrary, the specific rotation of polymer **31** increased with an increased of the M_1 unit in the polymer, but nevertheless, PMMA derived from **29** was optically inactive. Therefore, the comonomeric unit is required to convert the racemo sequence to a chiral chain. The number-average sequence

length (n'_1) of the M_1 unit can be calculated from the monomer reactivity ratios, r'_1 = 0.35 and r'_2 = 0.36, by the eq 7.27.[11]

$$n'_1 = 1 + r'_1 \frac{[M_1]}{[M_2]} \qquad (7.27)$$

The n_1 value increases from 1.04 for the M_1 mole fraction of 0.1 to 1.82 and 2.40 for those of 0.7 and 0.8, respectively. Consequently, the chirality in polymer **31** should originate from the isolated M tetrad sequence due to the M_1M_1 diad unit. Since the probability of the formation of the racemo diad in the intermolecular reaction is higher than that in the intramolecular cyclization, the decisive process for the chirality induction is attributable to the formation of the enantiomeric racemo diad in the intermolecular reaction in cyclocopolymerization.

7.3 Conclusions

Optically active poly[(methyl methacrylate)-*co*-styerne] was synthesized through the cyclocopolymerization of 1,2:5,6-di-*O*-isopropylidene-3,4-di-*O*-methacryloyl-D-mannitol (**29**, M_1) with styrene. The specific rotation of template-free polymer **31**, i.e., poly(MMA-*co*-St), increased with an increase of the M_1 unit in the polymer in contrast to the cyclocopolymerization of bis(4-vinylbenzoate) with styrene. In addition, the intermolecular reaction to form M_1M_1 sequence showed the higher probability of the formation of the racemo MM diad than that in the intramolecular cyclization. Consequently, the origin of chirality was assigned to the chiral tetrad MMA sequence separated by comonomer units.

7.4 Experimental Section

Measurements. ^{1}H and ^{13}C NMR spectra were recorded using JEOL JNM-EX270 and JNM-A400II instruments. The molecular weight of the resulting polymers was measured by gel permeation chromatography (GPC) in tetrahydrofuran on a Jasco Intelligent HPLC system (880-PU pump and 830-RI detector) equipped with three polystyrene columns (Shodex KF-804L). The number-average molecular weight (M_n) was calculated on the basis of a polystyrene calibration. Optical rotations were measured with a Jasco DIP-140 digital polarimeter.

Materials. Toluene was refluxed over sodium benzophenone ketyl and distilled just before use. 2,2'-Azobis(2-methylpropionitrile) (AIBN) was recrystallized from methanol.

1,2:5,6-Di-*O*-isopropylidene-3,4-di-*O*-methacryloyl-D-mannitol (29). 1,2:5,6-Di-*O*-isopropylidene-D-mannitol (13.1 g, 50 mmol) was dissolved in anhydrous pyridine (130 mL) and then methacryloyl chloride (12.5 g, 120 mmol) was added with ice-cooling. The mixture was heated at 70 °C for 7 hrs and then allowed to stand overnight at room temperature. The entire mixture was poured into water and then extracted with ether. After removal of the solvent, the resulting oil was purified by column chromatography on silica gel with hexane/diethyl ether (vol. ratio 7:3) to yield a colorless crystal. The product had a m.p. of 53 °C after recrystallization with hexane. Yield 5.1g (12.8 mmol, 26 %). $[\alpha]_{435} = +79.7°$, $[\alpha]_D = +38.8°$ ($CHCl_3$, 24 °C, *c* 1.0); ^{1}H NMR (270 MHz, $CDCl_3$): δ (ppm) = 6.15 (s, 2H, $=CH_2$), 5.64 (s, 2H, $=CH_2$), 5.43 (dd, ^{3}J = 2.5 Hz, ^{3}J = 7.8 Hz, 2H, OCH), 4.27-4.21 (m, 2H, CH), 3.97-3.86 (m, 4H, CH_2), 1.96 (s, 6H, α-CH_3), 1.35 (s, 6H, CH_3), and 1.31 ppm (s, 6H, CH_3). ^{13}C NMR (67.8 MHz, $CDCl_3$): δ (ppm) = 166.0 (C=O), 135.6 (=C-), 126.6 ($=CH_2$), 109.3 (C), 74.7 (CH), 71.6 (CH), 65.5 (CH_2), 26.3 (CH_3), 25.1 (CH_3), 18.2 (α-CH_3). IR (KBr): ν (cm^{-1}) = 1760 (C=O st), 1636 (C=C st). Anal. Calcd for $C_{20}H_{30}O_8$ (398.5): C 60.29; H 7.59. Found: C 59.99; H 7.56.

Cyclocopolymerization. The polymerization was conducted at 60 °C using toluene (45 mL) and AIBN (46 mg). The total concentration of both monomers was 0.2 mol·L^{-1} in each of the copolymerizations.

Poly[(methyl methacrylate)-*co*-styrene] (31). To polymer **30** (300 mg) in THF (3 mL) was added 25% methanolic KOH solution (15 mL). The mixture was heated under reflux for 5 h, then converted to be homogeneous by gradually adding water,

and boiled for ca. 100 h. After neutralization with hydrochloric acid, the solution was dialyzed using a cellophane tube, and later concentrated by freeze-drying. To a mixture of an ether solution (60 mL) containing diazomethane (ca. 30 mmol) and benzene (60 mL) was added the finely divided hydrolyzed polymer (ca. 100 mg: the amount of specimen used corresponded to 1.0 mmol of the C=O group). The polymer was dissolved with evolution of nitrogen gas. The entire mixture was set aside for 14 h and then the all solvent was removed. The residue was purified by reprecipitation with chloroform-methanol and dried *in vacuo*.

7.5 References

(1) Roovers, J.; Smets, G. *Makromol. Chem.* **1963**, *60*, 89.

(2) Aso, C. *J. Polym. Sci.* **1959**, *39*, 475.

(3) Aso, C. *Mem. Fac. Eng. Kyushu Univ.* **1963**, *22*, 119, *Chem. Abstr.* **1963**, *59*, 4045f.

(4) Katritzky, R.; Smith, A.; Weiss, D. E. J. Chem. Soc., Perkin Trans. 2 1974, 1547.

(5) Kato, Y.; Ando, I.; Nishioka, A. *Nippon Kagaku Kaishi* **1975**, 501; *Chem. Abstr.* **1975**, *83*, 28706.

(6) Aerdtsm, A. M.; de Haan, J. W.; German, A. L. *Macromolecules* **1993**, *26*, 1965.

(7) Kakuchi, T.; Kawai, H.; Katoh, A.; Haba, O.; Yokota, K. *Macromolecules* **1992**, *25*, 5545.

(8) Nakano, T.; Sogah, D. Y. *J. Am. Chem. Soc.* **1995**, *117*, 534.

(9) Guéniffey, H.; Kämmerer, H.; Pinazzi, C. *Makromol. Chem.* **1973**, *165*, 73.

(10) Nakano, T.; Okamoto, Y.; Sogah, D. Y.; Zheng, S. *Macromolecules* **1995**, *28*, 8705.

(11) Ito, K.; Yamashita, Y. *J. Polym. Sci., Part A: Polym. Chem.* **1965**, *3*, 2165.

Chapter 8
Conclusions

The effect of distance between two chiral centers of the template was examined by use of (2*S*,3*S*)-2,3-butanediol, (2*S*,4*S*)-2,4-pentanediol, and (2*S*,5*S*)-2,5-hexanediol as chiral templates. The cyclocopolymerization of (2*S*,3*S*)-2,3-butanediyl, (2*S*,4*S*)-2,4-pentanediyl, and (2*S*,5*S*)-2,5-hexanediyl bis(4-vinylbenzoate)s (**1a**, **1b**, and **1c**, respectively) with styrene homogeneously proceeded. The resulting polymer was converted into poly[(methyl 4-vinylbenzoate)-*co*-styrene] (**3**) by alkali hydrolysis and methyl esterification. Quantitative removal of chiral template from polymer **3** was confirmed by ^{1}H NMR spectroscopy. Polymers **3a**-**c** showed an optical activity and their CD spectra indicated that the segmental distribution of high content of (*R*,*R*)-racemo benzoate diads is favored in the polymer. Since the specific rotation of polymers **3a**-**c** increased with an increase in content of the isolated benzoate diad, the origin of chirality was attributable to the isolated benzoate diad. The chirality induction efficiency was improved in order of **a** < **c** < **b**, namely, 1,2-diol < 1,4-diol < 1,3-diol.

The radical cyclization of bis(4-vinylbenzoate) using tri-*n*-butyltin hydride was carried out to estimate the stereoselectivity in the intramolecular cyclization. The stereoselection in the radical cyclization was fairly agreed with that in the cyclocopolymerization. For 1,2-diol templates, the extent of stereoselectivity was increased with an increase in the A value of split Cotton effect in CD spectra of monomers. This result means that the chirality induction in intramolecular cyclization was driven by the chiral twist of two 4-vinylbenzoyl groups.

In order to estimate the stereochemical distribution of the cyclic units, radical cyclization of bis(4-vinylbenzoate) was carried out using allyltri-*n*-butyltin as a chain transfer reagent. The stereoslection between (*R*,*R*)- and (*S*,*S*)-configuration in the cyclization was entirely agreed with the results of the cyclocopolymerization. The second stereoselectivity in the intermolecular addition of cyclized radical significantly depended on the absolute configuration of the first chiral center.

In order to elucidate the chirality induction mechanism, the semiempirical molecular orbital calculation (MOPAC6-AM1 method) was applied to the simplified model of radical cyclizations of (2*S*,3*S*)-2,3-butanediyl, (2*S*,4*S*)-2,4-pentanediyl, and (2*S*,5*S*)-2,5-hexanediyl bis(4-vinylbenzoate)s (**1a**, **1b**, and **1c**, respectively). The search for minimum energy conformations was carried out using MM2 calculation. The results indicated that **1a** and **1b** practically took onyl one conformer but **1c**

distributed among three conformers because of flexibility. The MOPAC6-AM1 calculation was carried out in consideration of direction in radical addition for dissymmetric conformation as well as conformational distribution. The stereoselectivity in the intramolecular cyclization could be explained by the heat of formation on the transition states and consideration about the allowed angle of radical addition to carbon-carbon double bond. The chiral twist of two 4-vinylbenzoyl groups selects the prochiral face of vinyl groups to meet the allowed angle of radical addition.

On the other hand, The stereoselectivity in the intermolecular cyclization of the cyclized radical could be explained by the heat of formation of the cyclized radical and equilibrium on the conformational interconversion. The stability of the cyclized radical significantly depended on the configuration of the first chiral center. This dependecy could be explained by considering the stereoelectoronic effect of cyclized radical and the steric effect of the penultimate group. The stereoelectronic effect of cyclized radical affects the direction of the benzene ring which is closely connected with the carbonyl groups because of conjugation. Hence, the chiral orientation of two carbonyl groups has an influence on the stability of the cyclized radical.

Chiral template biases two conformational elements, i.e., chiral twist of two 4-vinylbenzoyl groups and chiral orientation of two carbonyl groups. According to abovementioned mechanism, the former and latter conformational elements play an important role on the stereoselction in the intra- and intermolecular addition, respectively.

The chirality induction mechanism established on the basis of the computational results included the conformational interconversion of the cyclized radical. The rate of the interconversion is independent of total monomer concentration, whereas propagation is proportional to total monomer concentration. Then, the effect of total monomer concentration on chirality induction were examined to clarify whether conformational interconversion functions or not. The DP_n' of template-free polymer has no influence on the chiroptical property within the DP_n' ranging from 32 to 21. In this DP_n' range, the specific rotation of the template-free polymer increased with a decrease in total monomer concentration. This effect could be explained on the basis of the chirality induction mechanism.

The computational study on the chirality induction indicated that chiral template controls two conformational element, i.e., chiral twist of two 4-vinylbenzoyl groups and chiral orientation of two carbonyl groups. In order to test the conformational effect, cyclocopolymerization of methyl, ethyl, and isopropyl 2,3-bis-*O*-(4-vinylbenzoyl)-L-tartarate (**1g**, **1h**, and **1i**, respectively) with styrene were examined. After removal of the template, the template-free polymer **3g-i** shows an extremely low specific rotation. The template-free polymer **3f**, which synthesized through the cyclocopolymerization of (2*S*,3*S*)-1,4-dimethoxy-2,3-butanediyl bis(4-vinylbenzoate) (**1f**, i.e., the decarbonyl analog of **1g**) with styrene, shows the considerably higher specific rotation than polymer **3g-i**. From the CD spectral analysis, two 4-vinylbenzoyl groups twisted counterclockwise for **1g-i** and clockwise for **1f**, whereas **1g-i** and **1f** have same configuration on the chiral center. Hence, the stable conformations of **1g-i** are different from that of **1f** and separate thier two 4-vinylbenzoyl groups. This leads to disorder the control of the carbonyl orientation in the cyclization, resulting in deterioration of the chirality induction efficiency.

In order to explore other approaches for characterization of the optically active polymer due to main chain chirality, the cyclocopolymerization of 1,2:5,6-Di-*O*-isopropylidene-3,4-di-*O*-methacryloyl-D-mannitol (M_1, **29**) with styrene (M_2) were examined. The resulting polymer **30** was converted to poly[(methyl methacrylate)-*co*-styrene] (**31**) by hydrolysis and methyl esterification. Although polymer **31** showed an optical activity, the specific rotation of polymer **31** increased with increase in mole fraction of M_1 unit in polymer **31** in contrast to polymer obtained from cyclocopolymerization of bis(4-vinylbenzoate) with styrene. From the ^{13}C NMR spectral analysis, the probability of racemo addition in the intermolecular reaction was higher than that in the intramolecular cyclization in this polymerization system. Therefore, the optical activity of polymer **31** was attributable to the chiral tetrad sequence rather than chiral diad sequence.

inches 1 2 3 4 5 6 7 8

cm 1 2 3 4 5 6 7 8 9 10 11 12 13 14 15 16 17 18 19

Kodak Color Control Patches

Blue Cyan Green Yellow Red Magenta White 3/Color Black

Kodak Gray Scale

C Y M

A 1 2 3 4 5 6 **M** 8 9 10 11 12 13 14 15 **B** 17 18 19